The role of the bedrock groundwater in the hydrology of a mountainous hillslope affected by gravitational deformation and the implications in the generation of deep-seated landslides

The role of the bedrock groundwater in the hydrology of a mountainous hillslope affected by gravitational deformation and the implications in the generation of deep-seated landslides.

January 2014

CRISTÓBAL PADILLA MORENO

The role of the bedrock groundwater in the hydrology of a mountainous hillslope affected by gravitational deformation and the implications in the generation of deep-seated landslides.

A Dissertation Submitted to
The Graduate School of Life and Environmental Sciences,
The University of Tsukuba
in Partial Fulfillment of the Requirements
for the Degree of Doctor of Philosophy in Science
(Doctoral Program of Integrative Environmental Sciences)

CRISTÓBAL PADILLA MORENO

Contents

Abstract

The groundwater response of hillslopes to rainfalls has critical importance in the study of hillslope stability. Deep seated landslides (DSL) often involve the movement of soil (sediment) and bedrock which make difficult the groundwater modeling. The study of groundwater in hillslopes requires the observation of groundwater in fractured bedrock. However few studies have based the analysis on direct observations and the mechanisms of DSL generation are still not well known. This study is aimed to clarify the role of the bedrock groundwater in a hillslope with fractured sedimentary bedrock and establish its implication in the generation of DSL. The study is based on extensive hydrometric and hydrochemical observations of groundwater and catchment discharge in an area where DSL were generated. The study was carried out in a hillslopes of Mt. Wanitsuka (1118 m asl), in Miyazaki prefecture. In the area heavy rainfall caused several DSL events in 2005. The geology of the bedrock is dominated by stratified sedimentary rock, part of the Shimanto accretionary prism units. Also the hillslopes present evidences of gravitational deformation, marked as precursor of DSL events. For the groundwater observations in the area, two boreholes were constructed in the hillslope; one is 10 m deep (Bh10) and the other 40 m deep (Bh40). Also, the discharge of a catchment next to the hillslope (catchment D) and others in adjacent areas (catchment U and M) were observed.

The data obtained from the boreholes showed fast and significant responses of the bedrock groundwater (observed in Bh40) with important change in the water quality in comparison to the response in the sediment cover groundwater (observed in Bh10). The bedrock groundwater presents single and double peaks responses mainly depending on antecedent rainfall (API) in short periods of time (API_6 (with 6 hours half-life)). The double peak responses are mainly associated to low and moderate rainfall events and single peak responses to higher rainfall events. Both types of response show similar initial fast response but different recession curve. The initial fast response is caused by rapid flows of groundwater in bedrock. The

chemical analysis suggests that this rapid flow is composed by a mix of infiltrated rainfall water and groundwater that remains in the unsaturated fractured bedrock. These rapid flows are attributed to high degree fractures (HDF) in the bedrock that act as conduits of groundwater. This HDF were identified in the borehole core and they can be related to the gravitational deformation of the slope. In the single peak response, the bedrock groundwater showed a maximum level at 11.5 m below the ground surface approximately. This phenomenon suggested the existence of another fracture flow mechanism that can causes an exfiltration of groundwater from the bedrock aquifer during heavy rainfall events. The analysis of catchment runoff evidenced that this exfiltration can affect the runoff characteristics of catchment D. The runoff only in catchment D reveals a delayed discharge and significant chemical similarities with the BG during base level and storm flow. A hydrograph separation analysis was carried out using three end members; the rainfalls and two end members for groundwater. The groundwater end members were separated in the base level groundwater and the groundwater during response due to their significant chemical differences. The analysis of two rainfall events revealed an important contribution of BG during storms.

As a conclusion, it is possible to affirm that the BG controls most of the hydrological response of the hillslope analyzed. A fracture system related to the gravitational deformation facilitates a rapid infiltration of rainfall water into the bedrock aquifer. Additionally, another set of fractures plays an important role in the establishment of a maximum level of bedrock groundwater and its eventual exfiltration to superficial flows. The short term response of the bedrock groundwater can be associated to the timing of the landslides events of 2005 which is coincident with the maximum intensity of rainfall. Due to the dynamics of gravitational deformation, changes in the fracture setting are possible in the future. A probable reduction in the efficiency of the exfiltration mechanism can eventually generate DSL in the future due to an increase of groundwater pressure in bedrock fractures.

Keywords: Deep-seated Landslides, Bedrock Groundwater, Gravitational Deformation, Shimanto Accretionary Prism Complex, Borehole Observation, Bedrock groundwater – runoff interaction, Mountainous catchment, Environmental Isotopes.

List of Figures

List of Photographs

List of Tables

Chapter 1: Introduction

1.1. Deep-seated landslides characteristics

Landslides are a common mass movement process in mountainous areas. These processes are classically classified depending on the material involved and the mode of movement (Varnes, 1978). In terms of depth of failure surface many terrestrial mass movements can be considered as shallow-seated failures (Figure 1). These shallow-seated failures, such as debris flows or shallow landslides, can be studied using established methods in soil or rock mechanics (Petley and Allison, 1997). In contrast, deep-seated landslides (DSL) are less common and involve mechanical deformation at considerable depth. This deformation is known as deep-seated slope gravitational deformation, DSGSD (Agliardi et al., 2001; Zerathe and Lebourg, 2012) or mass rock creep (Chigira, 2009). The deformation driven by gravity is commonly observed as small movements of the hillslope in comparison to its dimensions. The deformation can occur in short periods prior to the complete failure of the hillslope or can be extended during long periods (chronic deformation) and not necessarily cause a complete failure of the hillslope (Chigira, 2009). In the deformation state, certain conditions of seismic acceleration or groundwater pore pressure generated by heavy rainfall can trigger a rapid and catastrophic slide of the deformed rock mass defined as DSL (Petley and Allison, 1997). This study is focused on the DSL events generated by rainfalls and the changes in groundwater conditions in hillslopes.

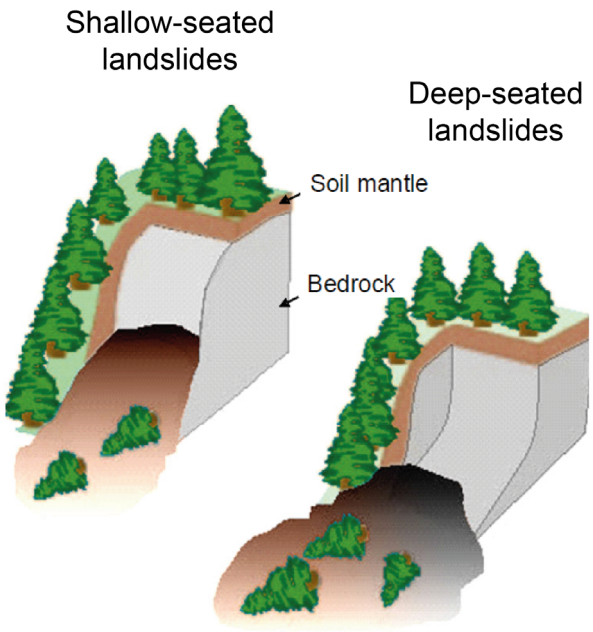

Figure 1. Shallow-seated landslides and deep-seated landslides (modified from Uchida et al. (2011)).

The DSL events induced by rainfalls are commonly associated to long rainfalls with moderate intensity in contrast to the shallow-seated landslides related to shorter and high intensity rainfall events (Crosta, 2004). Under long rainfall events it is expected a larger volume of rainfall water infiltrate deep into the fractured bedrock, increasing the groundwater pressure in bedrock fractures and eventually trigger the failure of the hillslope. The process of infiltration in fractured media to deep levels can have different elapsed time depending directly on the fracture system of bedrock (Tsou et al., 2011). This affect the timing of DSL occurrence which sometimes can be even days after of rainfall event finished (Chigira, 2009; Lollino et al., 2006; Tsou et al., 2011).

Recently in the Japanese territory several DSL event caused by heavy rainfall have been occurred. Heavy rainfall events in Japan are associated to the pass of typhoons during the summer season. The major DSL events were observed in Miyazaki Prefecture in 2005 caused by the typhoon No14, “Nabi” and in Kochi, Wakayama and Nara prefectures caused by the typhoon No12, “Talas” in 2011 (Figure 2). For the events of Miyazaki prefecture 124 landslides events

were observed (DSL, debris flows and earth falls) after 1013 mm of accumulated rainfall in 72 hours (Taniguchi, 2008). In 2011, the typhoon "Talas" was responsible of more than 70 DSL events observed mainly in the prefectures of Nara and Wakayama (Chigira et al., 2013). The measured accumulated rainfall exceeded 1000 mm in approximately 72 hours with a maximum of 2439 mm.

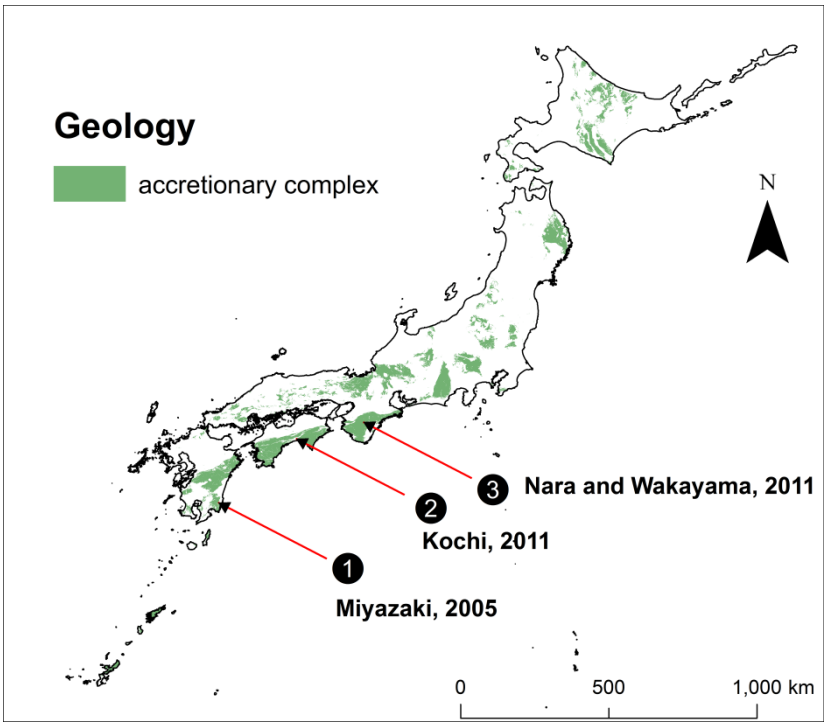

Figure 2. Recent DSL events in Japan and bedrock geology.

Additionally to the heavy rainfall that generates these events, the geology of the bedrock is another common factor between them. All these events are located in sedimentary rock part of accretionary complexes. Uchida et al. (2012) showed that tectonic uplift of bedrock is an important factor in the identification of areas prone to be affected by deep catastrophic landslides in Japan, based on historical record of these events. In the same work it is also concluded that in zones with geology of accretionary prism the frequency of landslide events is higher than in other bedrock geology. The fracture conditions and competence of the sedimentary rock of accretionary prisms seems to provide the conditions for the generation of DSL. In this case, the

characteristic of groundwater in the fractured bedrock as a response of heavy rainfalls seems to be very relevant in the analysis of DSL generation. However, these characteristics are poorly understood due to the scarcity of studies of bedrock groundwater conditions, especially in areas with fractured bedrock and DSL has been observed.

1.2. Previous studies in bedrock groundwater.

1.2.1. Bedrock groundwater and DSL studies.

The study of bedrock groundwater for the analysis of DSL is very limited. In landslides generation assessments the indirect analysis of groundwater conditions that could trigger landslide in hillslopes are frequently used. These indirect analyses correspond to conceptual models, generally based on rainfall data, used to interpret infiltration rates and water contents of sediments in hillslopes (Caine, 1980; Jain, 1993; Montgomery and Dietrich, 1994; Sugawara et al., 1984; Terlien, 1998). Even though these conceptual models interpret the conditions of hillslopes as a "black box", they are widely used because of their low-cost and easy implementation. Also, they have given good results defining threshold for failure in non-cohesive deposits, mainly for shallow-seated landslides such as debris flows and shallow landslides (Saito et al., 2010a; Saito et al., 2010b; Sepulveda and Padilla, 2008; von Ruette et al., 2011; Yano, 1990). Most of the time these models correctly interprets water conditions in homogeneous and isotropic media dominated by Darcy flows. In contrast, in the case of deep seated landslides the use of this type of methodologies becomes difficult (Onda et al., 2003; Zhang et al., 2006). The complexities inherent to groundwater flows in fractured media demand the direct observations of groundwater in order to understand its dynamics (Kosugi et al., 2011; Padilla et al., 2014; Salve et al., 2012). In these studies, direct observations are referred as the

use of observation boreholes for the direct measurements of the water table fluctuations and also other characteristics of bedrock groundwater.

Even though the awareness of the importance of direct observations there are almost no study that bases the analysis on borehole measurements. The remote conditions of mountainous areas and the cost of the observation well construction in high degree hillslopes has been marked as a main restriction of development of this kind of observations (Gabrielli et al., 2012). One of the first studies that used direct bedrock groundwater observations correspond to the work of Okunishi and Nakagawa (1977). In the study, the authors carried out a quantitative analysis and modeling of the groundwater and spring discharge in a hillslope affected by a large-scale landslide. The study area is located in Kochi prefecture and the geology also corresponds to fractured sedimentary rock, part of accretionary complexes. In the area, particular patterns of groundwater flows and spring discharge such as double peak were identified. These patterns were attributed to different flow path in the fractured bedrock and soil cover. The modeling of groundwater, based on tank model methodology, demonstrate the complexity in the use of simple models to estimate the groundwater behavior in fractured bedrock. After this study, the study of bedrock groundwater using borehole in fractured bedrock related to the occurrence of DSL is very limited. Since then the development of DSL analysis and bedrock groundwater has been based on the conceptual models described before.

Recent studies have used bedrock groundwater observation boreholes in hillslopes but they are mainly focused on shallow-seated landslides processes. Wilson and Dietrich (1987a) defined important flow through the fractured bedrock by deep piezometric observations (15 m maximum depth). These flows define the saturation conditions and possible generation of landslide in the sediment cover of a low degree hillslope. Similar observations were made by Montgomery et al. (2002) analyzing the response of shallow fractured bedrock groundwater using piezometric observations. In the study an important influence of bedrock flows in the

generation and timing of shallow landslides was determined. These studies are not related with deep landslides processes; however, they show the important role of bedrock groundwater even for hillslopes with low fractured bedrock.

The scarcity of studies of bedrock groundwater in mountainous hillslopes can be covered by the studies in fractured aquifer. The comparison with those studies can provide important information to correctly interpret the observations made in fractured aquifer in hillslopes.

1.2.2. Bedrock groundwater and catchment runoff generation studies.

Recently, important advances in the understanding of bedrock groundwater have been reported in studies focused on the analysis of runoff generation in mountainous catchments. Classically in mountainous (headwater) catchments the storm runoff generation has been restricted to surface (overland flows) or subsurface flows in the sediment cover mantle (soil or saprolite), assuming a very low or null hydraulic conductivity of the underlying bedrock (Figure 3a) (Banks et al., 2009; Kampf and Burges, 2007; Salve et al., 2012). The assumption of the bedrock as an impermeable barrier during storms is progressively changing. More studies are showing that bedrock can be permeable and affect the hydraulic response of the catchment (Figure 3b). Also some studies proposed the importance of bedrock groundwater flows in the storm runoff (Anderson et al., 1997; Gabrielli et al., 2012; Haria and Shand, 2004; Iwagami et al., 2010; Katsuyama et al., 2005; Montgomery et al., 1997; Onda et al., 2006; Wilson and Dietrich, 1987b). Many of these studies had estimated the contribution of shallow weathered or fractured bedrock groundwater using indirect observations of bedrock groundwater such as pressure heads measurements in the soil-bedrock interface, chemical tracer analysis or measurements in bedrock spring discharge.

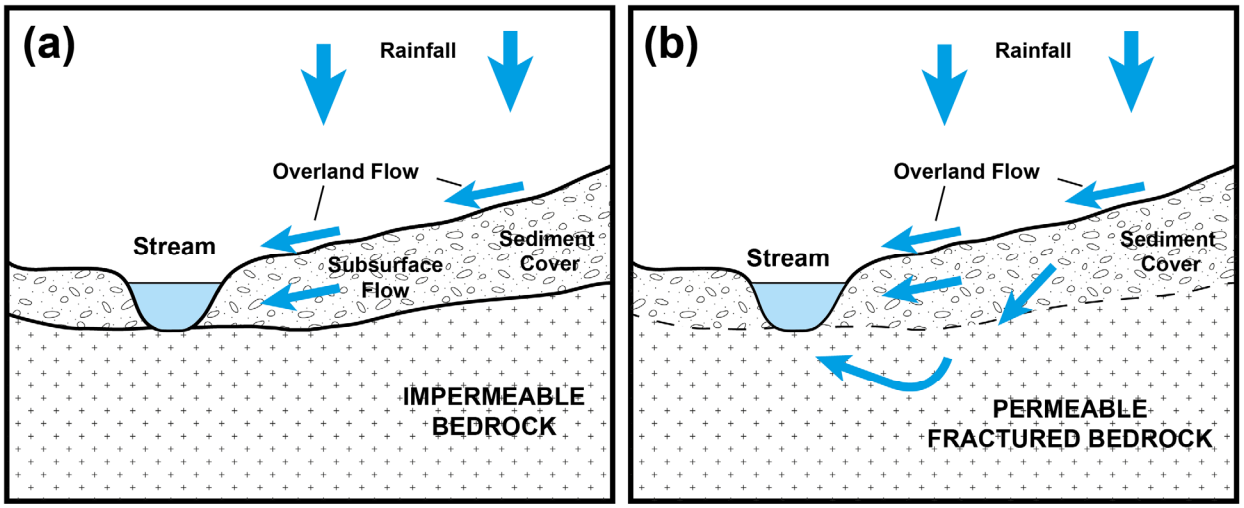

Figure 3. Conceptual models for the bedrock groundwater interaction with the storm runoff. (a) Impermeable bedrock (b) Permeable bedrock. Modified from Banks et al. (2009).

Anderson et al. (1997) and Montgomery et al. (1997) identified important flow path through the shallow weathered sandstone bedrock with a thin colluvial soil cover (less than 2 m). Uchida et al. (2003) estimate a contribution of bedrock groundwater from 50% to 90% of the storm runoff of headwater catchment underlain by granite bedrock. This contribution was estimated based on measurements in tensiometers, observation wells over the soil-bedrock interface and the discharge of bedrock springs. Similar data set was used by Onda et al. (2006) in order to compare two catchments with different underlain geology (granite and shale bedrock). The authors found a major contribution of bedrock groundwater to the runoff in the catchment with sedimentary bedrock. Moreover, the contribution of bedrock groundwater was expressed as a delayed discharge in the hydrographs. In the study the author addressed the importance of the analysis of the contribution of bedrock groundwater under different geological conditions. The fracture settings that characterize different type of bedrock can also determine different types of bedrock groundwater contribution. In some cases a possible contribution of deep bedrock groundwater was proposed.

The studies based on direct observations of bedrock groundwater in weathered or fractured bedrock are still few (Gabrielli et al., 2012; Iwagami et al., 2010; Salve et al., 2012).

Katsuyama et al. (2005) using a net of tensiometers and observations wells with penetration in the weathered granite bedrock, identified important responses of the bedrock groundwater to storms and the generation of flows that can even exceed the saturated throughflow in the soil-bedrock interface. Gabrielli et al. (2012) by comparing two well-known catchments, one underlain by relatively shallow weathered and fractured volcanic rock and the other by moderately weathered sedimentary rock, observed an significant response of the bedrock water table in the catchment with more fractured bedrock (volcanic). In that catchment the authors identified a shallow high fractured zone in the bedrock (1 - 2 m below the soild bedrock interface) that actively participate in the storm runoff. This zone acted as a conduit of subsurface flows of soil water and rainfall water but no deep groundwater. The low fractured bedrock below this zone did not show any potential contribution in the storm runoff.

Studies in catchments with deeper fractured bedrock have reported important responses in the deep bedrock groundwater that also influenced the storm runoff. The study of Iwagami et al. (2010) showed deep percolation of rainfall water until 20 m in the bedrock (weathered andesite) in a small mountainous catchment. The discharge characteristics in that catchment were strongly dependant on the groundwater table location, including the generation of delayed discharge. Using very dense net of observation boreholes (20 m to 70 m depth) in a headwater catchment in granite bedrock, Kosugi et al. (2011) identified a three bedrock aquifers separated by possible geological structures (faults). In the study, the bedrock groundwater clearly determines the characteristics of the catchment runoff in short and long terms. Two delayed peaks in the catchment discharge were identified, both of them associated to the bedrock groundwater response. These studies reveal that deep groundwater can affect the hydrological response of headwater catchments with deep fractured bedrock. Also, geological structures can define the characteristics of the interaction bedrock groundwater – runoff. However more studies under this line of investigation had not been reported.

1.3. Studies in Mt. Wanitsuka.

The review of previous studies showed the general scarcity of the bedrock groundwater observations in mountainous hillslopes, especially in areas where DSL are more frequent. In Japan the areas prone to be affected by DSL were identified as the areas with geology dominated by sedimentary rock, specifically part of the accretionary prism complexes (Uchida et al., 2012). At the time of starting this investigation, the DSL events observed in Miyazaki in 2005 were the most favorable option for the study of bedrock groundwater and the interaction with DSL. In this area, particularly the DSL events observed in Mt. Wanitsuka (Miyazaki Prefecture), presented advantages in front of the rest of the areas where DSL were observed. Mt. Wanitsuka, located 18 km to the southwest of Miyazaki city, counts with easy accesses from the city to the areas where DSL occur in 2005. This fact has a vital important in the access of machinery needed for the construction of boreholes in the required areas. Moreover, the geology of the area corresponds to layers of sedimentary rock part of the Shimanto Accretionary Prism Complexes.

After the DSL events of 2005, in Miyazaki prefecture, including Mt. Wanitsuka, were carried out several studies oriented to determine the particular characteristics observed in the area. The DSL events in Miyazaki prefecture were caused by the slowly pass of the typhoon No14 “Nabi” during September 5th and 6th (Figure 4).

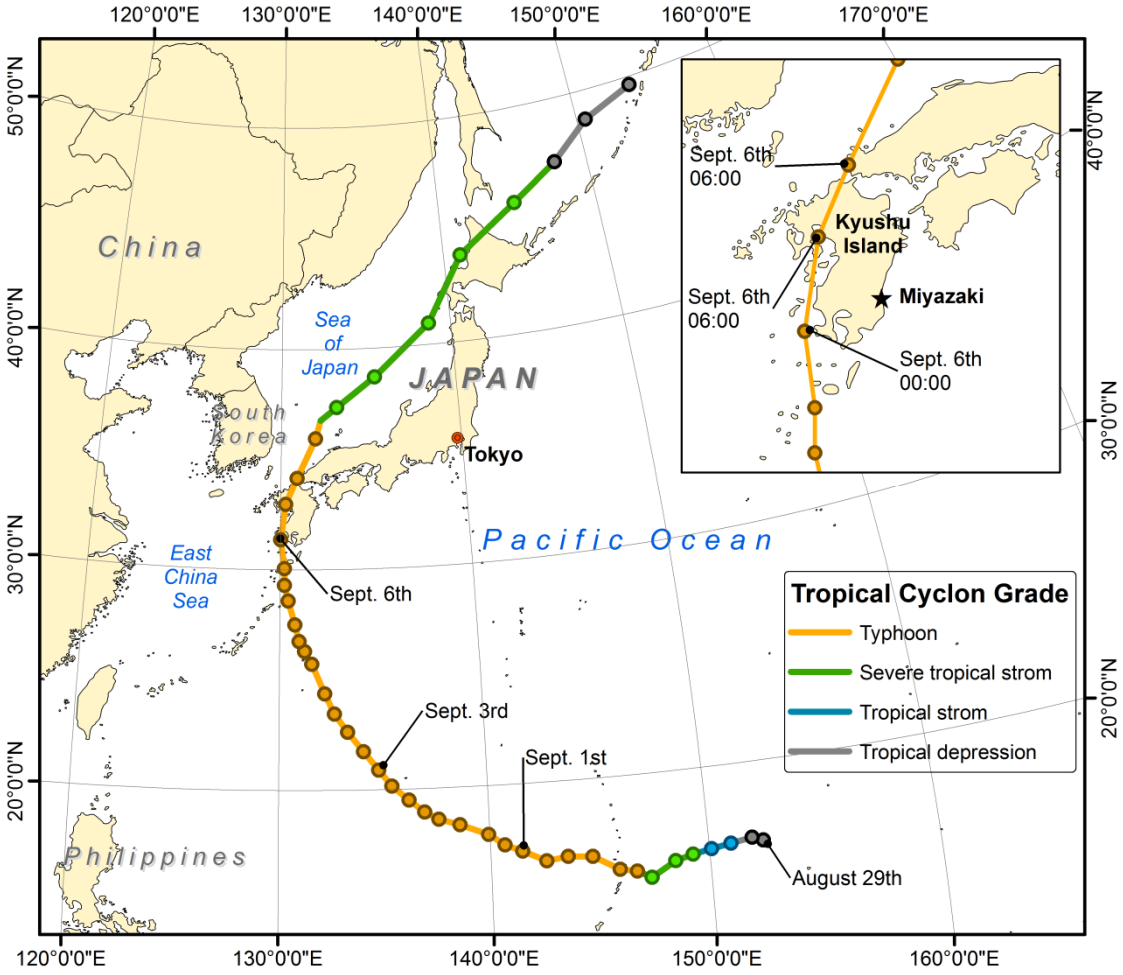

Figure 4. Track of typhoon No14 (0514) Nabi.

According to locals information collected by Taniguchi (2008) the occurrence time of most of DSL was estimated at the morning of September 6th. In particular, the occurrence of the Mt. Wanitsuka events was estimated between 7:00 and 8:00 am. This is coincident with the peak of intensity of rainfall of 46 mm/h measured in the top ot Mt. Wanitsuka. As it was mentioned previously, the coincidence of maximum rainfall intensity and occurrence of DSL is not common. This fact can suggest particular conditions of this area about the infiltration of rainfall water in the bedrock aquifer. The accumulated rainfall measured at the estimated time of the DSL occurrence was 914 mm in 71 to 72 hours, measured in the top of the Mt. Wanitsuka.

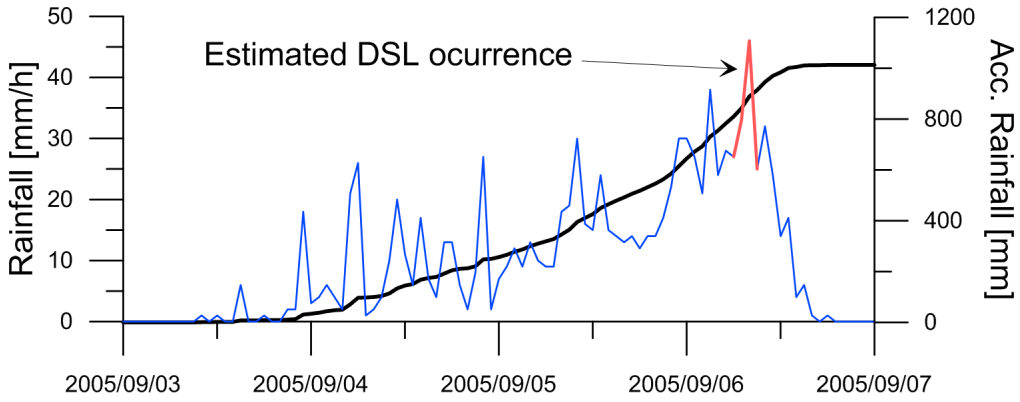

Figure 5. Hyetograph of rainfall event caused by the Typhoon Nabi. Blue line: rainfall (mm/h); Black line: Accumulated rainfall (mm); red line: rainfall at estimated time of DSL occurrence.

Studies in Mt. Wanitsuka identified several hillslopes with tension cracks or downhill-facing scarps evidencing the deformations of the hillslopes in the area (Akther et al., 2011; Onda et al., 2010; Uchida et al., 2011; Yokoyama et al., 2011). Akther et al. (2011), based on historical inventory of maps and aerial photographs, identified a chronic deformation of the hillslopes. Uchida et al. (2011) developed a new methodology for the assessment of DSL susceptibility. With this new methodology the authors demonstrated that catchment that presents ancient DSL, chronic deformation and large steep slopes are prone to be affected by DSL. Most of the landslides that observed in Mt. Wanitsuka satisfied these criteria. Onda et al. (2010) analyzing the chemistry of groundwater and the runoff of catchment in Mt. Wanitsuka proposed an important contribution of bedrock groundwater in areas near of DSL occurrence. This was proposed based on the comparison of Ca^{+2} concentrations and the EC characteristics of groundwater and different streams of Mt. Wanitsuka.

The previous studies permit to demonstrate the importance of Mt. Wanitsuka as a favorable area in the analysis of bedrock groundwater and its relation with the DSL.

1.4. Objectives

The objective of this research is to identify the role of the bedrock groundwater in the hydrogeological response of a hillslope underlain by fractured bedrock. For this purpose a geological and hydrometric analysis of a hillslope was carried out in a hillslope of Mt. Wanitsuka. This mountain is build on fractured sedimentary rocks of the Shimanto acretionary complex and also presents evidence of gravitational deformation. The final purpose of the study is to clarify the participation of the bedrock groundwater in the generation DSL, using as a reference the events generated by the Typhoon No 14 “Nabi”.

Chapter 2: Study Area

2.1. General Description

The study area is located in Mt. Wanitsuka (1118 m asl) in Miyazaki prefecture. The region has sub-tropical climate (humid and temperate) with average temperatures of 18°C. The average annual precipitation measured in the top of the mountain is 2669 mm and the main rainfall occurs during summer, from June to September, as part of the East Asia monsoon. In this period, the Japanese territory is also lashed by severe tropical cyclones known as typhoons. Most of the heavy rainfalls observed in Japan are attributed to typhoons or summer storms over the territory.

The field observations of the study area were concentrated in the Byutano River basin with 15.2 km^2 of drainage area. In this basin, approximately seven DSL events where generated during the heavy rainfalls observed in 2005 (Figure 6). Within this basin a particular hillslope was studied. This studied hillslopes is part of Shirinashi River basin, a sub basin of Byutano River. This area was selected from others because its accessibility by vehicle to near areas where DSL took place and its location next to a DSL scarp, part of the 2005 events.

The average slope of the hillslope corresponds to 35° to 40°. The altitude ranges from 390 m asl to 540 m asl. The hillslope is partially covered by Japanese cypress. Due to the works to stabilize the DSL deposit area, part of the forest cover was cut off.

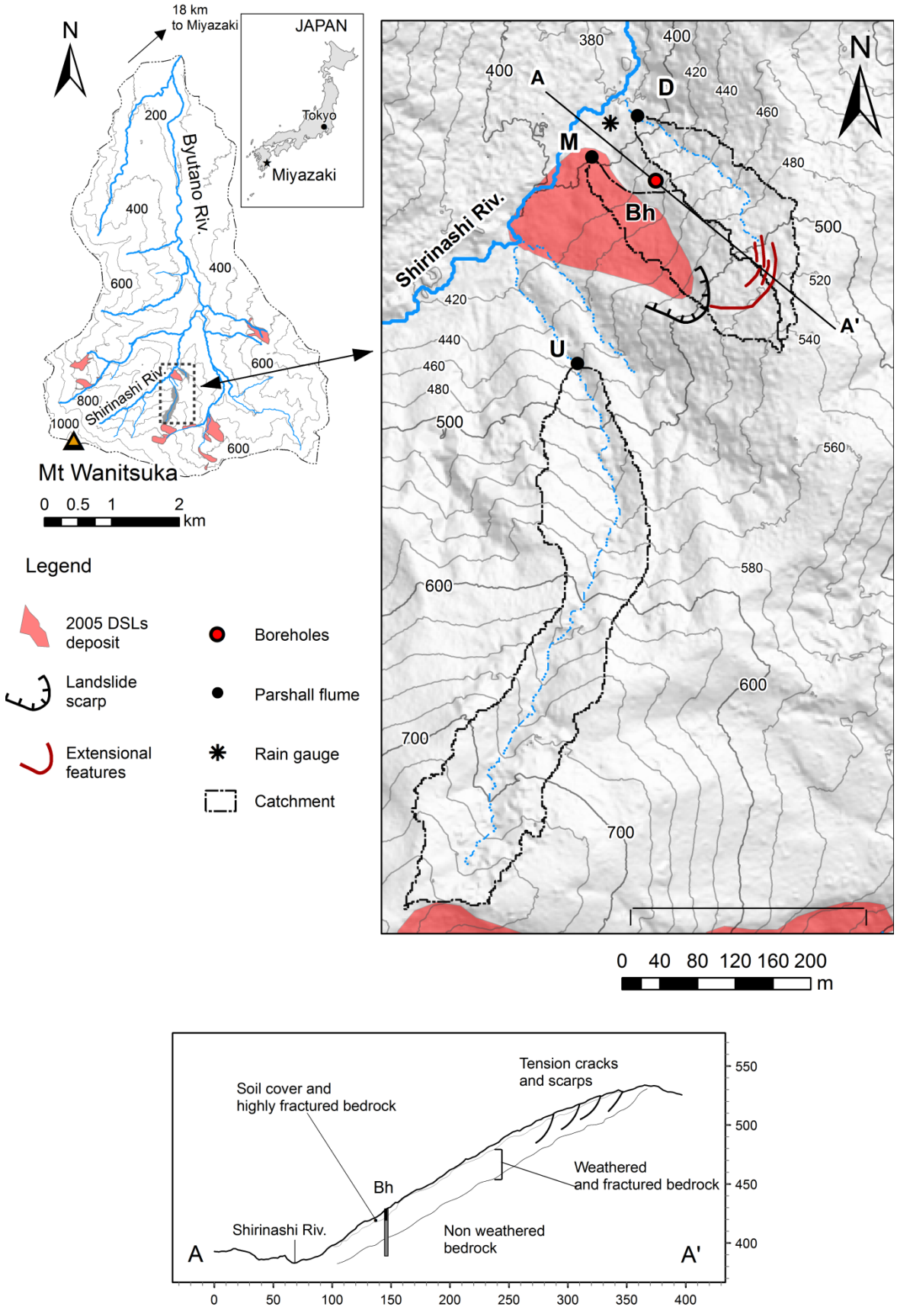

Figure 6. Study area map and instruments location.

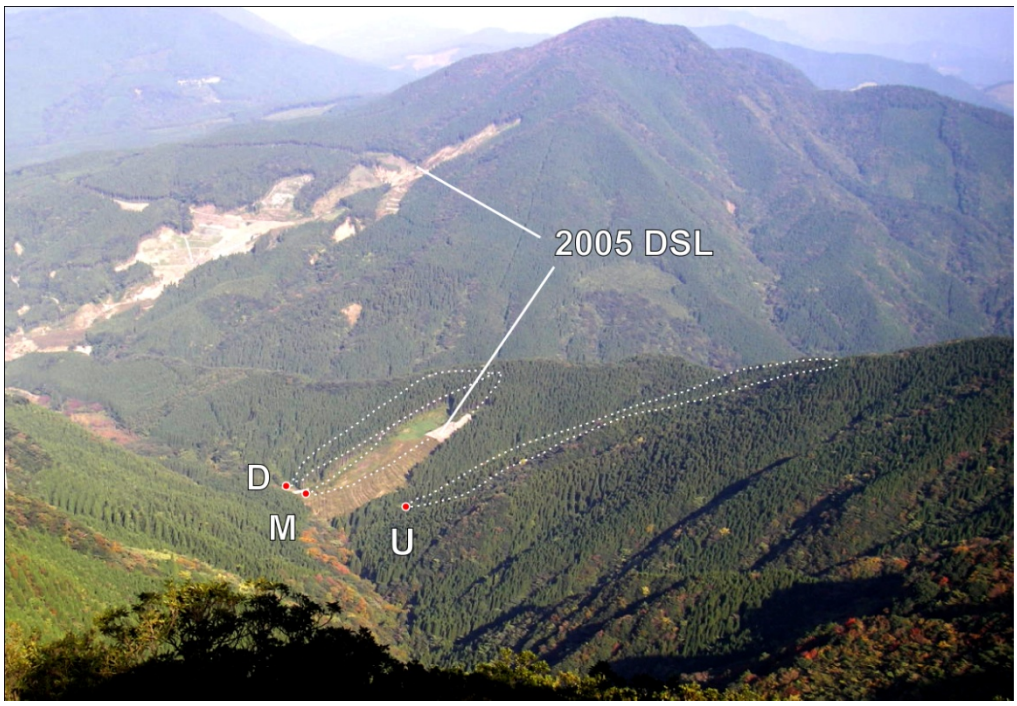

Photo 1. General view of the studied hillslope from the top of Mt. Wanitsuka.

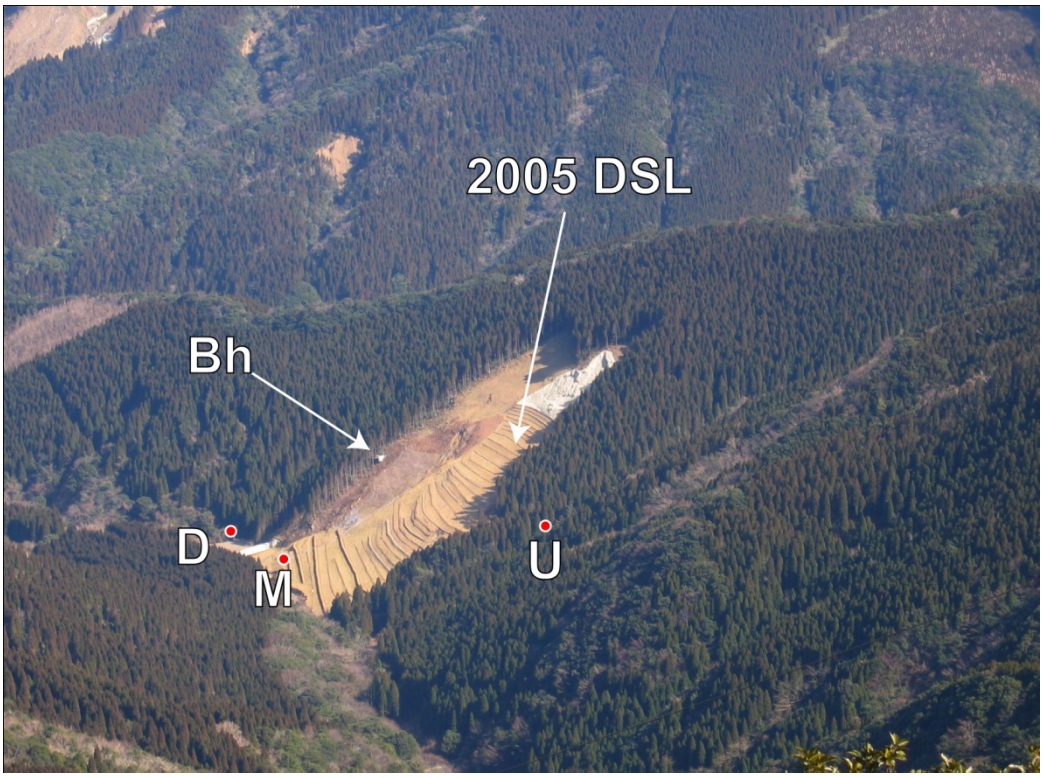

Photo 2. Detailed view of the studied hillslope from the top of Mt. Wanitsuka.

2.2. Geology and geomorphological features of the Study area

According to the Geological Survey of Japan, the area of Mt Wanitsuka is mainly dominated by sedimentary rocks. The bedrock is composed by an alternation of sandstone and shale from the Nichinan Group and the Hyuga Group, part of the Shimanto Terrane complexes (Late Early Oligocene - Early Miocene). In general, the layers show dips between 15° and 40° with a SW dip direction. The thickness of the sandstone layers varies from 5 - 15 cm to 1 – 1.5 m, whereas shale is found in layers from 5 cm up to 1 m. The outcrops in the area showed that the shale layers are highly fractured, forming small sheets of a few centimeters of thickness parallel to the bedding. In general, the sandstone layers are very competent rock with low weathering and fracturing. Mainly the fractures are discontinuous between layers and they are oriented perpendicular to the bedding.

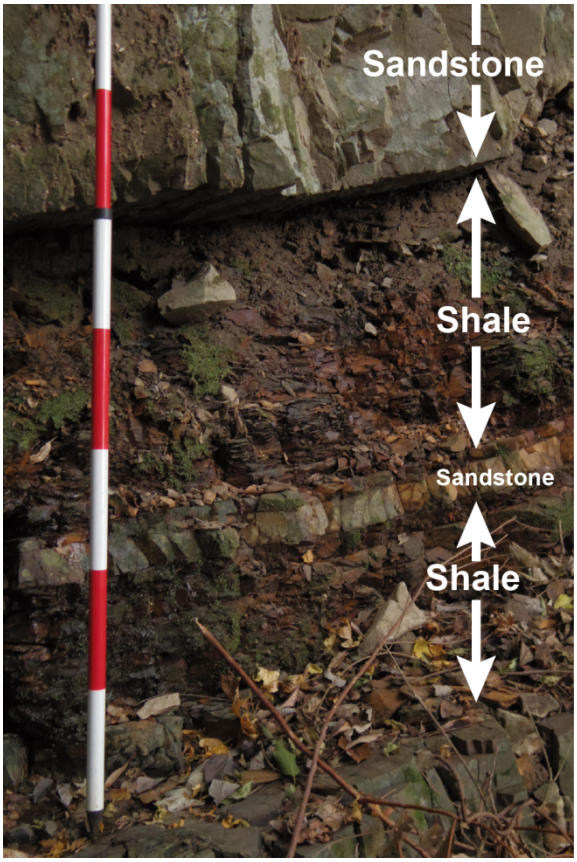

Photo 3. Outcrop showing the fracture characteristics of sandstone and shale beds in the study area.

In the studied hillslope, the construction of a borehole provided more information about specific geological characteristics observed in the hillslope (Figure 7). In the borehole core a soil cover of approximately 2 m depth was observed. This cover is composed by a thin layer of tephra from the eruptions of the volcanic complexes in the near areas. Below this, an unconsolidated sediment deposit until 9.3 m below the ground surface (bgs) covers the fractured bedrock. The presence of isolated rock fragments of approximately 60 cm could indicates that this unconsolidated material correspond to regolith or highly fractured bedrock, mainly sandstone. This highly fractured regolith cover was not clearly observed in surface. Near to the ridge of the hillslope, only fractured bedrock was observed below the soil cover. There, the soil cover does not exceed the 1.5 m of thickness in the rest of the hillslope according to observations in some tension cracks and bedrock outcrops in the area. Additionally, in the foothill an excavation performed for the construction of a slit dam revealed part of the bedrock with a deposit cover that does not exceed 50 cm in depth. Under this regolith, a moderately to highly weathered bedrock is observed in the borehole core from 9.3 to 24 m bgs. For the description of bedrock observed in the core, the rock quality designation index (RQD) is used (Deere, 1964). This index (generally used for engineering purposes) grades the quality of rock mass by the frequency of fractures in a defined unit of length. The index ranges from 0% to 100% for highly fractured to non fractured bedrock respectively. In the highly weathered bedrock zone, the RQD values per meter of the core range from 0% to 20%. In this zone, two clear highly fractured zones were identified from 13 m bgs to 15 m bgs and from 20 m bgs to 24 m bgs. Additionally, the bedrock presents high-degree open fractures (more than 70° from the horizontal), which are mainly observed in the layers from 15 m bgs to 24 m bgs. These fractures are open, unfilled and exhibit low weathering. The maximum length of the fractures is 20 cm approximately. Moreover, rock fragments in the high fractured zone present striated high degree fault plains (Photo 4). The striation indicates normal faults with dominant vertical component movement of the fault walls. The borehole core was not oriented so it inferred that the hanging wall falls to downhill direction.

The presence of this set of vertical fractures and fault zones can be considered evidence of the active deformation in the bedrock at that depth. Below 24 m bgs the bedrock does not shows weathering. The RQD values per meter of core in this section vary from 10% to 69%, and high-degree fractures are not observed.

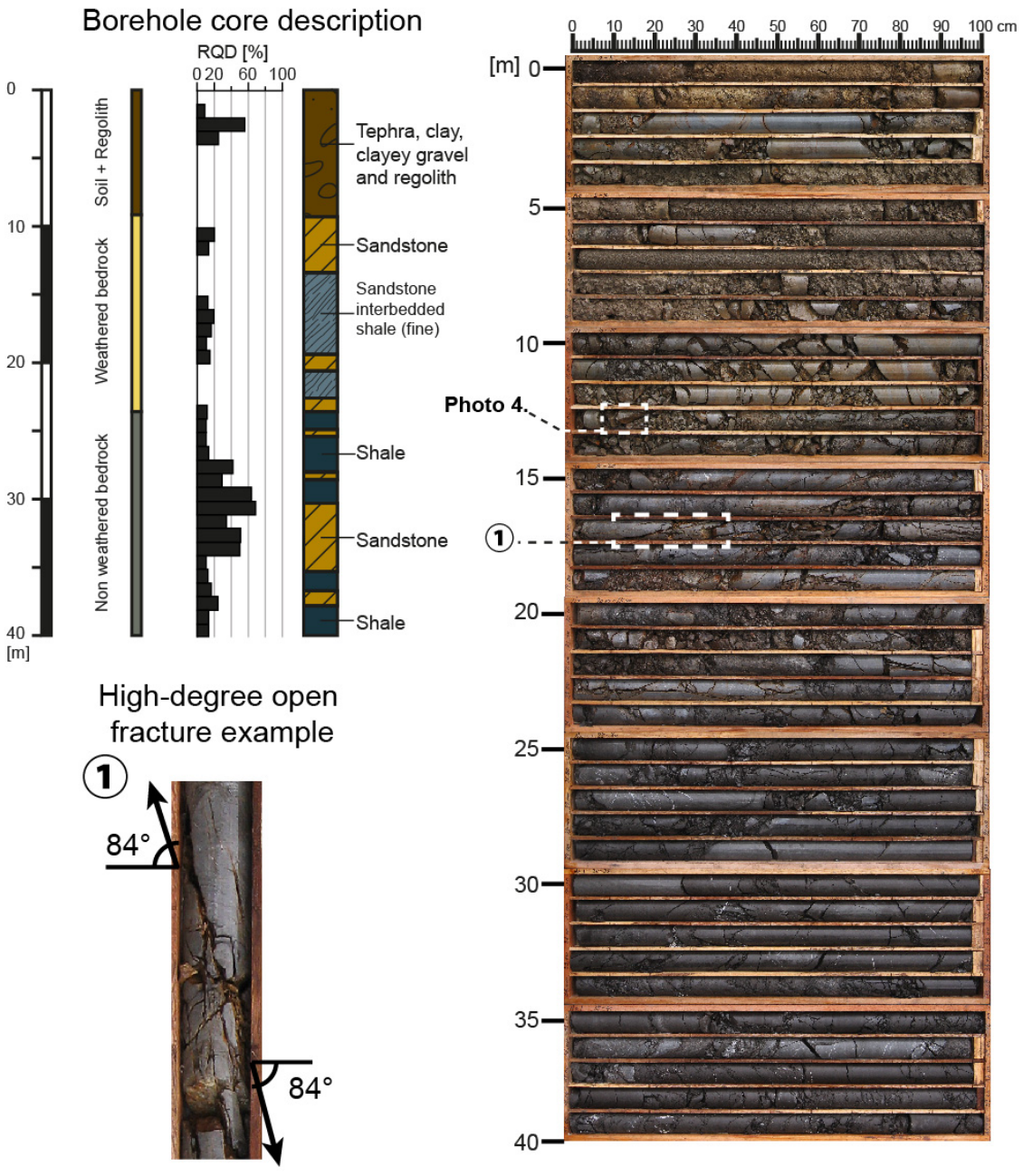

Figure 7. Simple borehole core description and photograph of the core sample.

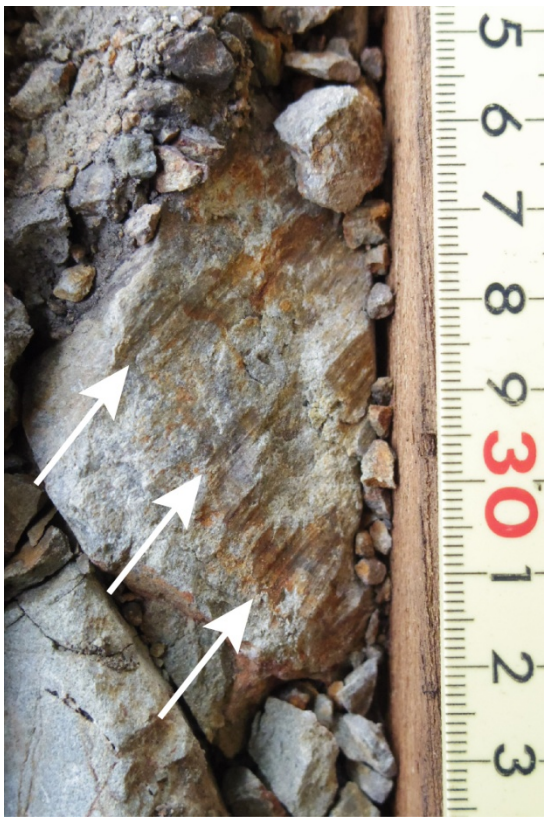

Photo 4. Evidences of faulting in core sample. The arrows show the striation direction.

Observations in outcrops in the basin of Byutano River revealed zones with quartz-calcite veins that cross the bedrock layers (sandstone and shale) (Photo 5). The veins were also observed in the bedrock core (40 m bgs maximum depth). In the weathered area (from 9.3 m bgs to 24 m bgs) most of the veins present high weathering and in some cases the vein filling is partially or completely removed (Photo 6). It is assumed that this high weathering can implies the dissolution and posterior removal of calcite portions of the veins in the weathered zone.

Photo 5. Quartz-calcite veins in outcrop of sandstone.

Photo 6. Quartz-Calcite vein partially removed. The picture shows a rock fragment from the borehole core sample.

In terms of geomorphological features, the studied hillslope presents extensional features near to the ridge (Photo 7). These features correspond to downhill facing scarps and tension cracks. The scarp represents steps of no more than 2 m of depth and it extension seem to be related to the landslide scarp next to this area. The tension cracks do not exceed the 1 m of depth. The rest of the hillslope presents morphology of micro steps that are clearer in the upper section of the hillslope. The appearance of this morphology seems to suggest the existence of sets of normal faults in the hillslope. Normal faulting forming steep-like slope surface has been

described in some models of deep-seated deformation by Chigira and Kiho (1994) (Figure 8). This also could be counted as evidences of deformation in the studied hillslope.

Photo 7. Gravitational deformation scarp near to the ridge in the studied hillslope.

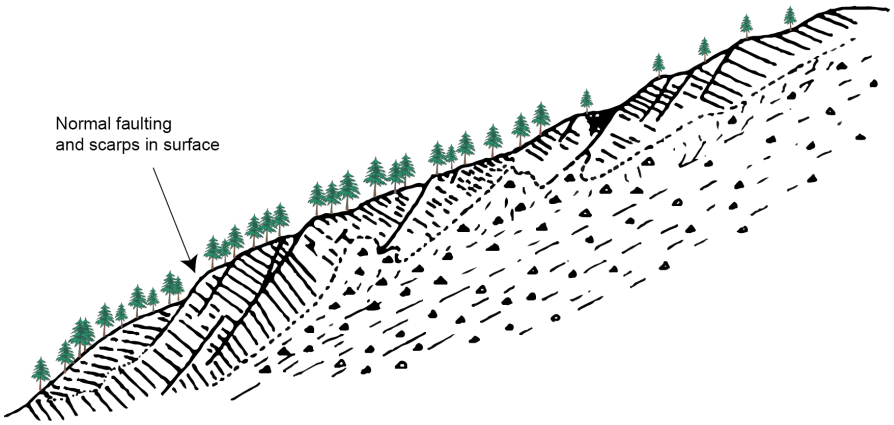

Figure 8. Representation of deep-seated gravitational deformation in Senmaida-Kuzure (Akaishi Mountains, Central Japan). Modified from Chigira and Kiho (1994).

Chapter 3: Methodology

3.1. Field Observations Methodology

To analyze the hydrogeological response of the studied hillslope, the groundwater level, the rainfall in the area and the discharge of nearby catchments were measured and sampled.

3.1.1. Groundwater observations methodology

For groundwater observations, two boreholes of 10 m and 40 m in depth were installed in the studied hillslope at 430 m asl (Photo 8). Both are approximately 1 m separated. The 10 meters depth borehole (Bh10) is screened from 1 to 10 m in order to observe the hydrogeological response of the superficial section of the hillslope. This superficial section corresponds to the soil cover and the unconsolidated material defined as regolith over 9.3 m bgs. The 40 meters depth borehole (Bh40) is screened from 10 to 40 m aimed to observe the groundwater response of the bedrock. From 2008 (June) to 2009 (July), two water-level sensors (Hobo Water Level Logger, Onset Computer Corp., Cape Cod, Massachusetts, USA) were used to measure the groundwater levels in both boreholes. These devices measured the water pressure head every 10 minutes. After 2009, the sensors were replaced by water-level loggers (S&DL water sensor from OYO Corp., Tokyo, Japan) capable of measuring the groundwater pressure head and the electrical conductivity (*EC*) of the groundwater. The water loggers were installed at 10 m and 24.8 m depths in Bh10 and Bh40, respectively, and measurements were taken every 10 min. Due to the dimensions of the new water logger in Bh10 and the location of the water level sensor in the device, it was not possible to measure water levels deeper than 9.55 m bgs.

Photo 8. Boreholes location (Bh point in map of Figure 6).

From 2010 a system of water samplers were installed in both boreholes. The samplers collect the groundwater samples when the groundwater level rises (Response samples). In Bh10, 17 5-ml bottles attached to the logger and logger cable were installed every 6 cm between 9 m and 10 m bgs. In Bh40, 15 10-ml bottles were installed every 1 m between 7 m and 20 m bgs (Photo 9). From 2011, additional sample bottles were added in Bh40. This new samples were spaced in 10 cm and installed between 14 m bgs to 16 m bgs. The water sampler bottles in Bh40 were equipped with a sealing system, wherein a floating ball seals the bottle when it is filled with water (Figure 9). Thus, the samples from Bh40 were collected as the groundwater level increased. This sealing system was not installed in the Bh10 water sampler bottles. Additionally, samples were collected from the boreholes (Base level samples) using a bailer every 2 months.

Photo 9. Sampler installed in the 40 m depth borehole (Bh40).

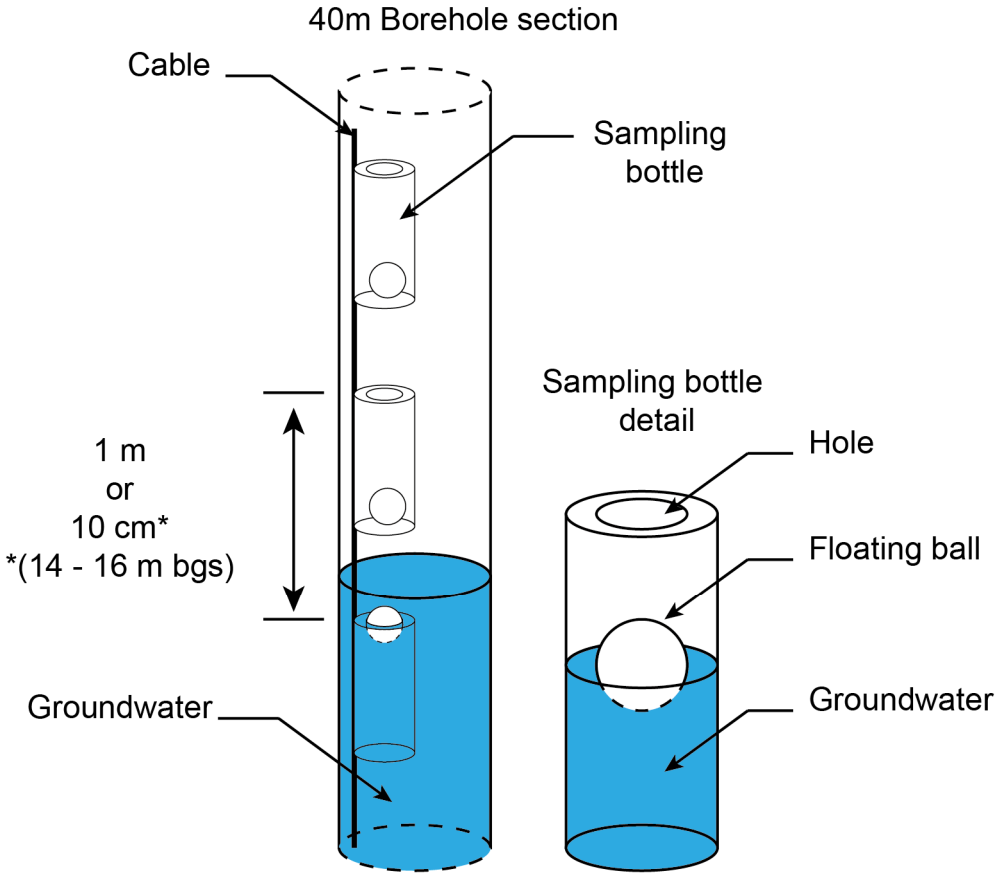

Figure 9. Details of groundwater bottle sampler installed in the borehole Bh40.

All samples collected were analyzed to measure the *EC* values and the isotopic compositions ($\delta^{18}O$ and deuterium, δD). The *EC* values of the samples were measured using a manual conductivity meter (HORIBA Twin compact meter, Kyoto, Japan). The isotopic compositions were measured using a Picarro L1102-I isotopic liquid water and water vapor

analyzer (wavelength-scanned cavity ring-down spectroscopy, WS-CRDS). Additionally, the concentration of major cations (Ca^{+2}, Mg^{+2}, K^{+2}, Na^{+2}) and silica was analyzed by optical emission spectrometry, ICP (Perkin Elmer Optima 7300DV).

3.1.2. Catchment observations methodology

In order to understand the role of bedrock groundwater in the hydrological response of hillslopes, the discharge of three catchments, D, M and U were observed. The catchments are located in the vicinities of the studied hillslopes. The boundaries of catchment D and M share the superficial runoff of the studied hillslope. The characteristics of each catchment are presented in Table 1.

Table 1. Catchment characteristics, periods of observations and size of parshall flume installed.

Catchments	Area	Length	Highest point	Period of observation	Parshall flume size
	[ha]	[m]	[m asl]		[inch]
D	1.44	352	520	2010-2012	6”
M	1.51	120	52	2010	6”
U	5.42	850	770	2010-2012	9”

Catchment M is partially over the deposit of DSL of 2005. In this area the catchment runoff is canalized in order to prevent the interference of the slope stabilization works in the DSL deposit (Photo 10).

The discharge of the three catchments was measured by Parshall flumes (Photo 11, Photo 12). The water level in the discharge was measured by 50 cm TruTrack data logger (WT-HR500) installed in the Parshall flumes. The equations to transform the water levels into discharge (m^3/s) are showed in Table 2.

Table 2. Parshall flume equations.

Parshall flume Size [inch]	Equation: Water level in sensor (H) – Discharge (Q)
6”	$Q\ [\frac{m^3}{s}] = 0.3812 \cdot (\frac{H[mm]}{1000})^{1.58}$
9”	$Q[\frac{m^3}{s}] = 0.5354 \cdot (\frac{H[mm]}{1000})^{1.53}$

The collection of samples was carried out manually during fieldwork activities (every 2 month). These samples correspond to base level samples. Additionally samples of the discharge during rainfall events (event samples) were collected by automatic samplers (Sigma 900 Standard Portable Sampler, HACH) located upstream of the Parshall flume (Photo 13). These samples were collected every 2 hour or 3 hours. The start of the automatic sampling was also given manually or by a floating level trigger installed in the Parshall flumes. The water samples obtained were chemically analyzed following the same procedure to groundwater samples.

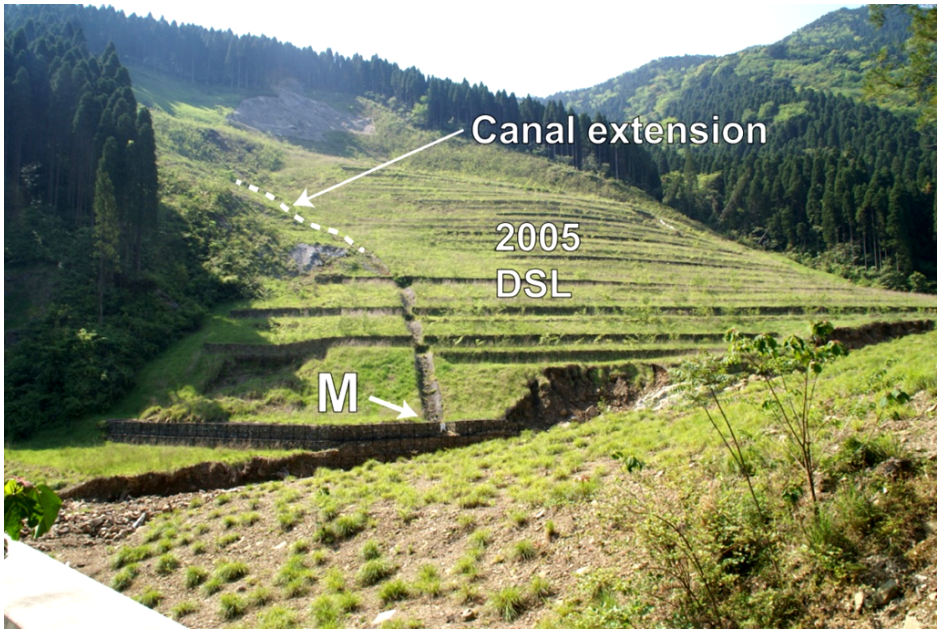

Photo 10. Details of catchment M definition. Dashed line indicates the complete extension of the canal of the catchment M stream.

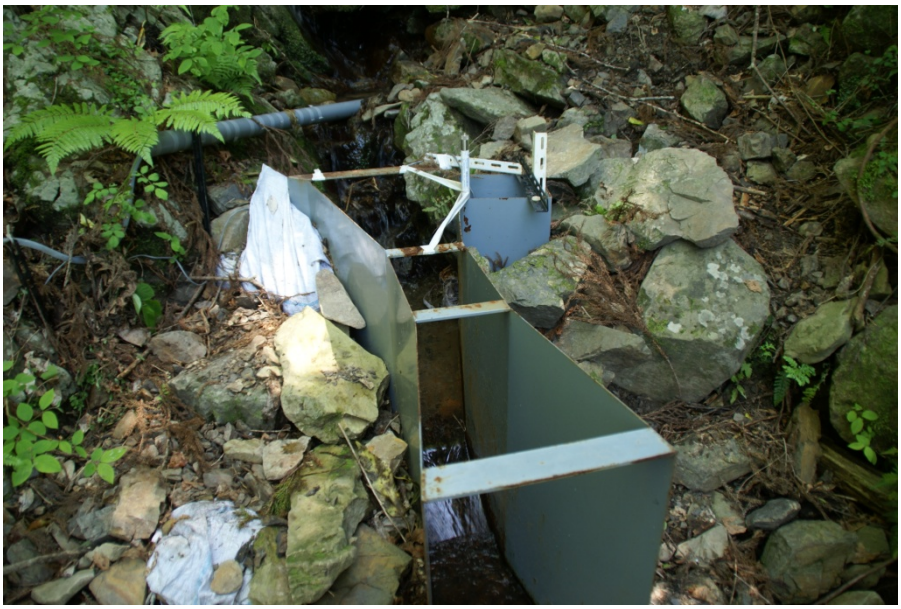

Photo 11. Parshall Flume in catchment D.

Photo 12. Parshall flume in catchment U.

Photo 13. Sigma Water Sampler.

3.1.3. Rainfall observations methodology

The measurement of rainfall was carried out by a tipping bucket gauge located in the foothill of the hillslope analyzed (Photo 14). The bucket size is 0.2mm and the data was collected in mm/10min from 2008 until 2012. Also, the precipitation data (mm/10min) from the pluviometric station of Mt. Wanitsuka, Tano and Ote was used in order to compare with our measurement. These stations are administrated by the local government agencies of Miyazaki Prefecture.

Photo 14. Open tipping bucket rainfall gauge.

The rainfall water was sampled as a bulk using a water tank of 18 litters (Photo 15). The accumulation period of the bulk sample was 2 month. However, during the rainfall season of 2010 (24th June to 16th July) bulk samples after individual rainfall events were collected.

Photo 15. Rainfall Bulk Sample collector.

3.2. Theoretical methodology

3.2.1. Antecedent Precipitation Index API

To characterize the different precipitation events, the antecedent precipitation index (API), or Effective rainfall (as defined by Yano (1990)), was used. This index permits the estimation of the water content in a mass of soil as function of the antecedent rainfall, which decays with time according to a defined half-life (Hong et al., 2005; Kosugi et al., 2008; Matsuura et al., 2003; Moriike et al., 2009; Uchida et al., 2004). This index, which is based on the application of a linear succession of tank models (Sugawara et al., 1984) has been commonly used to define precipitation conditions that generate shallow landslides or debris flows.

The expression of the API index is:

$$API_T = r_t + \sum_{n=1}^{x} \left(\frac{1}{2}\right)^{\frac{n}{T}} \cdot r_{t-n}$$

Where API_T, the antecedent precipitation index for a half-life of T (in hours), is equal to the precipitation at time t (r_t) plus an expression that represents the antecedent rainfall decay. In this study, the calculation of API was based on the precipitation record unit of mm 10 min-1.

Although this index is used to interpret the water contents in soil masses, it has also been used to estimate water conditions in rocks to approximate the runoff from catchments (Moriike et al., 2009). In this study, the API index was used to estimate antecedent rainfall periods that can determine the hillslope responses.

3.2.2. Triple hydrograph separation – End Member Mixing Analysis (EMMA)

In order to estimate the possible contribution of groundwater in the discharge of the catchment observed, a triple hydrograph separation was carried out using an End Member Mixing Analysis (EMMA). The triple hydrograph separation is based on simple mass balance equations (Dewalle et al., 1988; Hooper et al., 1990):

$$Q_1 + Q_2 + Q_3 = Q$$

$$A_1Q_1 + A_2Q_2 + A_3Q_3 = AQ$$

$$B_1Q_1 + B_2Q_2 + B_3Q_3 = BQ$$

Where Q represents the total discharge of the catchment. A and B represent the concentration of the tracer selected. The sub-index numbers 1, 2, 3 permits to differentiate the discharge and concentration of tracers of the three end members selected.

Chapter 4: Results - Groundwater observations.

4.1. Groundwater Hydrograph observations

The groundwater levels in the observations boreholes show the significant differences in the responses of the soil and regolith cover of the hillslopes and the response of the bedrock groundwater (Figure 10, detailed graphs in Appendix I). General information about the annual precipitation and groundwater levels is provided in Table 3. The groundwater level in Bh40 is more variable than the levels in Bh10. The groundwater level of Bh10 ranges from 9.9 m bgs and 9.2 m bgs, whereas the corresponding Bh40 varies from 20 m and 11.5 m bgs. For Bh40, the base level is usually between 16 m and 17 m bgs, but during the dry season in winter, the groundwater level continuously decreases, reaching very low levels near to 20 m bgs, as observed during the winter season of 2011. This variation implies that the aquifer represented by Bh40 was constantly discharging water and did not achieve a stable base level. In contrast Bh10 presented a stable base level of 9.85 m bgs, observed in the data from 2008 and 2009. In the other hand, a very particular characteristic of groundwater in Bh40 is the maximum level of approximately 11.5 m bgs. This level was never exceeded during the observed period and it is not observed in the responses of Bh10.

Table 3. Rainfall characteristics by year and number of maximum peaks in Bh40. (*) data from June until December.

	Total annual rainfall	**Daily maximum**	**Hourly maximum**	**Maximum groundwater level**		**Number of maximum peaks in Bh40**
				Bh10	Bh40	
	[mm/year]	[mm/day]	[mm/h]	[m bgs]	[m bgs]	[ ]
2008*	3146.4	532.8	73.2	9.23	11.49	3
2009	3337.2	214.4	35.6	9.44	11.59	2
2010	4360.6	194.2	56.4	9.31	11.54	5
2011	5411.6	382	62	9.31	11.54	8

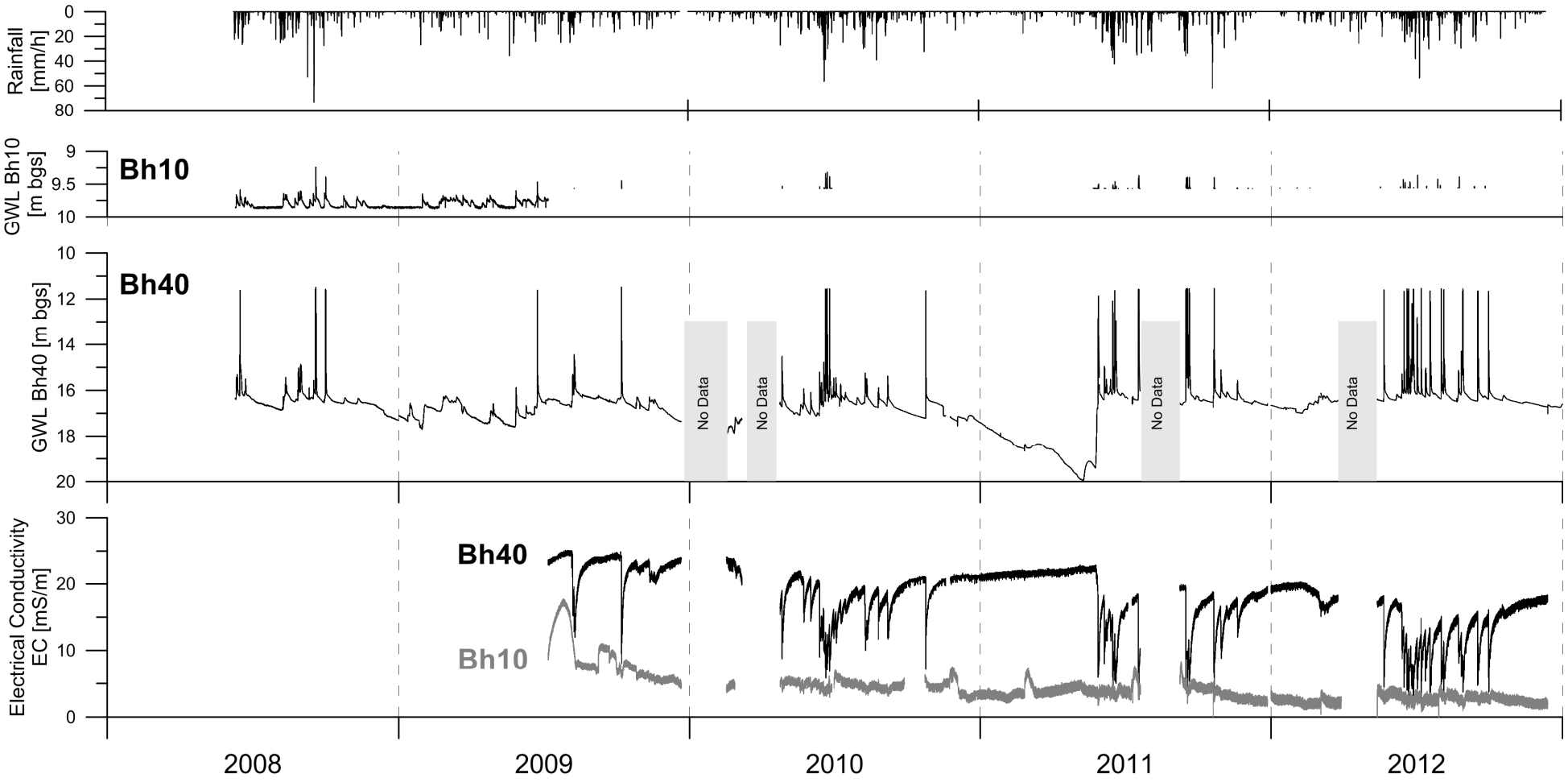

Figure 10. Rainfall and groundwater observation in Bh10 and Bh40.

The differences in the response of groundwater level between the two boreholes are also observed in the changes of EC values. Bh40 presents variation approximately from 5 mS/m to 20 mS/m in the peaks and base level respectively. During the peaks the values of EC in Bh40 are similar to the values in Bh10. Bh10 does not show significant changes in EC values as the observed in Bh40.

Observing in details the response of groundwater, both boreholes present a particular fast response to rainfalls. The responses are more significant in Bh40 where in general it is observed a fast rise and fall of the level until reach the base level. These rapid changes in the groundwater levels are partially followed by EC values which present a fast decrease of values but not so fast recovering to the base level values. In terms of the response, in particular the recession curve, it is possible to identify two zones of response of the bedrock groundwater. The first zone is represented by fast rise and fall of levels which is depth it is observed from 11.5 m bgs to 16.2 m bgs approximately. The second zone is located below 16.2 m bgs and it represented by a fast rise of levels but in contrast, the recession curve correspond to the slow recession of the base level. The first zone as been labeled as Primary response zone (PR) where the more significant responses are observed and the second zone correspond to the Secondary response zone (SR).

In order to model these two zones of responses, the hydrographs of Bh40 was compared with the antecedent precipitation index (API) for different half-lives, from 6 hours to 20 days (Figure 11). Due to the relatively high-degree limbs of PRs, these responses can be associated with API values with half-lives equal to or less than 12 hours. The SRs seems to be more correlated to the API value with half-lives in days (3 to 10 days half-life). These correlations define two terms of the hillslope response to the main rainfall events: short term (*PR*) and long term (*SR*). The analysis will be focused on PR, as PR demonstrates highly dynamic groundwater levels and is the main response of the hillslope to rainfall events.

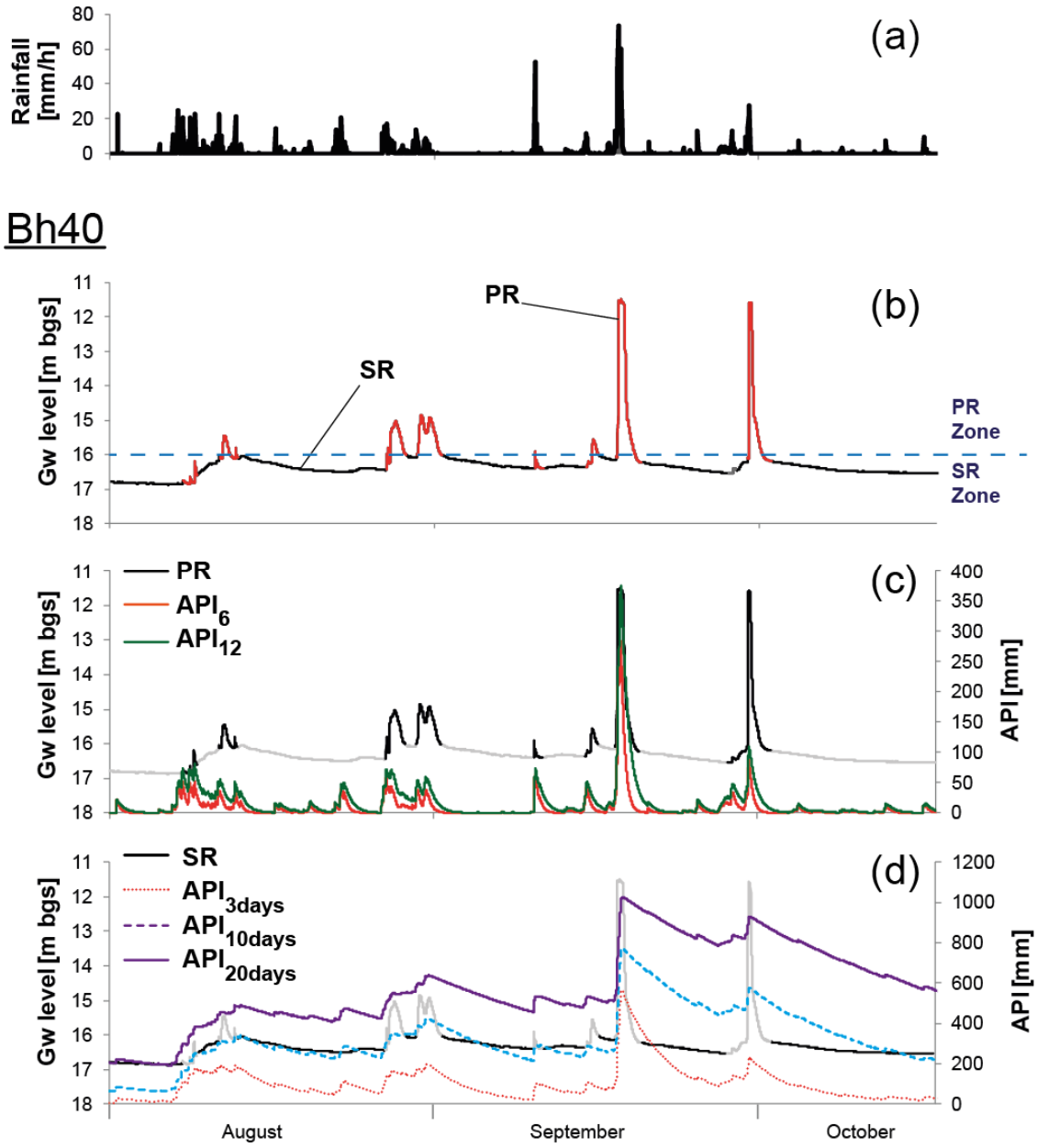

Figure 11. Correlation of PR and SR zone responses in Bh40 and API for different half-life periods. (a) Rainfall data. (b) bedrock groundwater levels and definition of responses. (c) PR responses and API correlation. (d) SR responses and API correlation.

Correlating these two types of response with what it is observed in the borehole core of Bh40 it is identified particular characteristics of the fracture system and the type of response (Figure 12). The PR zone is mainly observed in a zone where the bedrock present high fracturing (RQD = 0 %). The SR zone is located in depth with more competent bedrock dominated by vertical fractures with low frequency of lower angled fractures. The low frequency of low angled fractures can imply a lower horizontal hydraulic conductivity of groundwater. This characteristic can explain the fast rise of the levels but the slow recession. The maximum level also presents a particular distribution of fractures in bedrock. Between 10 to 12 m bgs the bedrock becomes again more competent but in this case the fractures system is dominated by low degree or horizontal fractures. These horizontal fractures could be responsible of the maximum level allowing fast horizontal flows.

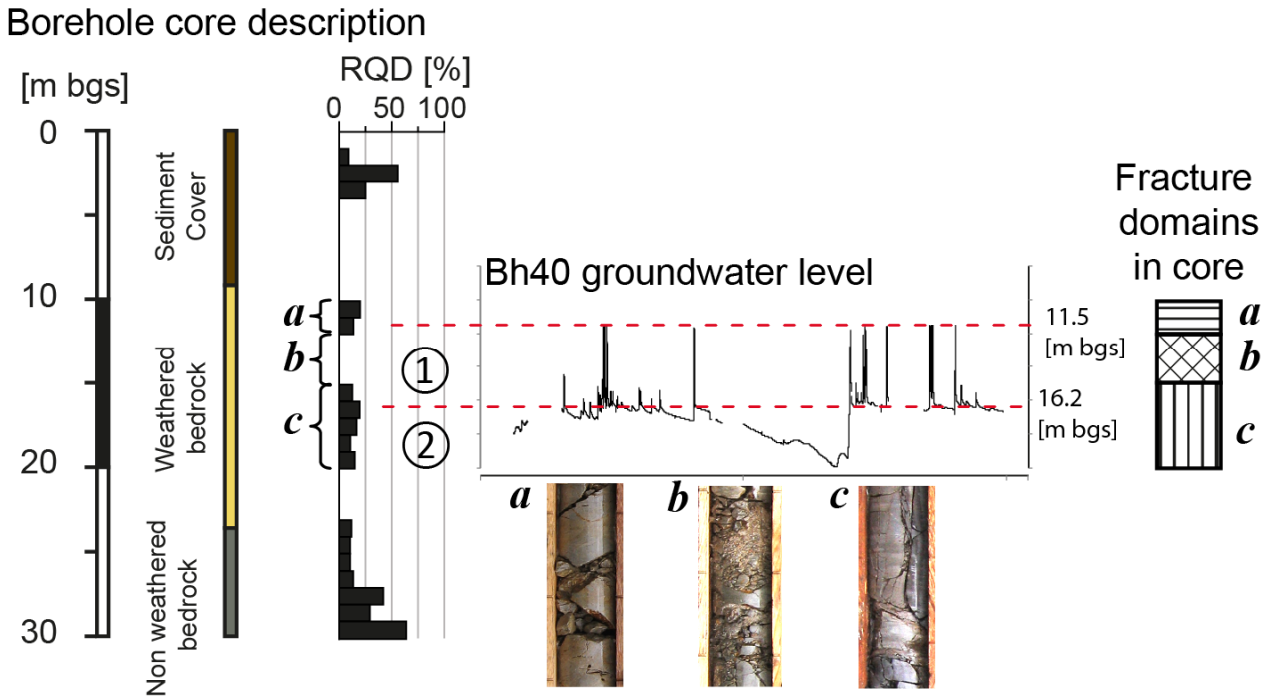

Figure 12. Characteristics of bedrock observed in the borehole core and the bedrock groundwater response associated. ①: PR zone; ②SR zone. Domains of fractures: (*a*) Horizontal or low degree angled fractures; (*b*) highly fractures bedrock; (*c*) Vertical or high degree fracture domain.

In order to identify the characteristics of the rainfall that generates this maximum level in the bedrock groundwater, observed in Bh40, the correlation between peaks or groundwater and API values at the time of the peak was analyzed (Figure 13). According to the previous analysis of PR and API, half-lives of 12 hours or less were selected. In the correlation the maximum level at 11.5 m bgs approximately is clearly observed.

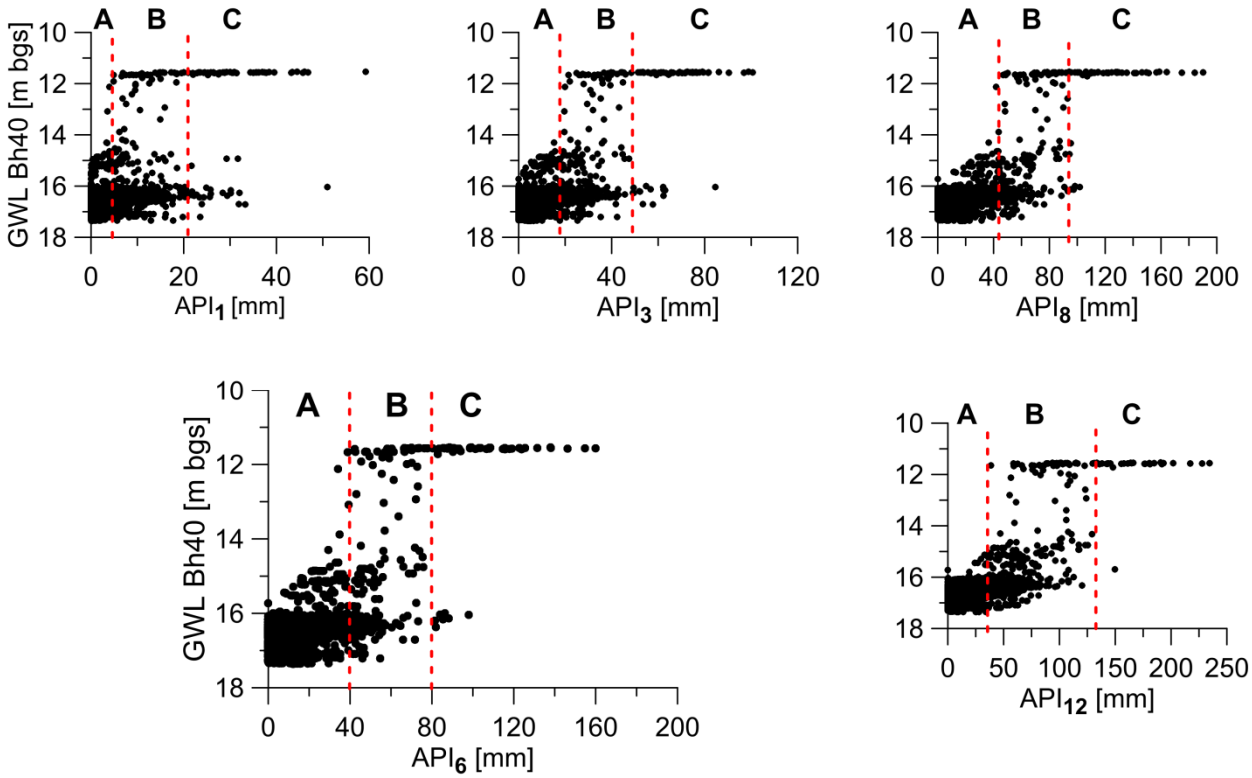

Figure 13. Correlation between peaks of Bedrock groundwater (Bh40) and API with a, 3, 6, 8, and 12 hours half-life. A: Zone of lower peaks (Lp). B: Transition zone (Lp and Hp). C: Zone of maximum peaks (Hp).

The criterion to determine the best correlation corresponds to select the API index that permit to define a triggering rainfall of the maximum peaks. In Figure 13 this criterion can be explained by selecting the API index with narrower B zone and with few peaks (black dots) inside. For all the API correlations, a boundary between maximum peaks and lower peaks was not clearly determined, however the best results were obtained with API_6 (a 6-hour half-life). Peaks with API_6 values below 40 mm were observed deeper than 14 m bgs. Between 40 mm and 80 mm it is defined a transition zone where the maximum peaks start to appear in Bh40 but still it is possible to observe lower peaks. For API_6 values greater than 80 mm, the maximum peaks

dominate the responses in Bh40. Only few lower peaks are observed with API_6 values over 80 mm and are related to particular intense rainfall events with very short duration.

4.1.1. Details in bedrock groundwater response.

The correlation of peaks of bedrock groundwater in Bh40 and the API permit partially separate the maximum peaks with the rest of the lower peaks. With this it is possible to define two types of peaks, maximum peaks (Hp) and lower peaks (Lp). Observing in details these two types of peaks, it is possible to identify clear differences in the shape of peaks. In one side, the lower peaks, Lp, are characterized by a double peak for s single rainfall pulse whereas Hp peaks are associated to a single peak as a repose to rainfalls. The characteristics of each type of peak are described as follows.

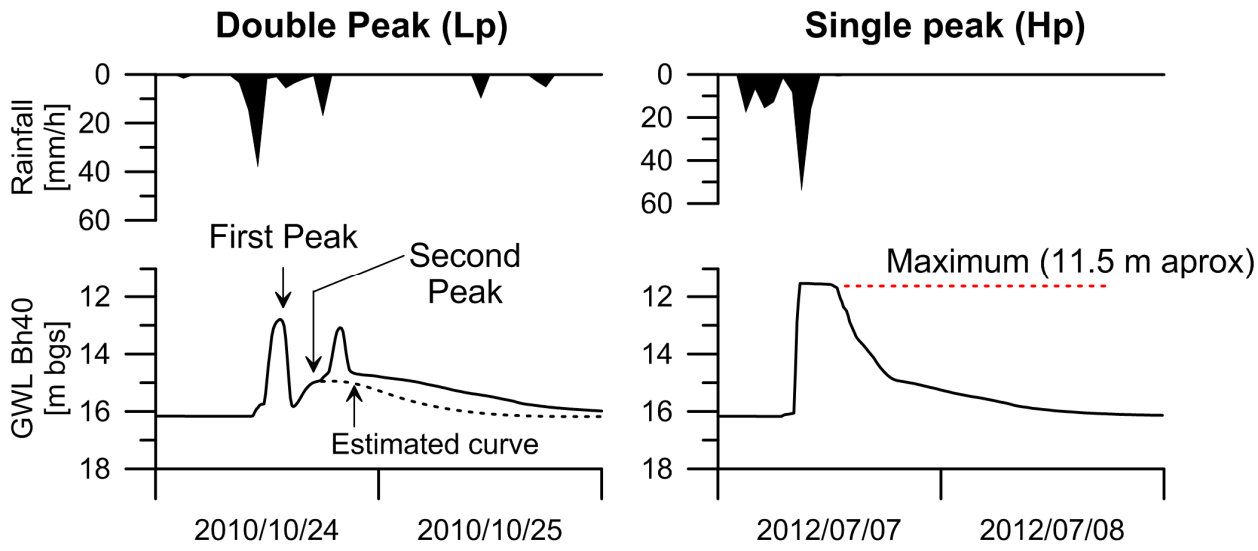

Figure 14. Type of responses observed in bedrock groundwater (Bh40). Double peak (Lp) figure, the second peak is defined by estimated curve due to the superposition of a later rainfall event. Single peak (Hp) presents maximum peak at 11.5 m approximately.

4.1.1.1. Lp peaks: Double peak responses.

The Lp peaks are compounded by two peaks with different characteristics each other. These characteristics are clearly observed for single pulse of rainfall. Successive pulses of rainfall could hide and overlap the different peaks in the groundwater response as it is shown in Figure 15.

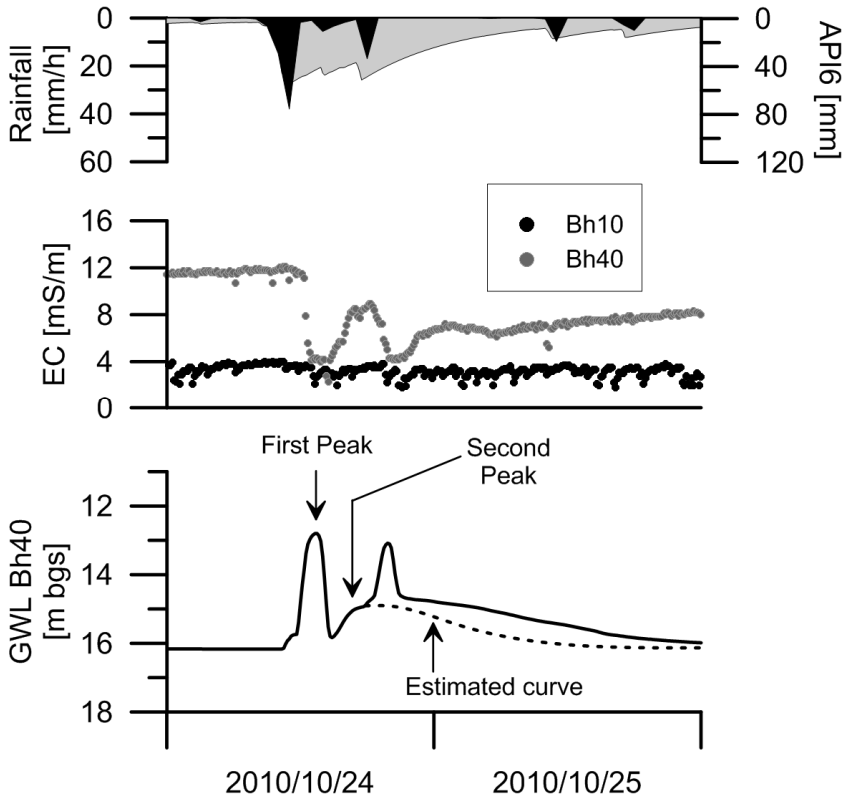

Figure 15. Double peak in bedrock groundwater (Bh40) and EC values during the response.

The first peak corresponds to peak that commonly presents fast rise of the levels and also fast recession curve. This first peak is related to the peak of rainfalls and presents high variability in its levels, ranging from the base level until the maximum level of 11.5 m bgs. The second peak, clearly different to the first, is round in shape with relatively slower rise of the levels and very low degree recession curve. This second peak corresponds to the main response of the groundwater for rainfall events with API_6 below 40 mm. This peak is commonly observed below 15 m bgs and very few cases exceeded this value.

The lag time between the first and second peak decreases as the first peak increases it height. The lag time ranges from 25 hours to 1 hour, however most of the cases the lag time never exceeded the 15 hours (Figure 16).

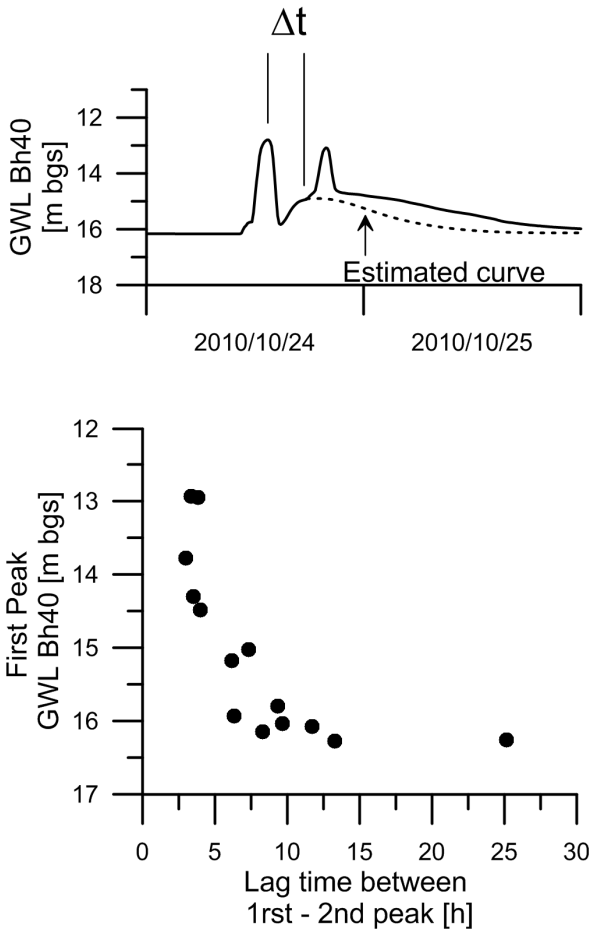

Figure 16. Lag time between first peak and second peak in double peak responses (Lp) and correlation with the first peak level.

4.1.1.2. Hp peaks: single peak responses.

For higher rainfall events the responses of groundwater in bedrock present a single peak (Figure 17). This single peak shows a very steep rising limb that drastically stops until reach the maximum area, near to 11.5 m bgs. After reach this maximum, the groundwater level shows small variations of the levels in centimeters that represent the different peaks of rainfall observed during this conditions. Two to three hours after the rainfall decrease below 5 mm/h approximately, the groundwater levels start to descend or fall from the maximum level. The recession curve is characterized by three clear segments or slopes. This pattern is observed in the same proportion every time when the maximum is reached, independently the antecedent precipitations. The segments are observed from 11.5 m bgs to 13.5 m bgs (first segment), 13.5 m bgs to 15 m bgs (second segment) and 15 m bgs to 16.2 m bgs (third segment). The third segments end when the levels falls into de base level (SR zone).

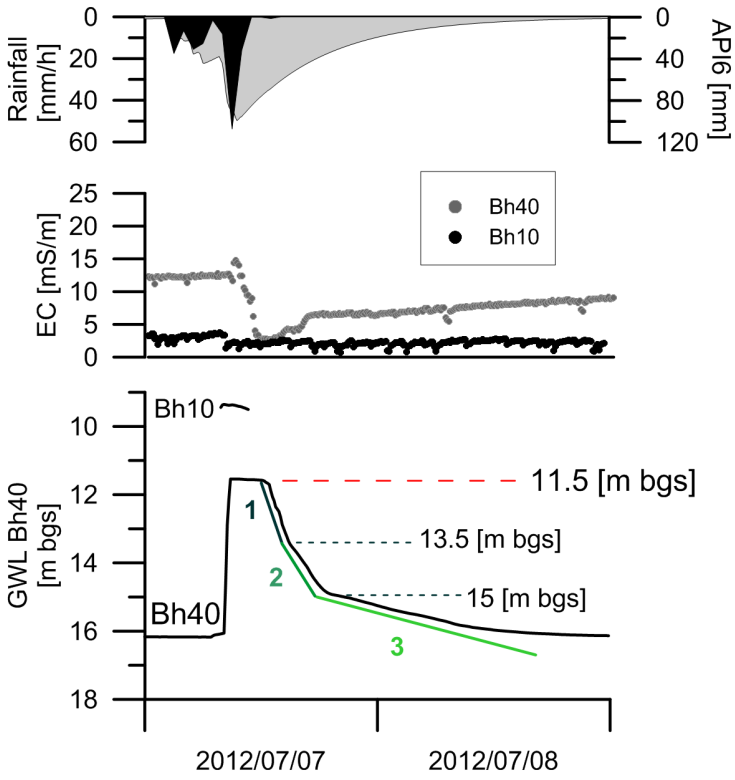

Figure 17. Single peak in bedrock groundwater (Bh40) and EC values during the response. The green lines indicates the three segment of the recession curve.

During the maximum level, small peaks of few centimeters are observed in bedrock groundwater (Bh40). These small peaks present a much reduced lag time between the peaks of rainfall (characterized by API_6) compared with the first peak in double peak (Figure 18). In the maximum peaks (Hp), the lag time is generally less than 1 hour and decrease for higher peaks. For the first peak in double peak responses (Lp) the lag time is generally more than 1.5 hours and increase for higher peaks. The lag time in Bh10 decrease for higher peaks and it has similar values to the maximum peaks in Bh40. Although, in most of the cases the peaks during the maximum in Bh40 tends to be few minutes earlier than the peaks in Bh10.

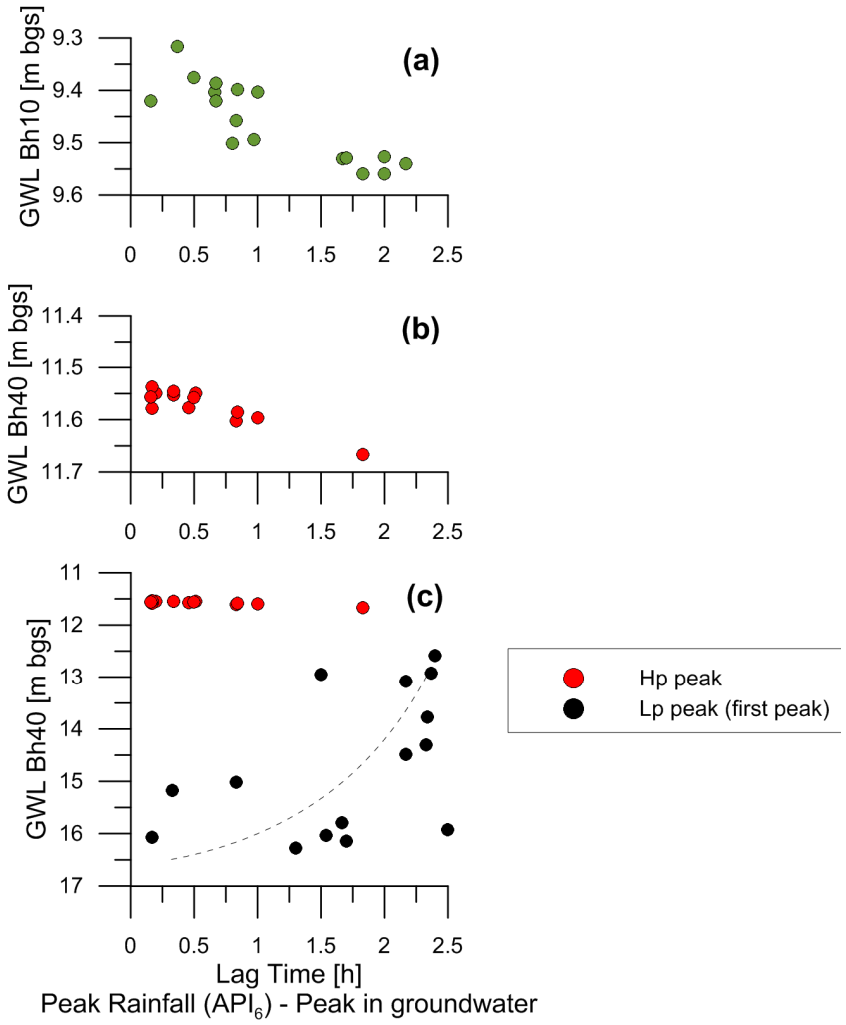

Figure 18. Lag time peak of rainfall (API_6) and peak of groundwater levels. (a) Correlation in Bh10. (b) Detail of the correlation during the maximum level in Bh40. (c) Correlation in Bh40; Black Dots: first peak in double peak responses (Lp). Red dots: Small peaks during the maximum level in Bh40 (Hp).

4.2. Groundwater electrical conductivity (*EC*)

The *EC* values in the groundwater were measured in both boreholes, Bh10 and Bh40, every 10 min as same as the water levels. To correlate the variation of *EC* and the groundwater levels, the electrical conductivity is presented in reverse order, with 0 mS m^{-1} *EC* located at the top of the charts. The *EC* values are between 2.5 mS m^{-1} and 22 mS m^{-1} in Bh40 and between 2.5 mS m^{-1} and 7 mS m^{-1} in Bh10. The values above 7 mS m^{-1} observed in Bh10 are attributed to errors induced during the collection of samples.

The *EC* values in Bh40 exhibit higher variability than those in Bh10 (Figure 10). Moreover, as observed in the detailed hydrograph analysis, the *LP* and *HP* peaks show different shapes with regard to the *EC* values. The Lp peaks present the same double-peak pattern in *EC* as in the groundwater hydrograph with steep limbs in the first peak and a smooth and wider second peak (Figure 19). The double peaks in EC have a delay with the peaks in groundwater levels. This delay is greater for the second peak than the first peak.

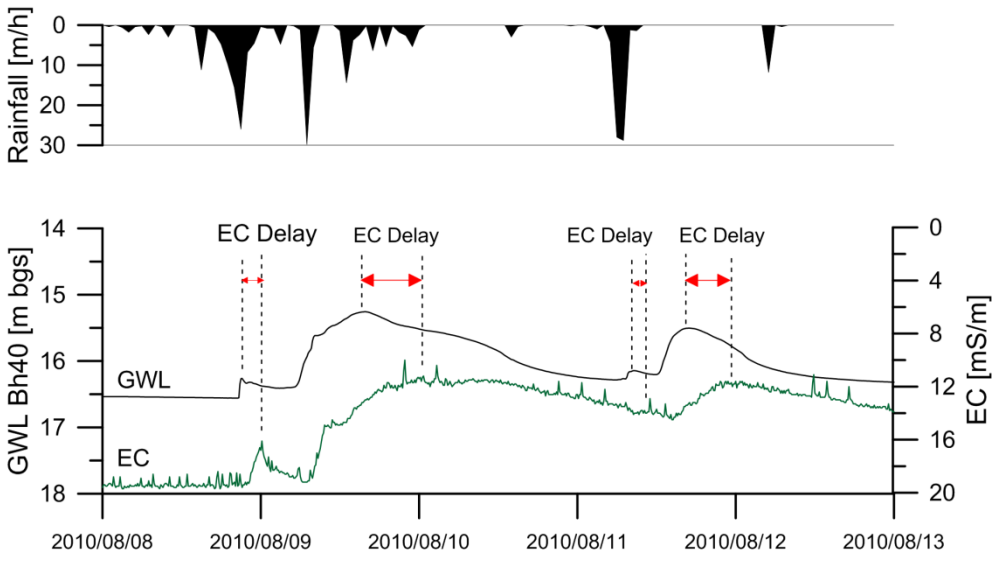

Figure 19. Double peak in groundwater levels (black line) and EC values (green line) in Bh40. Second peak of Bh40 has greater delay of peak of EC values than the first peak. The EC values are showed with the 0 value in the top for better comparison with peaks of groundwater.

For Hp peaks, the rapid rise in the groundwater levels is also observed in the *EC* values. However, during the rising of the maximum peaks a delay in the change of EC values is observed (Figure 20). The delay is not clearly observed for the first peak of Lp peaks. This indicates different characteristics of the groundwater that generates the different peaks.

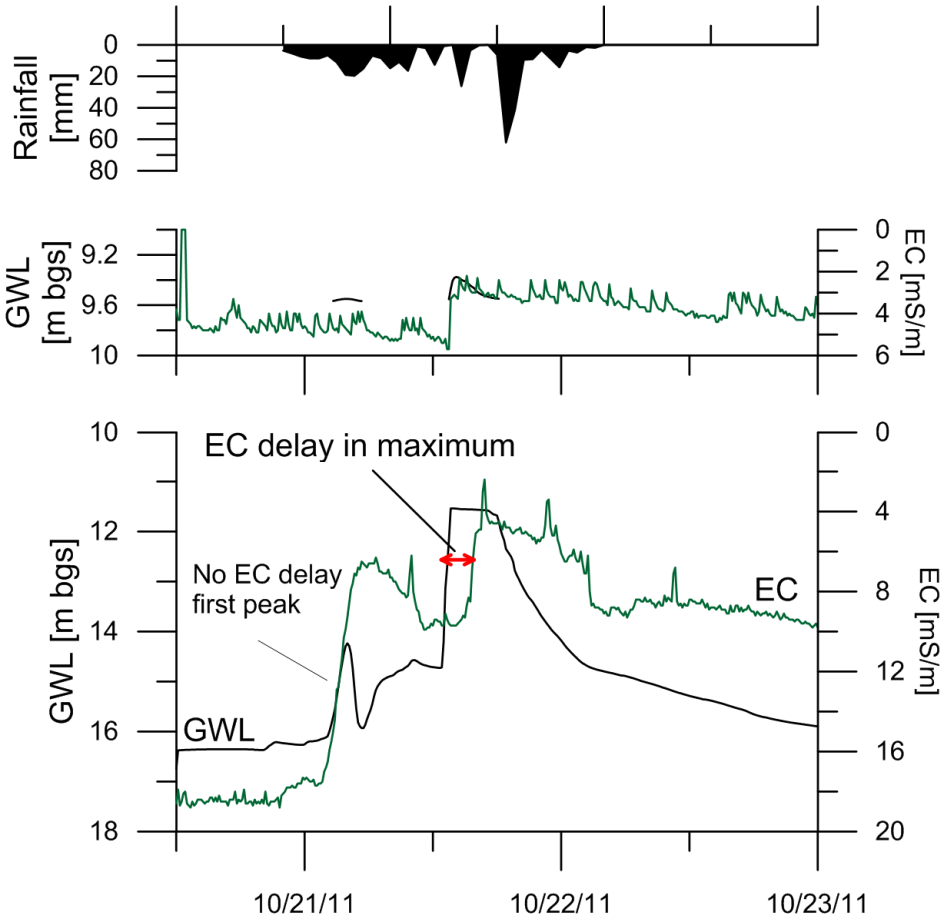

Figure 20. Example of delay in EC values (green line) at the initial maximum level (Hp). Compared with a fist peak (Lp) with no delay in EC. The EC values are showed with the 0 value in the top for better comparison with peaks of groundwater.

The correlation in both boreholes between the groundwater peak levels and the *EC* values at the peaks shows that the *EC* values in Bh40 decrease as the peak levels increase until the peak levels reach the maximum defined by the Hp peaks (Figure 21). For Bh10, it is not possible to define a similar relationship, and most of the values are concentrated from 2.6 mS m^{-1} to 5.5 mS m^{-1}, which is narrower than the corresponding range for Bh40. At the Bh40 maximum (Hp peaks), the *EC* values do not necessarily follow the increasing trend of the lower peaks, and the values vary from 2.6 mS m^{-1} to 11.5 mS m^{-1}.

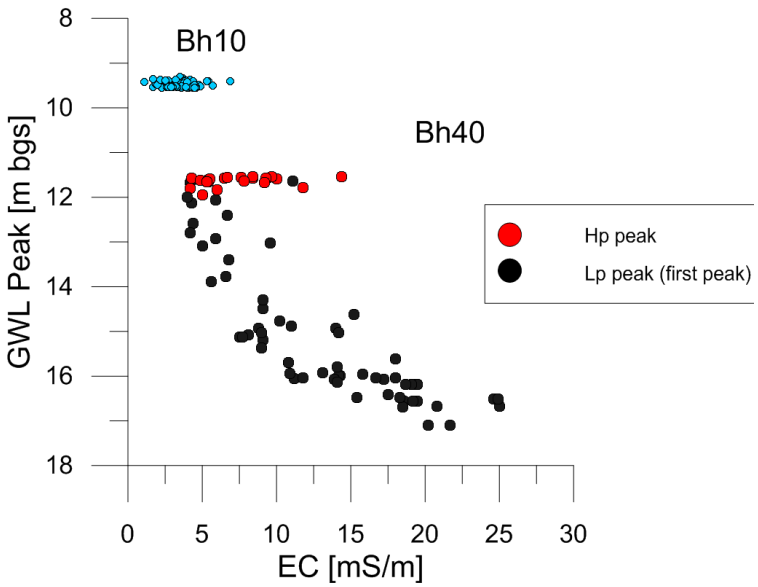

Figure 21. Correlation peak in groundwater (Bh40 and Bh10) and EC values at the moment of the peak. Red dots: EC values for the moment when the maximum in bedrock groundwater (Hp) is reached. Blue dot: EC values of peaks in Bh10.

Although the *EC* values of Bh10 exhibit little variation, there is an anomalous increase in the *EC* values in September 2011. This increase is synchronous with the *EC* values measured in Bh40. Under these high-precipitation events, the *EC* values are expected to decrease, especially in the most superficial part of the hillslope. However, in this case, the *EC* values are observed to shift in the opposite direction, which could suggest a contribution of deep groundwater in the most superficial part of the hillslope. A similar situation can be observed in the event of July 2011, but the increase in the Bh10 *EC* values is not significant (unlike in the September event). The data were collected during 2011, which featured high-precipitation events due to the passing of typhoons, but the specific conditions for this occurrence are unknown.

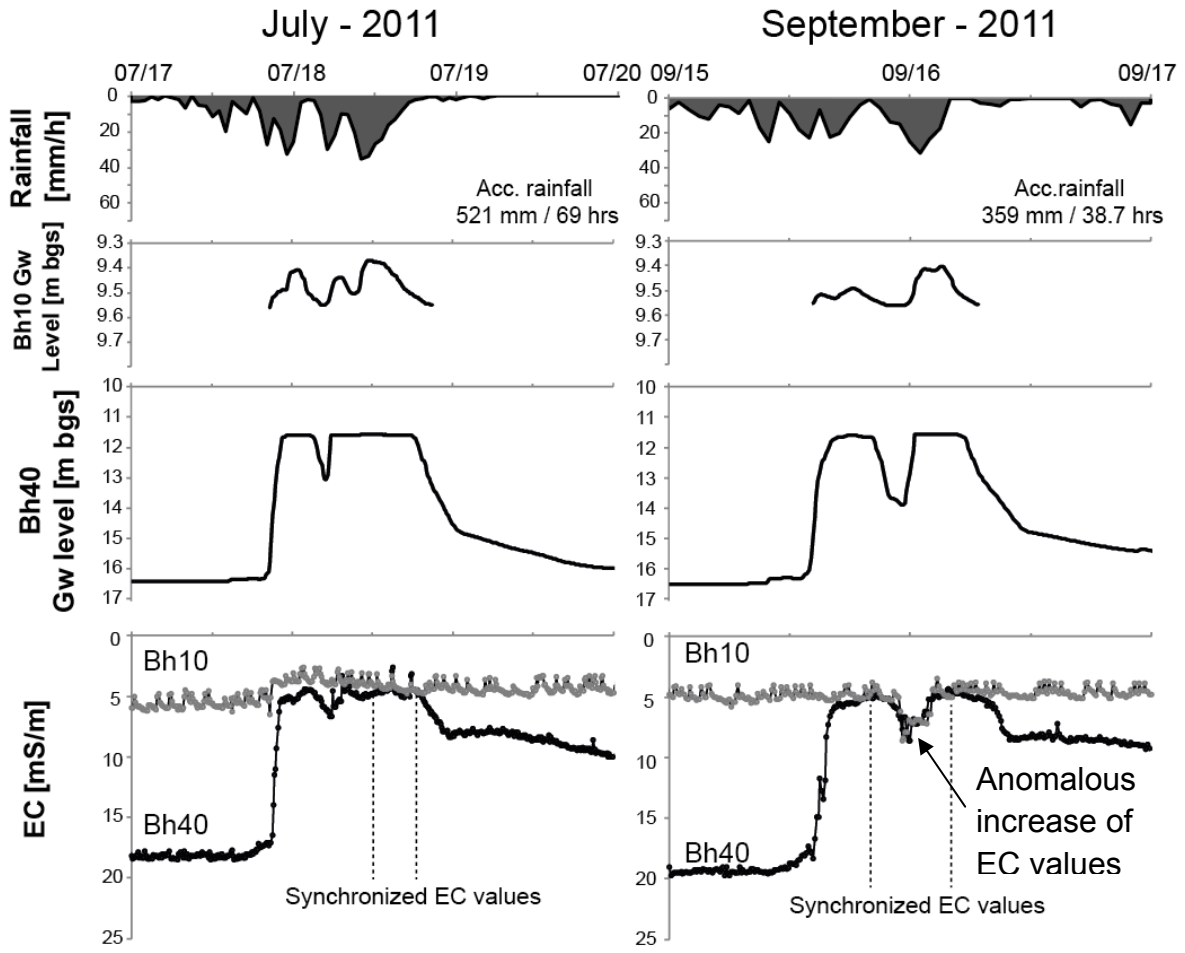

Figure 22. Cases of EC values synchronization between BH10 and Bh40 in July and September 2011. The accumulated rainfall refers to the rainfall accumulated until the synchronization starts.

4.3. Stable isotope concentration in groundwater.

In this study, groundwater samples from the two boreholes (Bh40 and Bh10) and bulk rainfall samples were analyzed during 2010 and 2012. The compositions of $\delta^{18}O$ and $\delta^{2}H$ measured in the samples are shown in Figure 23. In this figure, the local meteoric water line (LMWL) was drawn using the linear correlation of the $\delta^{18}O$ and $\delta^{2}H$ compositions of the rainfall samples.

Based on the analysis of the borehole base level samples and the bulk rainfall samples from 2010 to 2012, the rainfall water presents a high seasonal variation with respect to the $\delta^{18}O$ composition, and the Bh10 samples follow a pattern similar to that of the rainfall. The $\delta^{18}O$ composition of the Bh40 tends to be more stable throughout the year.

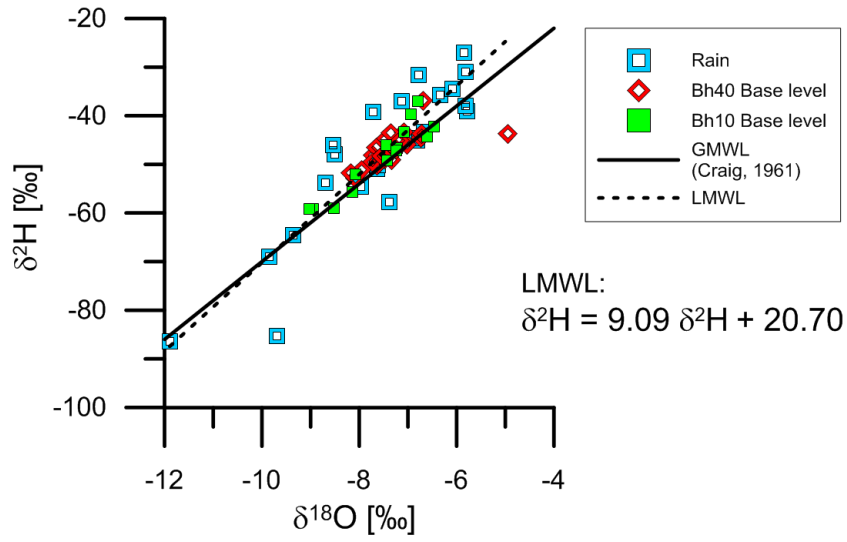

Figure 23. $\delta^{2}H$–$\delta^{18}O$ compositions of the water samples of groundwater (Bh10 and Bh40) in base level and rainfall. Dotted line: the local meteoric water line (LMWL). Solid line: Global meteoric water line (GMWL) of Craig (1961).

The event samples collected during the response of groundwater in both boreholes showed the changes of isotopic concentration for different depths (Figure 24 and Figure 25). These samples were collected during the rise of levels in nine maximum peaks (Hp) and two events where maximum level was not reached. The isotope concentration was compared with the bulk sample rainfall isotopic concentration. The rainfall showed an important variability of isotopic signature not completely followed by the response samples. In contrast the samples of Bh40 have a tendency to have similar values to Bh10 samples during the response and not to the rainfall values.

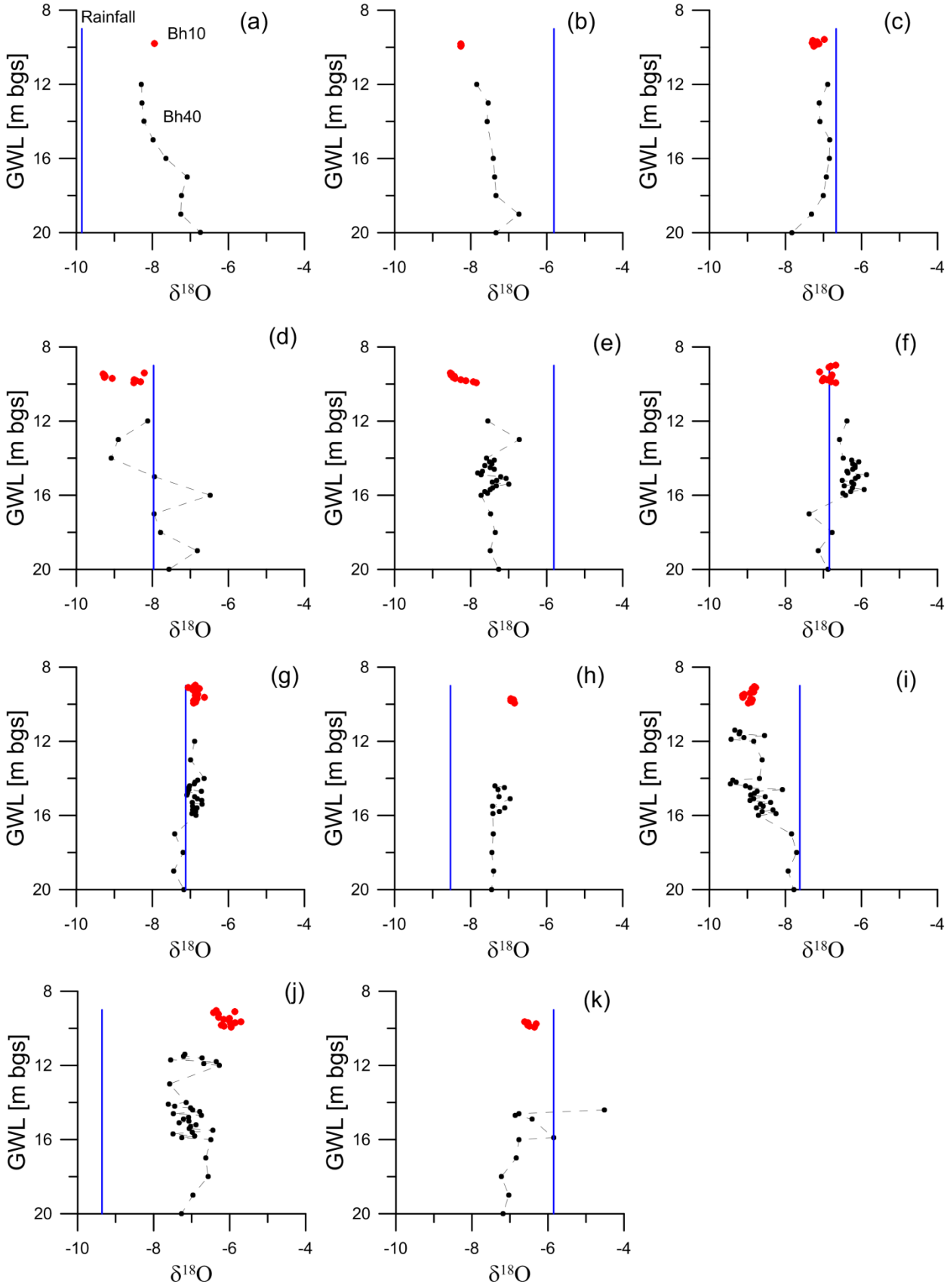

Figure 24. Concentrations of $\delta^{18}O$ in Bh40 (black dots) and Bh10 (red dots) in the response samples. Blue line shows $\delta^{18}O$ concentration in the correspondent bulk rainfall sample. Events date: (a) 2010/06/25, (b) 2010/10/24, (c) 2011/25/29, (d) 2011/06/16, (e) 2011/07/18, (f) 2011/09/16 (g) 2011/10/21, (h) January 2012, (i) 2012/05/21, (j) 2012/08/01, (k) November 2012.

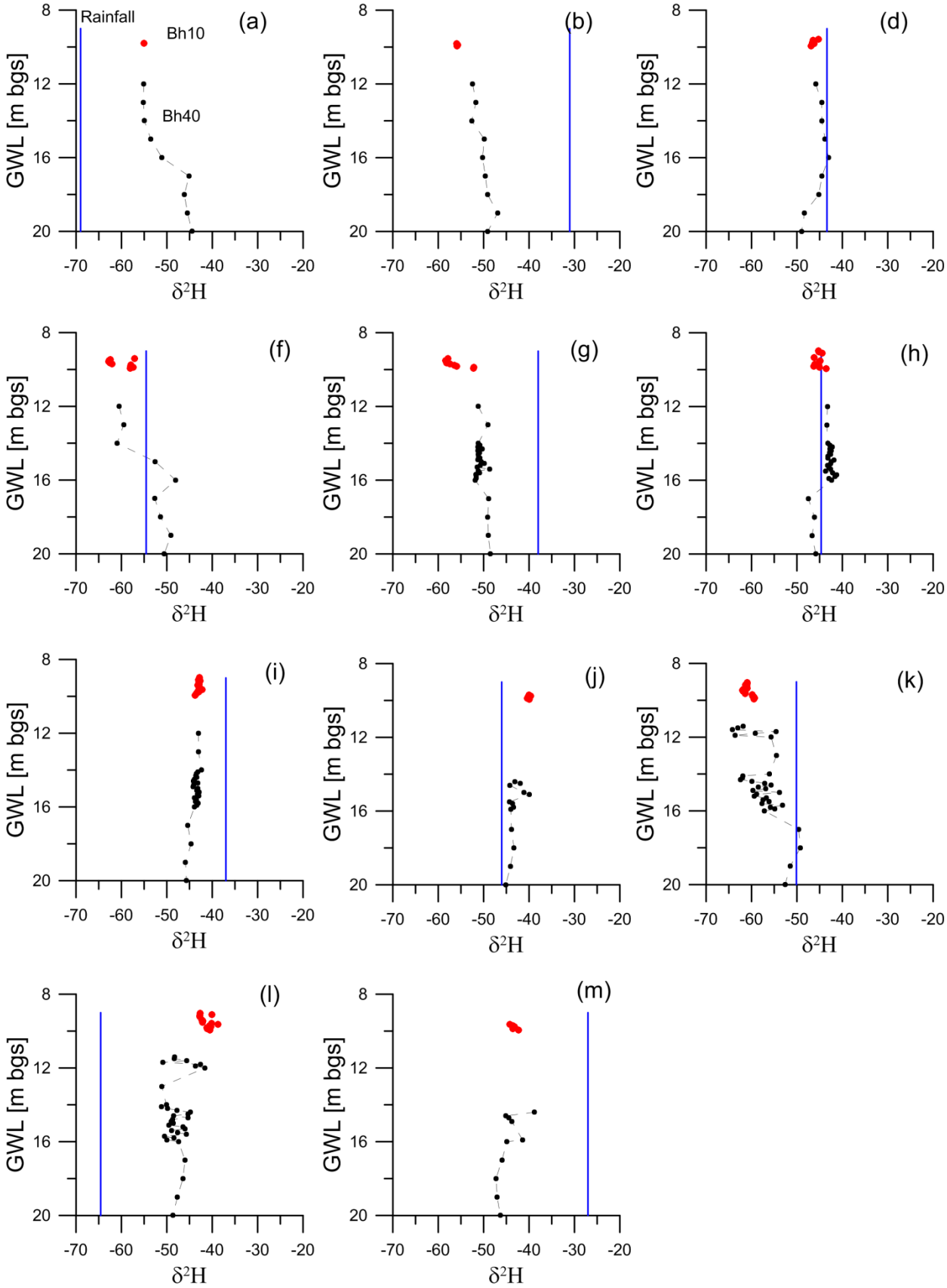

Figure 25. Concentrations of δ^2H in Bh40 (black dots) and Bh10 (red dots) in the response samples. Blue line shows $\delta^{18}O$ concentration in the correspondent bulk rainfall sample. Events date: (a) 2010/06/25, (b) 2010/10/24, (c) 2011/25/29, (d) 2011/06/16, (e) 2011/07/18, (f) 2011/09/16 (g) 2011/10/21, (h) January 2012, (i) 2012/05/21, (j) 2012/08/01, (k) November 2012.

4.4. Discussion: Groundwater observations.

The observations of groundwater response in the hillslope showed clear differences between the responses in the superficial parts (Bh10) dominated by sediments and regolith and the fractured bedrock (Bh40). These differences correspond to a significantly major change of groundwater levels and a significant change in the chemistry of bedrock groundwater in comparison with the sediment cover response.

Generally rapid response in the groundwater levels due to recharge is commonly observed in fractured rock aquifers (Banks et al., 2009; Gleeson et al., 2009; Rodhe and Bockgard, 2006; Salve et al., 2012; Shevenell, 1996). In these aquifers, the flow is determined by the hydraulic connections between fractures or structures, which, in some cases, permit a fast infiltration of recharge water into the bedrock. In the opposite case, when the fractures are more homogeneously distributed in the bedrock and not well connected, the responses tend to be slower, smoother and longer in duration. Shimada et al. (1980) and Kosugi et al. (2011) observed this trend by analyzing the groundwater response of hillslopes with weathered and fractured granite as bedrock. In these cases, the groundwater responses lasted for periods of months, similar to the SR zone recession in this study and contrary to the PR zone where the recessions are very short.

The short period of API (API_6, 6 hours half life) that determines the different response in bedrock groundwater do not depends on very long time antecedent rainfalls. However, this index is not helpful to make the distinction between the two types of response in the bedrock groundwater. This determines that the generation of the two types of responses does not depend on a certain volume of rainfall. It is suggested that the differences in the responses is given by the distribution of rainfall during the 6 hours and not the total amount of rainfall during that period.

The observation of two types of response in bedrock groundwater, single and double peak, has been not reported in any of the previous studies reviewed. These responses have been described individually but not in the same fractured aquifer.

Double peaks responses have been reported in few studies of fractured bedrock aquifer. Shevenell (1996) analyzing the bedrock groundwater flow in a karst area identified double peak responses as a common response of groundwater. In the study, the presence of double peak responses was attributed to different flow path of groundwater in bedrock. The first peak represents rapid flows in conduits that are commonly formed in carbonate rocks. After, the delayed peak observed was attributed to the flow of groundwater through slow hydraulic conductivity fractures in the bedrock matrix. In the other hand, Kosugi et al. (2011) identified double and triple peaks responses in a fractured granite. In this work, the different peaks are explained by the interaction of different aquifers in the bedrock separated by possible discontinuities, such as fault areas. In the study, no preferential flow path was reported and the peaks were attributed to flows in the bedrock fractures system. Recently, Salve et al. (2012) observing the bedrock groundwater responses in sedimentary rock (argillite) reported fast responses in deep fractured bedrock aquifer. Even though double peaks were not reported in the responses, the fast response observed in the aquifer was attributed to vertical or high degree fractures in bedrock. This fractures act as conduits of superficial water and helps in the fast response of the deep groundwater. The characteristics of these two studies can be useful to compare with the observation in this research.

The comparison of lag time between the first peak and rainfall peak (Table 4) shows the significant reduced lag time in this study. This reduced time is faster than the observed with the specific conduits developed in carbonates rock system but similar to the case of vertical fractures in sedimentary rock. In the study in karst area the extension or the distance traveled by the groundwater through these conduits is not mentioned, therefore a clear comparison with this study is not possible. However, it seems that the studies that suggest a special conduit of water

infiltration present very reduced lag time in comparison with the case of fractured granite. The existence of conduits in bedrock seems to be the main reason for the existence of fast peak responses.

Table 4. Comparison of lag time of first peak in groundwater response and Rainfall peak in this study and other studies reviewed.

	Bedrock	1rst peak	Lag time 1rst. peak GW– Rainfall peak
Shevenell, 1994	Carbonate rock	Conduits	5 – 7 hrs
Kosugi et. al., 2011	Weathered Granite	Fracture system	48 – 96 hrs
Salve et. al., 2012	Sedimentary	*vertical fractures (conduits)	Less 1 hour – 25 hours
This study	Sedimentary		10 min – 2.5 hrs

The reduction of the lag time between the first peak and second peak in bedrock groundwater responses (Figure 16) shows that there must be a relationship between these two peaks. In the previous studies reviewed the lag time between these peaks present significant differences. Shevenell (1996) defined a lag time in terms of hours (less than 1 day) in the carbonate bedrock aquifer whereas Kosugi et al. (2011) reported few days of lag time for the case in granite bedrock. In both studies a change in the lag time is not reported. For this study, the lag time is considerable short, ranging from 15 hours to less than 1 hour. Again, these values are more similar to the case when the first peak is generated by high conductive conduits. The evidences suggest that the rapid response associated to the first peak in the bedrock groundwater occurs by fast flows of water through conduits. It seems also that the same mechanism is the responsible of the fast rise of the levels during the single peaks.

Salve et al. (2012) carried out a detailed observation of the moisture conditions at different depth in the soil cover and fractured bedrock. The authors show that it is possible to observe fast responses in bedrock even if the moisture conditions of the unsaturated area are not

high. This fast response can be generated by a vertical fracture system in bedrock bounded by low-conductivity bedrock. Similar mechanism to generate fast responses is proposed for this study. The observations of a system of vertical and high degree fractures and some evidences of normal faulting in the borehole core demonstrate that similar structures are also observed in the hillslope. This type of fracture and normal faults system were describe by Chigira and Kiho (1994) as features observed in hillslopes affected by gravitational deformation. These fractures and faults can act as the conduit that helps the fast recharge of the bedrock groundwater. The fast flow in these structures can occur under unsaturated conditions of the bedrock. Evidences of this can be found in analysis of recession curve of the two types of response, single and double peak responses.

The analysis of the recession curves can provide information about the groundwater flow conditions in aquifers (Baedke and Krothe, 2001; Shevenell, 1996). Higher slope in the recession curve indicates high hydraulic conductivity of the media and the opposite for lower slope recession curve. In this study the differences and similarities in recession curve of the first peak, second peak and single peak demonstrate different saturation conditions for different peaks (Figure 26). The higher angle of recession curve in the first peak (Lp) (S1, Figure 26) compared to the recession curve in single peak demonstrate rapid discharge during the first peak. The recession curve of the second peak (Lp) and its similar slope to the recession in the single peak evidence similar flow conditions (S2, Figure 26).

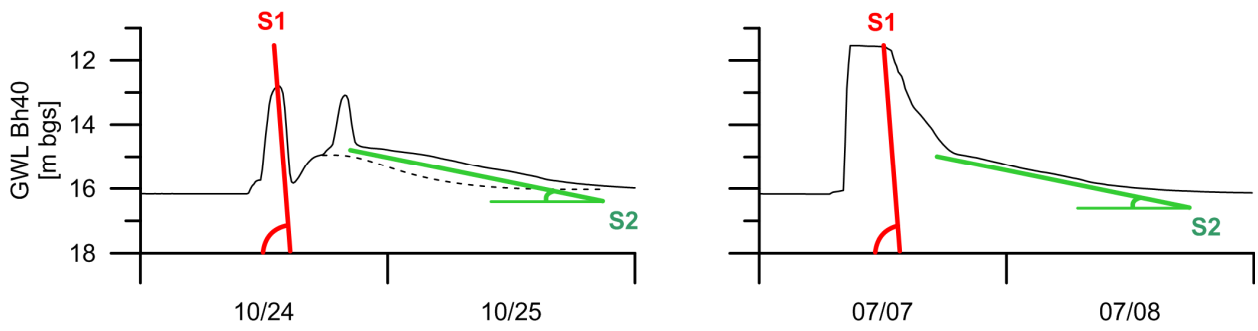

Figure 26. Comparison of recession curve slope. S1: Recession curve slope for first peak in double peak response (Lp). S2: Slope of the 3rd segment in the recession curve of single peak (Hp).

The observation of the high angled fractures (conduits) in the borehole core demonstrates the hydraulic connection of the borehole with these structures. Due to this hydraulic connection the rapid saturation of the conduits implies also a rapid rise of the groundwater levels in the borehole (Figure 27a). This rise of levels in the borehole does not imply a complete rise of the bedrock groundwater level which remains unsaturated. The flow of water through the conduits represents an injection of water into the bedrock that eventually recharges the bedrock aquifer. During this injection two scenarios can take place depending on the rainfalls characteristics:

1) If the rainfall stops soon after the generation of the first peak in Bh40, the conduit flow stops and a rapid fall of the levels starts (Figure 27; steep recession, S1 in Figure 26). This fast recession represents the rapid flow of groundwater from the saturated fractures (or borehole) to the bounded unsaturated bedrock aquifer (Shevenell, 1996). This flow of water into the unsaturated bedrock in addition to the injection of water from the sets of conduits up and down slope generates the secondary peak in bedrock groundwater (Figure 27c). Additionally a vertical infiltration of water through the soil cover must contribute to the secondary peak. The water that generates this secondary peak corresponds to a mix of water that flows in the different pathways (conduits + bedrock fractures). This groundwater also is mixed with water that eventually remains in the unsaturated bedrock. Assuming that the groundwater in the unsaturated area has high EC values as the base level, the mix of this groundwater with water from conduits can generates the delay in the peak of EC values for the secondary peak (Figure 19). This secondary peak represents the rising of the bedrock groundwater; therefore the recession curve is determined by the hydraulic conductivity of bedrock aquifer under saturated conditions (low degree recession) (Figure 27c; S2 recession curve in Figure 26).

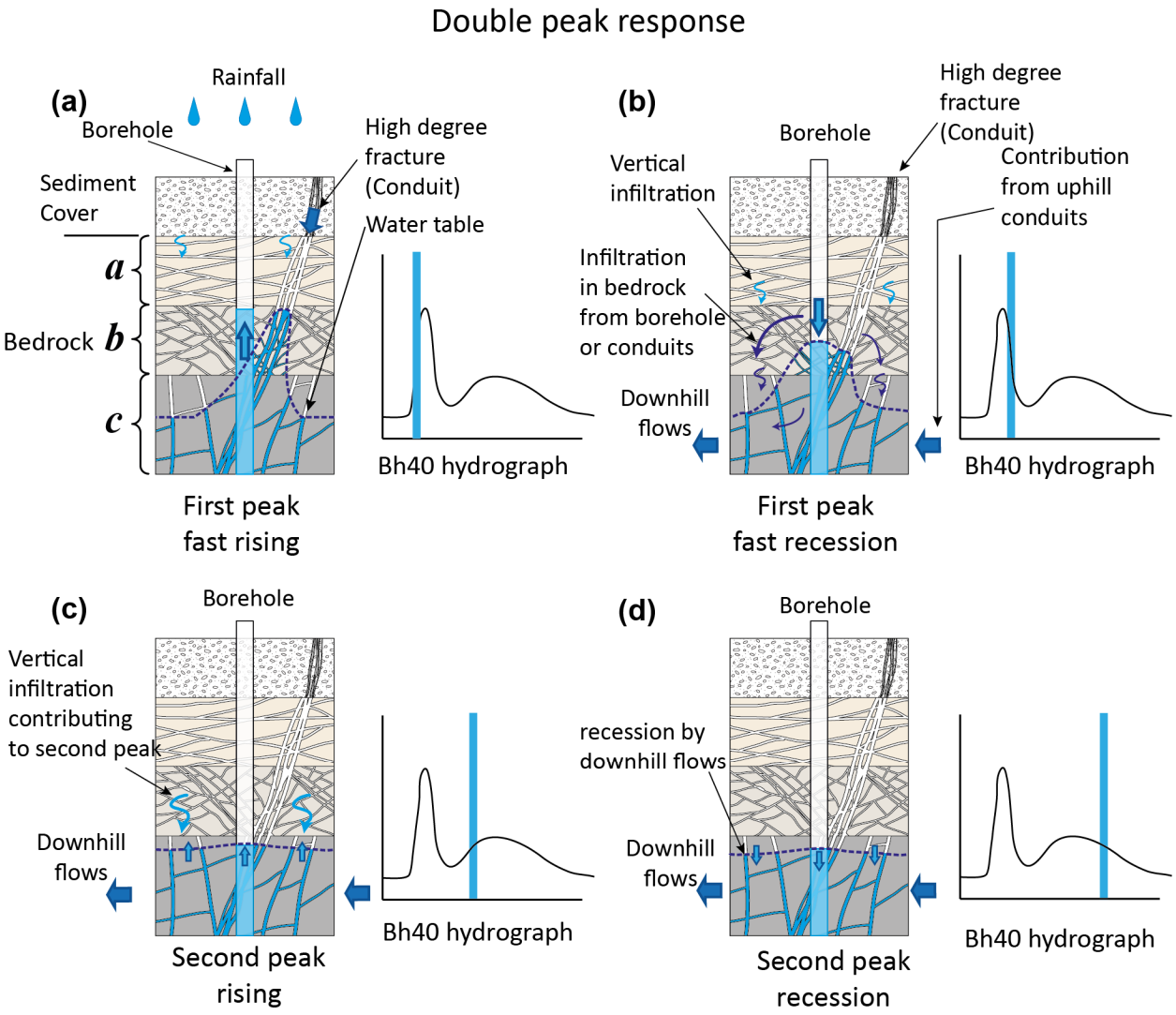

Figure 27. Proposed model to explain the double peak responses in Bh40. The bedrock is divided in tree domains (*a, b* and *c*) according to the fracture domains observed in the borehole core (Figure 12). (a) Infiltration by the high angle fracture generates rapid rise of the first peak in the borehole. (b) Rapid recession of the first peak due to flows from fractures or borehole to unsaturated bedrock (c) Second peak in Bh40 formed by the rise of the water table in bedrock. (d) After the second peak, the slow recession curve in the partially saturated bedrock is observed.

2) If the rainfall continues during the rising to the first peak, more water infiltrates and generates the maximum peak (Hp) (Figure 28). From Figure 16 we know that for greater first peak (Lp) the lag time with the secondary peak decreases. Under greater rainfall, the single peak can correspond to the union of these two peaks. The delay of EC values for the rising of single peak responses demonstrate that the maximum level is generated by a mix of water as same as the secondary peak in double peak responses. This mix is also observed in the values of isotopes concentration of the response samples. The samples collected in Bh40 during the rise of the groundwater levels tens to have isotopic concentration similar to the measured in Bh10. This isotopic concentration sometimes

differs completely with the rainfall bulk sample. The EC shows the same tendency, with similar values in both boreholes during the maximum level. The maximum levels remains stable thanks to the special fracture flow or exfiltration mechanism that prevent the rise of the bedrock groundwater levels (Figure 28b) After the rainfall ends, the recession curve is given by the hydraulic conductivity of the saturated bedrock aquifer which is different at different depth (Figure 28c). This generates the three segments in the recession curve and the similar slope for the 3rd segment and the recession in the secondary peak.

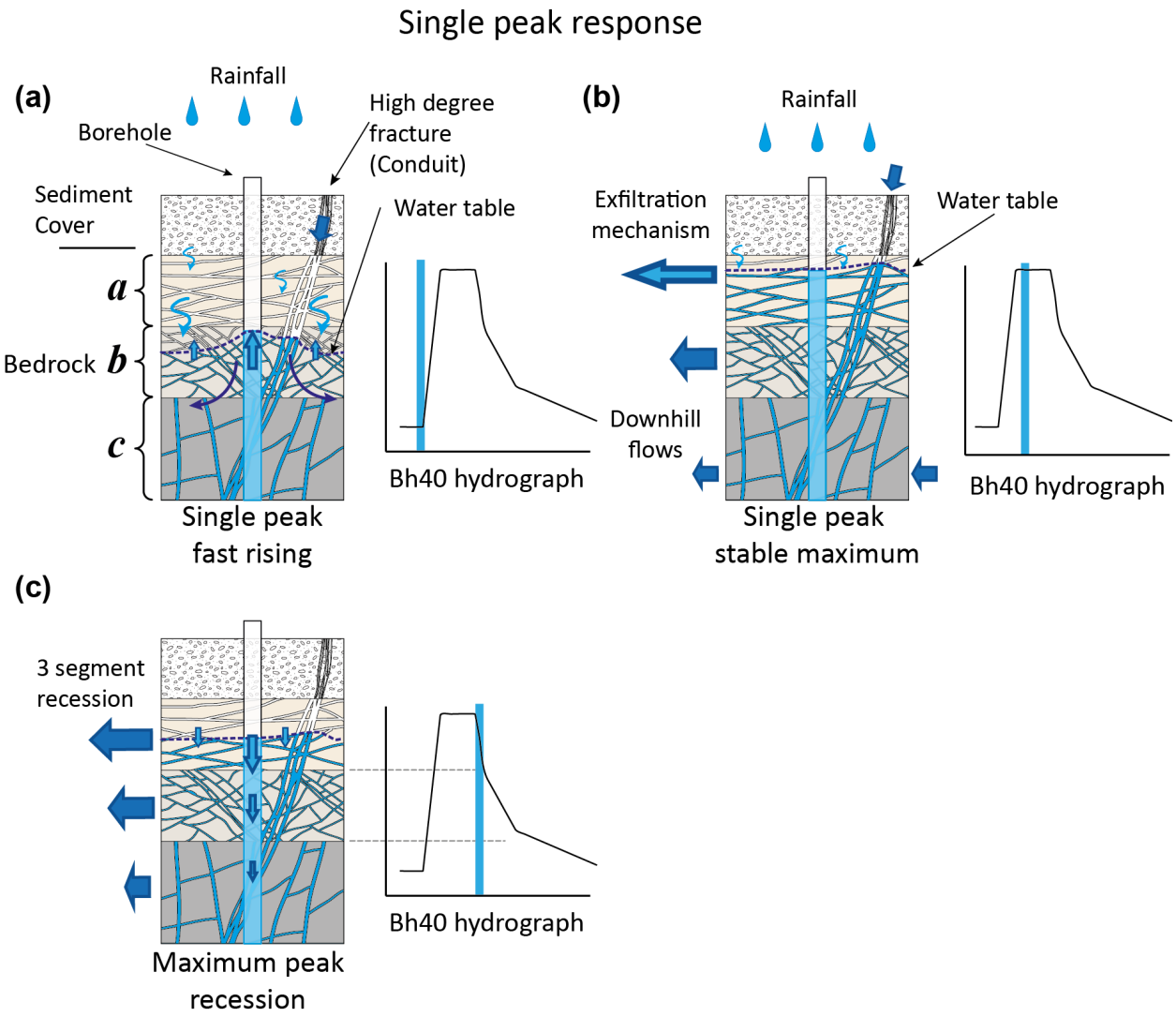

Figure 28. Proposed model to explain the characteristics of the single peak responses in Bh40. The bedrock is divided in tree domains (*a, b* and *c*) according to the fracture domains observed in the borehole core (Figure 12). (a) Infiltration by the high angle fracture generates the first peak in Bh40. A major contribution from vertical infiltration and from conduits contribute to the rapid rise of bedrock groundwater levels (b) The stable maximum is generated by the special fracture flow (exfiltration mechanism). (c) After the end of rainfalls, the groundwater levels descend according to the hydraulic conductivity at different depth (segments).

The condition of saturation observed in the maximum peak seems to be stable even if the rainfall amount increases. The similar time that it takes to the groundwater level descend to the base level after the rainfall decreases below 5 mm/h indicates that the maximum level also represents a maximum of water retained in the aquifer. This means that there is a system that allows the evacuation of water from the bedrock. The domain of low angle to horizontal fractures at the depth of maximum groundwater level suggests the existence of horizontal flows with high conductive fractures near to the contact to the sediment cover. This fracture system is an efficient mechanism to evacuate the fast infiltration of water and keep the saturation level at approximately 11.5 m bgs. However, this raises another question about the destination of the evacuated water. It is presumed that this water can contribute directly to superficial flow processes. Under this assumption the runoff of the near catchments was observed in order to identify contribution of bedrock groundwater in the surface processes and quantify it.

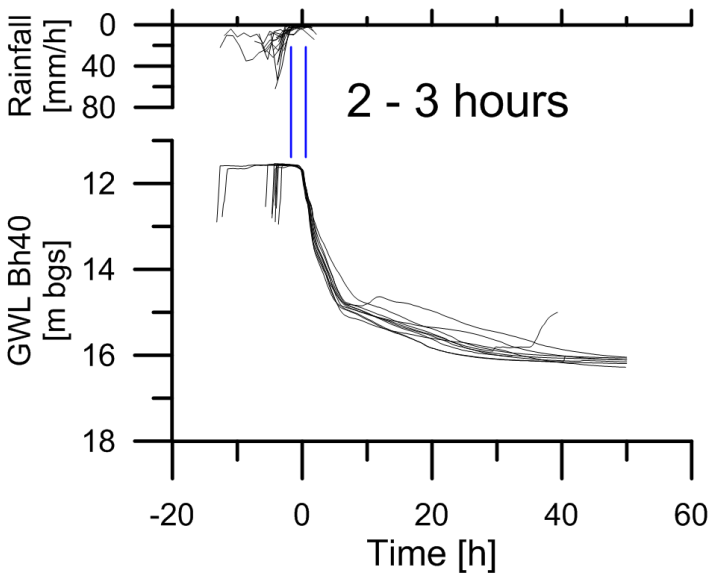

Figure 29. Observations in the recession curve of single peaks. Time 0 corresponds to the beginning of the first segment in the recession curve. The blue line interval represents the two to three hours after the decrease of rainfall and start of recession curve.

Chapter 5: Results - Interaction Groundwater and Catchment runoff

5.1. Hydrometric observations.

The observations of groundwater showed a very responsive groundwater levels. In this kind of conditions, an interaction between the groundwater and the superficial discharge in the area is expected. The runoff of three catchments in the area was analyzed to determine their possible interaction with bedrock flows. The complete record of discharges in the catchments can be seen in Appendix II.

A detailed analysis of the runoff of the three catchments analyzed showed clearly the differences and similarities between them (Figure 30).

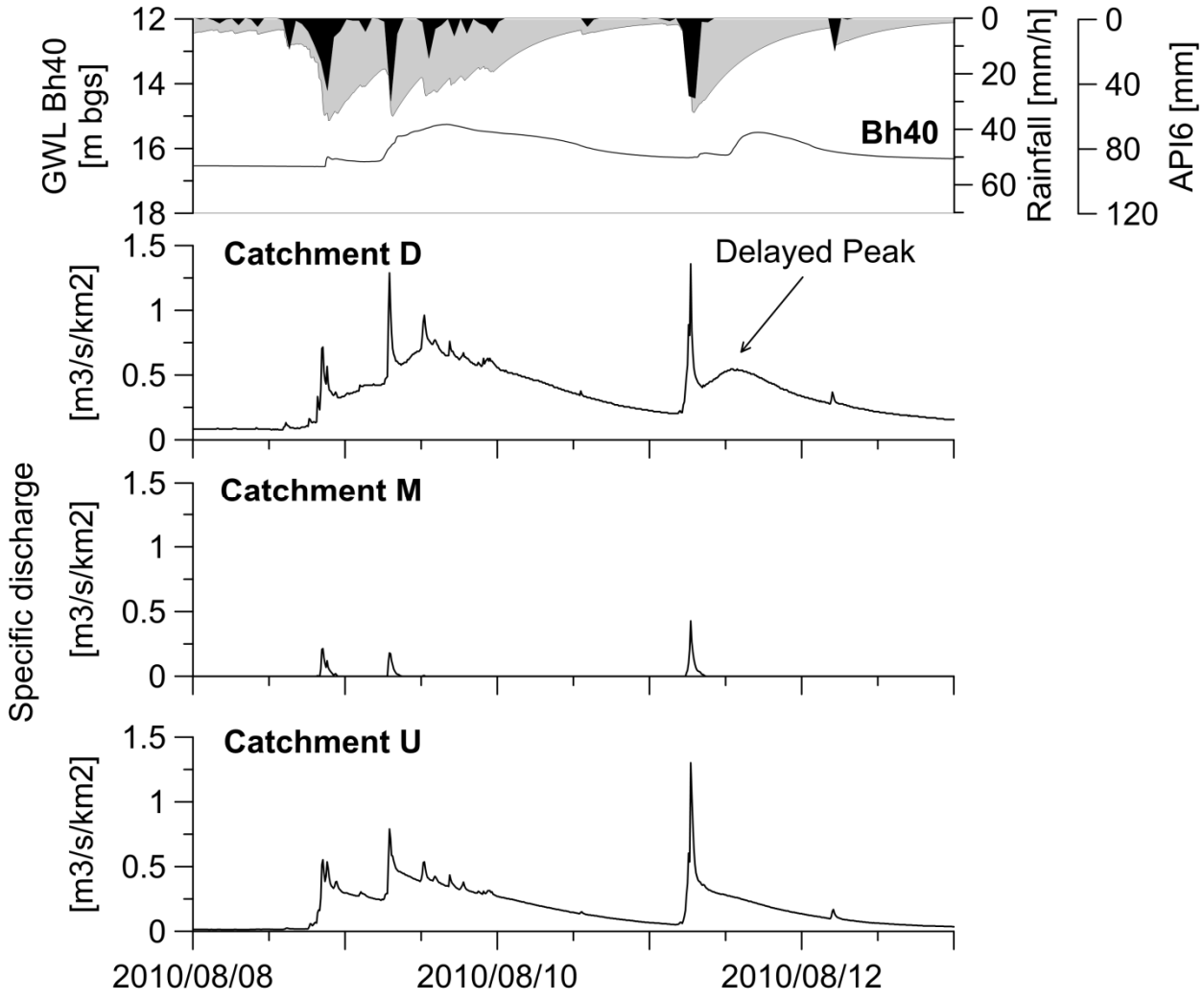

Figure 30. Comparison of hydrographs (specific discharge) for bedrock groundwater and the three catchments observed.

The three catchments are very responsive to rainfalls. The catchments show fast peaks in discharge after a peak of rainfalls. These responses seem to be mainly related to rapid saturation and overland flows (Anderson and Burt, 1978; Birkinshaw, 2008). The term quick flow will be used for this fast response. In the correlation between discharge (Specific discharge) and rainfall (Figure 31) catchment D generally present higher peaks than catchment U. Particularly for small rainfalls events (below 20 mm/h) are observed discharge that exceeded 2 $m^3/s/km^3$ not observed in U or M. Catchment M shows significant responses when the rainfall exceeded the 20 mm/h approximately, however is still much below than the other catchments.

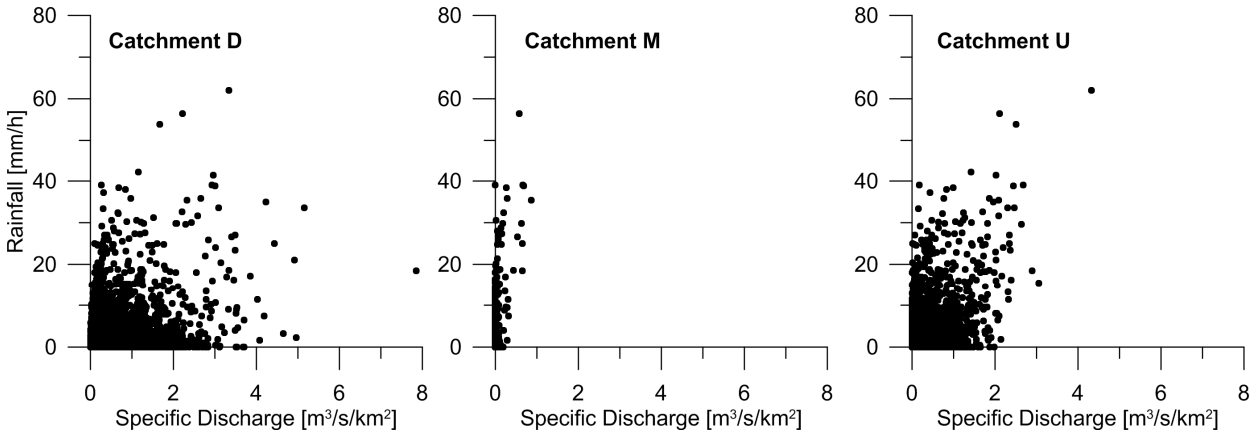

Figure 31. Graph rainfall vs. specific discharge in the three observed catchments.

Another remarkable difference in the three hydrograph is the delayed peak in catchment D, not observed in the other catchments. This delayed discharge causes greater quick storm runoff or quick flow for the immediately following rainfall peaks. The delayed discharge also generates a secondary peak in D. In catchment U, after a very fast decrease of discharge after rainfall peak, a linear recession curve is observed. The initial quick flow is very similar to the observed in catchment D. The linear recession curve in U and the delayed discharge in D seem to have very similar start point in the recession. Their characteristics evidence a different control of the runoff in both catchments. The recession of catchment M seems to be related directly to rainfalls and no extra discharge is observed.

Delayed discharges in runoff have been observed in several studies in different type of catchments. However, the observation of delayed peaks in mountainous catchment underlain by fractured bedrock is not well documented. Since some studies had attributed delayed responses in runoff to important contributions from groundwater to the runoff (Graeff et al., 2009; Onda et al., 2001; Onda et al., 2006) the characteristics of this discharge will be analyzed.

Most of the responses in D develop a delayed discharge, however the secondary peak is not always observed due to the overlap of rainfall and their responses. Two types of responses are defined depending on the generation of delayed response or not (Agata, 1997; Zillgens et al.,

2007). Type I responses are the quick flow peaks that do not generates delayed responses. Type II responses are the quick flow peaks with delayed response. In Figure 32 it is possible to visualize the frequency of both types of responses. The Type I responses are associated to very small discharges caused by relatively small rainfall events (Figure 32a). Previous studies had used the pre-event base level to represent the moisture conditions of the catchments before the rainfall event in order to identify conditions to separate Type I and Type II quick flows (Zillgens et al., 2007). For this study Type I and Type II quick flow are not clearly separated by using the pre-event base level parameter (Figure 32b). The generation of delayed responses does not seem to be related to the moisture conditions of the catchments. However, Type I quick flows are related with low levels of groundwater levels measured in Bh40.

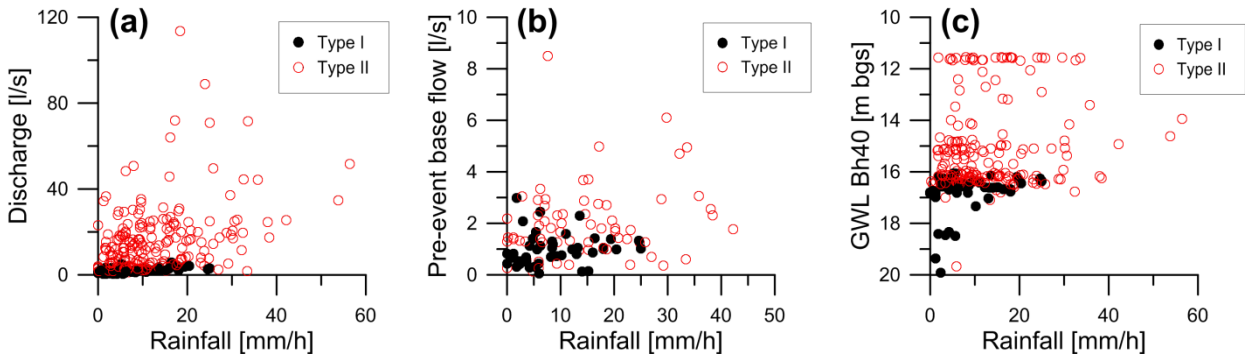

Figure 32. Analysis of quick flow in catchment D with no delayed discharge (Type I) and with delayed discharge (Type II). (a) Correlation discharge of quick flow and rainfall peak. (b) Correlation pre-event base flow discharge and rainfall peak. (c) correlation groundwater levels and rainfall peak.

The lag time between the peak of rainfall (or API) and the delayed peak also has been used to characterize the delayed discharge in runoff. The lag time between the peak of API_6 and the delayed peak was calculated In the responses where the secondary peak was clearly observed (Figure 33). Due to the groundwater responses are related to API_6, this index is also used to characterize the secondary peak. This permit to compare rainfall conditions for delayed peaks in discharge and for the response in groundwater.

The lag time between peaks of API_6 and peaks of delayed discharge ranges from 17 hours to less than 1 hour for higher rainfalls (Figure 33). Most of the delay times are below 8 hours.

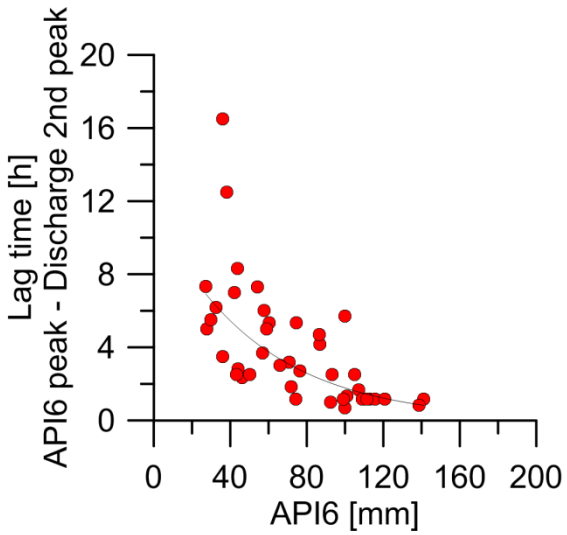

Figure 33. Correlation of API6 and lag time between the API6 peak and the second peak in D.

The correlation between the discharge in D and groundwater level of bedrock groundwater (Bh40) did not show clear correlation (Figure 34). During the double peak responses in Bh40 it is possible to elucidate some correlation in the timing of the delayed response in D and the rise of groundwater levels in Bh40 (first peak). For single peak in Bh40, the correlation with the discharge in D seems to be clearer. The quick flow peak in catchment D is faster than the peak in groundwater but there is a correlation between the discharges during the maximum of level in groundwater. The discharge in D is very similar at the beginning and at the end of the maximum in Bh40. It seems that the delayed peak dominates the discharge in D in high precipitations events and this discharge coincides with the peak of bedrock groundwater.

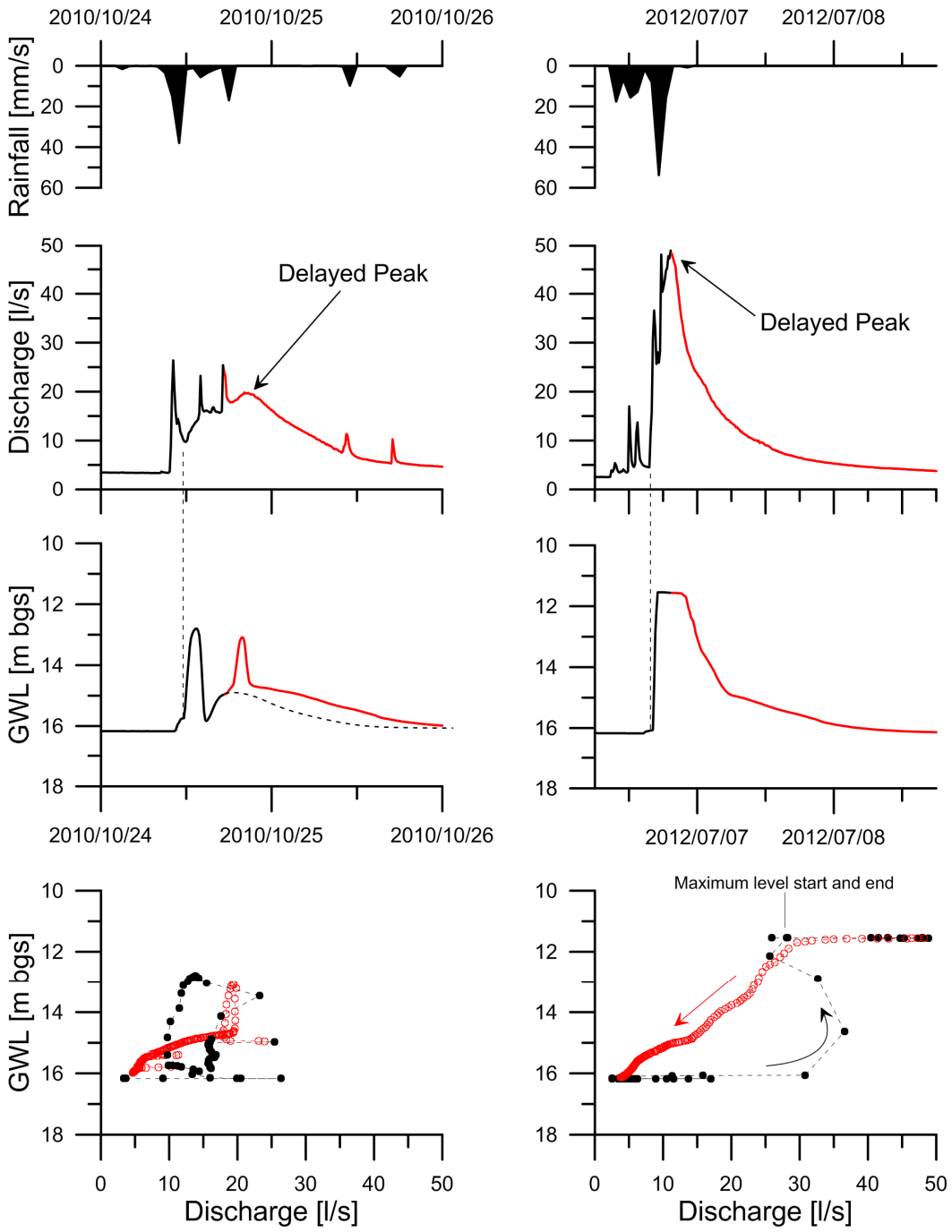

Figure 34. Correlation between bedrock groundwater levels (Bh40) and discharge in D for double peak response in Bh40 (Lp) (left column) and for single peak response in Bh40 (Hp) (right column. Black line (circles): rising limb in catchment D discharge. Red line (circles) Recession limb in catchment D discharge.

Observing the correlation between the delayed peak discharge and the peak in the bedrock groundwater response they show a good correlation (Figure 35 a and b). In the graphs, the peaks in bedrock groundwater correspond to the first peak for double peak responses in Bh40.

The delayed peak showed an important increment of the discharge when the maximum level in bedrock groundwater is observed a (Figure 35 b). For groundwater peaks below the maximum, the delayed peak never exceeded the 20 l/s. When the maximum is reached, there is a linear correlation between the small peaks during the maximum in bedrock groundwater and the discharge of the delayed peak (Figure 35 a). Small changes of bedrock groundwater levels during the maximum imply significant changes in the discharge of the delayed peak.

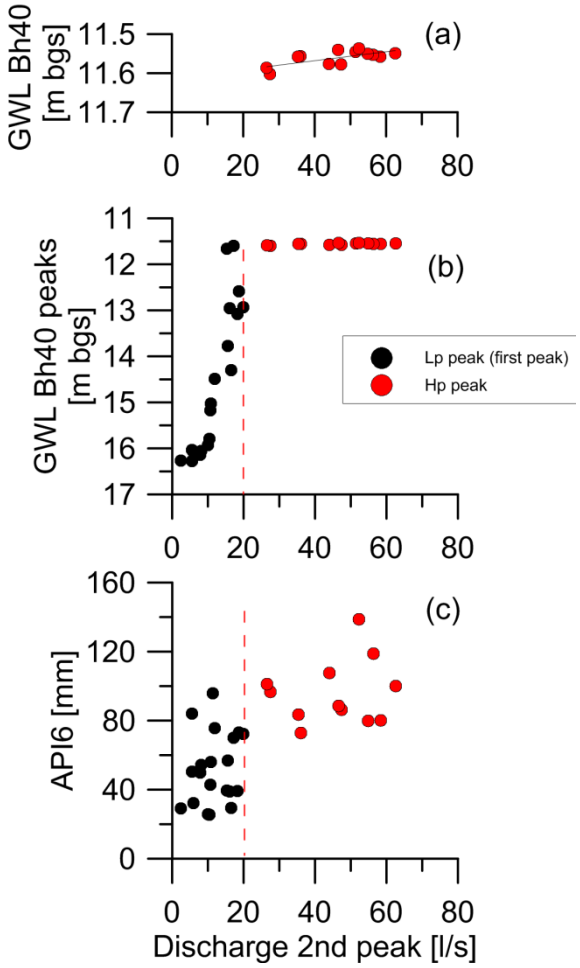

Figure 35. Correlation of delayed peak discharge (catchment D) and groundwater peaks (a and b) and API6 (c). (a) Details of the correlation Second peak and bedrock groundwater and bedrock groundwater peaks during the maximum level. (b) Black dots: correlation between first peak of double peak responses in Bh40 and delayed peak in discharge of catchment D; Red dots: Correlation between peaks during the maximum level at Bh40 and delayed peak in discharge of catchment D. (c) Black dots: rainfalls that generate Lp Peaks; Red Dots: rainfall that generate Hp peaks.

For API_6 peaks over 80 mm most of the discharge of delayed peak exceeded the 20 l/s (Figure 35 c). This limit is the same as the one which defines the precipitations that only generates maximum peaks in the bedrock groundwater (boundary between B and C in Figure 13).

The assumption of a discharge from the bedrock aquifer when it reached the maximum level seems to be correlated to the significant increment of the discharge in the delayed peak in D. The hydrochemical analysis of the responses could bring more information about the source of the water in the discharge of D and the possible strong connections with bedrock groundwater during the maximum level.

5.2. Hydrochemical observations

The use of tracers in the chemical analysis of the water sources is a wide spread technique that helps to identify water flow path in catchments and allows a quantitative analysis of them. A summary of the concentration in water of the elements analyzed are shown in Figure 36. The summary shows the concentration for Deuterium, Ca^{2+}, Mg^{2+} and silica for the base level samples in catchments and groundwater and for the event samples in Bh40. The analysis of each component is shown as follows.

Stable isotopes concentrations:

The rainfall samples present the high variability of deuterium concentration due to its seasonal variation with high isotopic concentration in winter ($\delta^{18}O$: -5.5 ‰ ~ -6.5 ‰; $\delta^{2}H$: -30 ‰ ~ -40 ‰) and low concentration in summer ($\delta^{18}O$: -8 ‰ ~ -9 ‰; $\delta^{2}H$: -60 ‰ ~ -50 ‰) generated by different rainfall origins (Kabeya et al., 2007; Kondoh and Shimada, 1997; Uemura et al., 2012).

The event samples of Bh40 show a progressive increase on the variability of $\delta^{2}H$ with height. In the lowest levels, from 17 m bgs to 20 m bgs, the deuterium concentrations remain relatively stables, similar to the values in the base level of the catchment D. In contrast, the

highest storm samples in Bh40 have similar range of variability as in Bh10 and the rainfalls samples. Higher variability in Bh10 samples and the highest samples in Bh40 can denote a major influence of rainfall water than for the base levels.

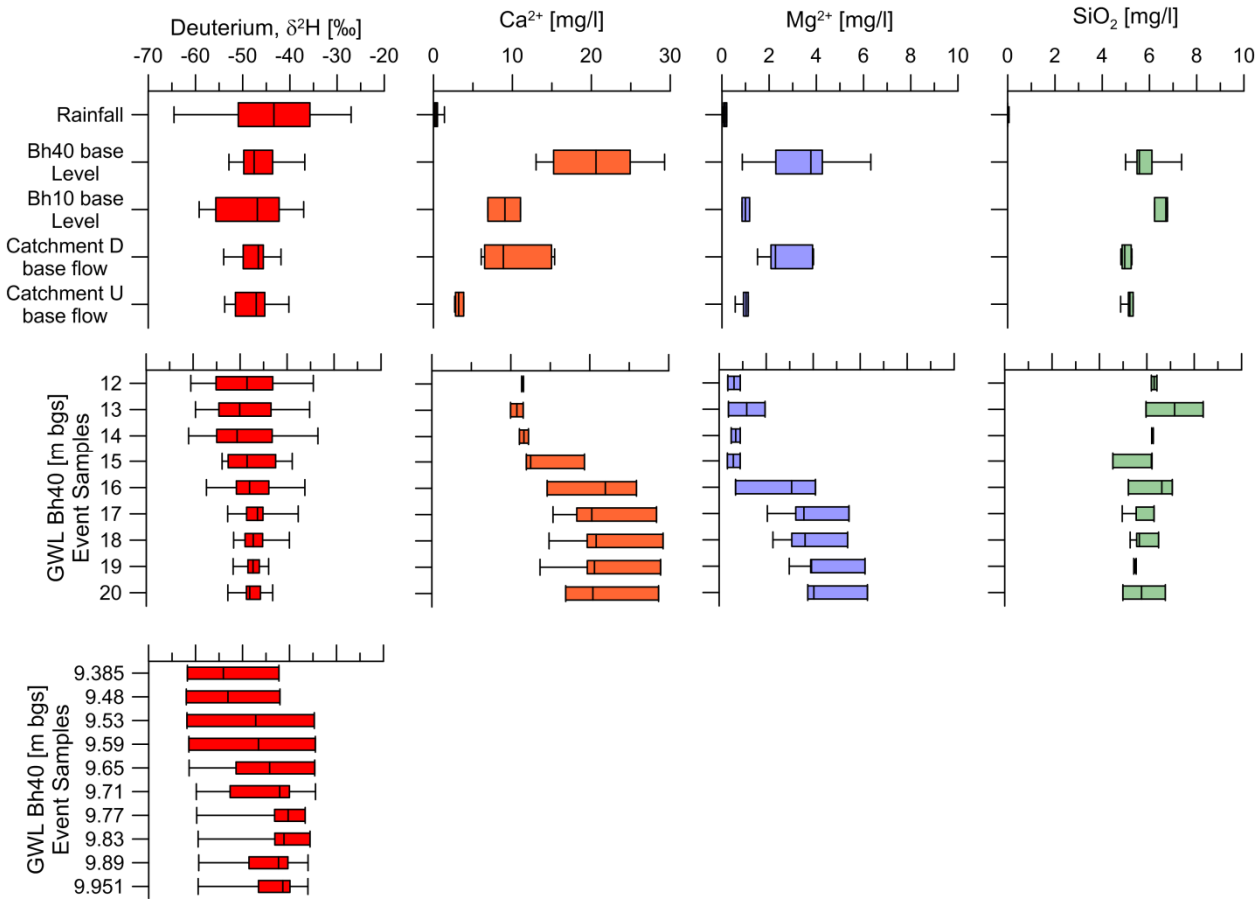

Figure 36. Concentration of deuterium (^2H), Ca^{2+}, Mg^{2+}, and Silica (SiO_2) in the water samples of the study area.

Concentration of Ca2+, Mg2+ and Silica.

As it is expected, the concentration of cations and SiO_2 in rainfall water is very low compared with the rest of the water samples. Ca^{2+} and Mg^{2+} show similar behavior in their concentrations in samples. The higher concentrations are observed in the deep bedrock groundwater followed by the base level of catchment D suggesting a major connection between them during the base level. For the event samples in Bh40 a clear decrease in the concentrations of both cations is observed and these values are similar to the measured in the base level of Bh10. Even though the similar pattern of concentration of these two cations, Mg^{2+} present more clear

differences between samples from deep groundwater (below 16 m bgs) and more superficial groundwater samples. This property is useful to trace and separate deep groundwater and shallower groundwater contributions to the catchment discharge.

In contrast to the cation concentrations, the concentration of SiO_2 is relatively stable and similar in all the samples of groundwater and stream water. The average concentrations fluctuate between 5.5 mg/l to 6.5 mg/l. The evident difference in SiO_2 concentrations of all the samples with the concentrations observed in rainfall makes the silica a good candidate for a tracer of rainfall water in the system.

5.2.1. Chemistry of water samples during rainfall event

In order to quantify the possible contribution of deep groundwater to the storm runoff of catchment D, the water chemistry of two storm event was analyzed based on the concentrations of the tracer described previously. The summary of groundwater levels, discharge in D and the water chemistry during the storm responses is s shown in Figure 37 and Figure 38.

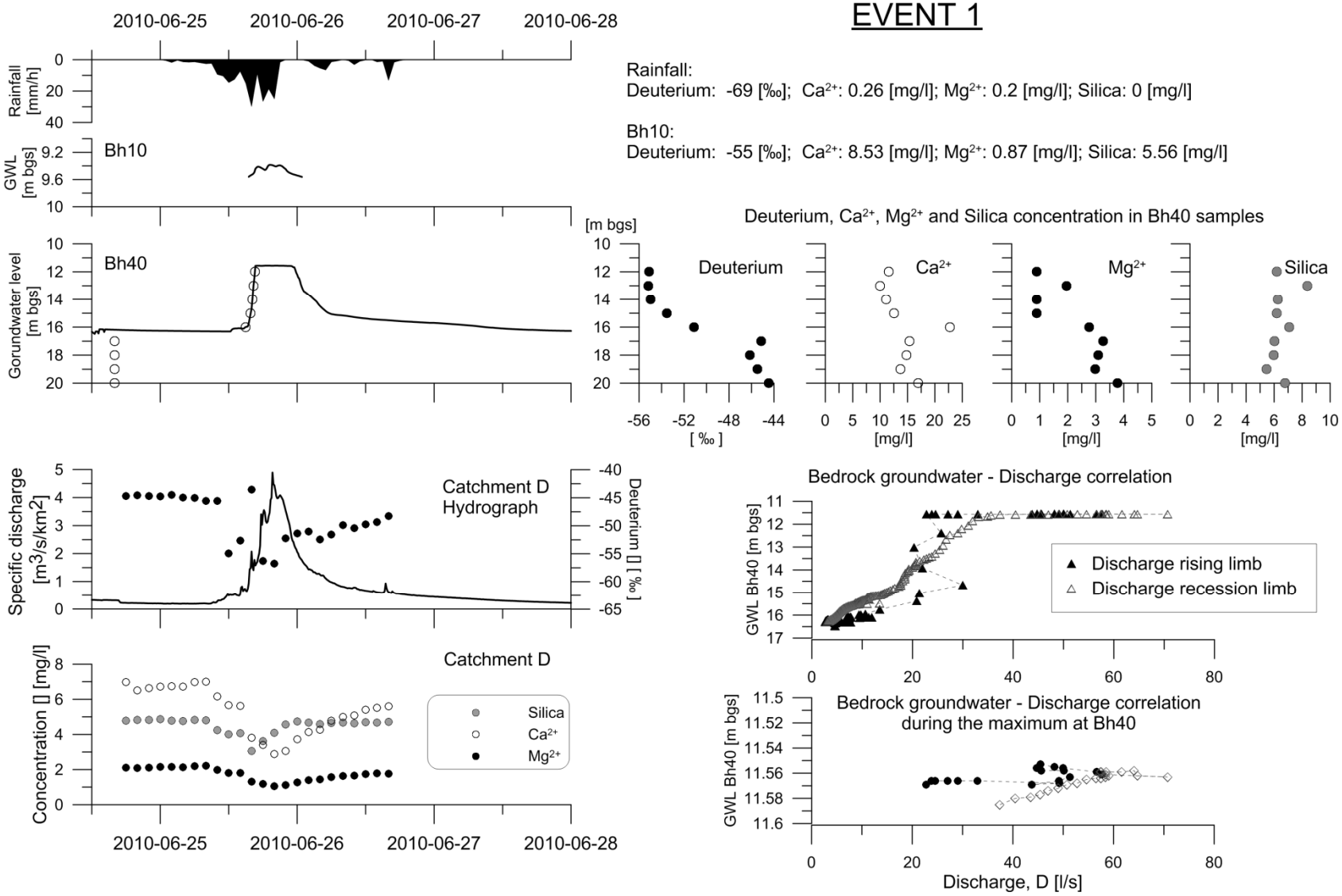

Figure 37. Hydrometric and hydrochemical measurements in groundwater, rainfall and catchment D for event 1.

Event 1:

The groundwater reached the maximum level with its characteristic hydrograph. The accumulated rainfall measured was 239mm. The evolution of the deuterium (^{2}H) concentration in the runoff of catchment D starts with concentration in the base level -45 ‰, similar to the base level of Bh40 (-44‰ to -46‰) . The storm runoff shows a depletion of ^{2}H (-56.7 ‰) in accordance with the concentration of the rainfall bulk sample of -69 ‰. However, in the peak of rainfall (29.5 mm/h) a strong pulse of water with isotopic signature similar to the base flow (-43 ‰) was measured. That pulse is coincident with the rising of the groundwater levels at Bh40. During the rising of groundwater level, the samples collected in Bh40 show also a decrease of the ^{2}H concentration from -45 ‰ in the base level to -55.1‰ at 12 m bgs, similar to the lowest concentration in the storm runoff of catchment D (-56.7 ‰). Even though the pulse occurs at the same time as the rising of groundwater level suggesting a contribution from the groundwater, it is known that also rainfall can have significant changes in the isotopic composition within hours or days (Coplen et al., 2008; Mcdonnell et al., 1990). Even these changes in the rainfall isotopic concentration, the rainfall bulk sample still clearly represent the storm signature and explain the general behavior of concentrations in storm runoff and groundwater.

A general reduction in concentration of Ca^{+2}, Mg^{+2} and SiO_2 is observed in runoff and groundwater but with differences between the timing of lowest concentration. For SiO_2, the lowest concentration seems to be correlated with the peak of the rainfall event. In contrast, the lowest concentrations of Ca^{+2} and Mg^{+2} are correlated with the maximum runoff and also with the delayed peak immediately after.

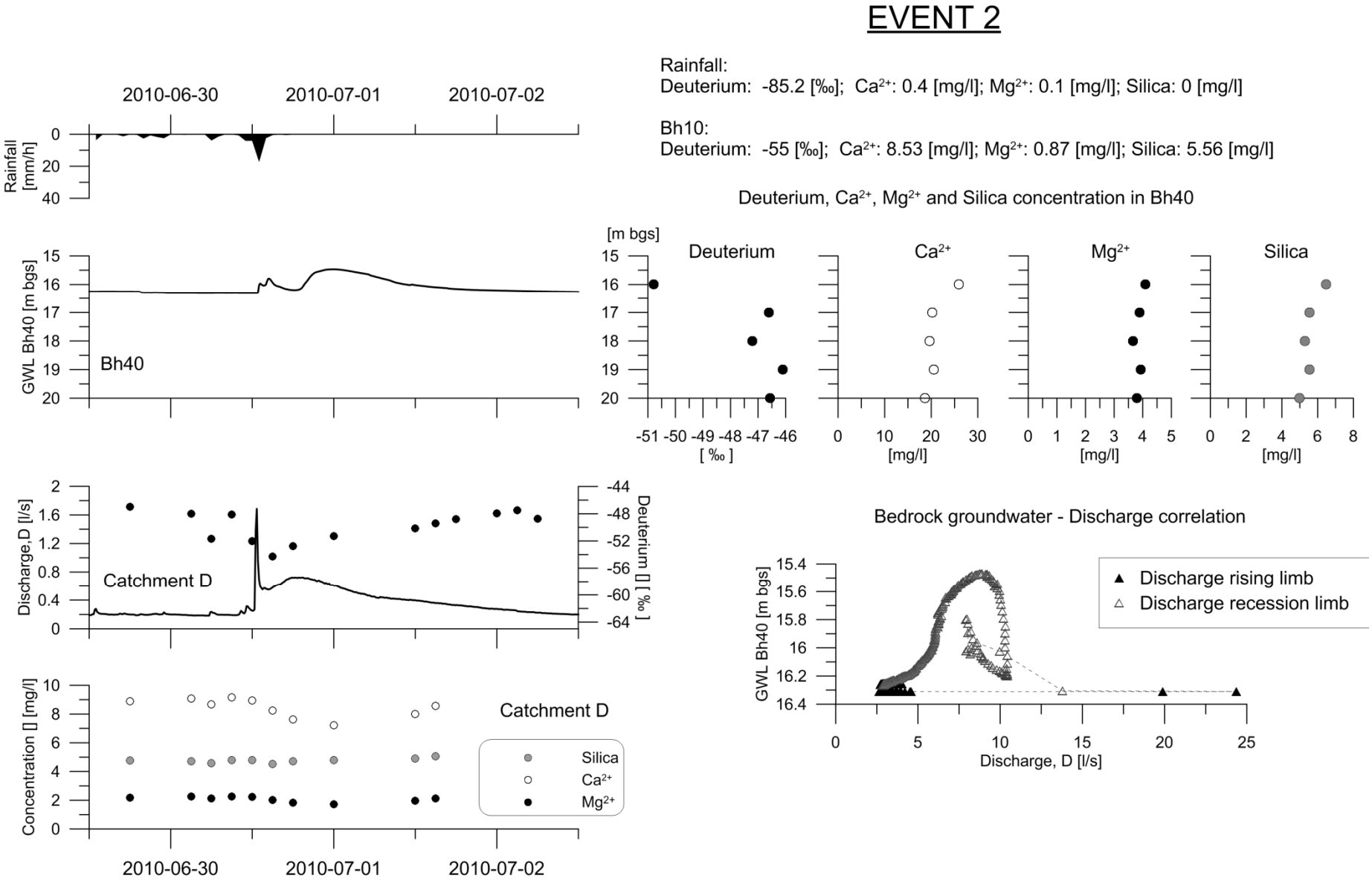

Figure 38. Hydrometric and hydrochemical measurements in groundwater, rainfall and catchment D for event 2.

Event 2:

The event took place immediately after the event 1. This is characterized by smaller rainfall with 58 mm of accumulated rainfall and shows clearly the double peak in the deep groundwater (Bh40) and catchment D. The bulk sample has a deuterium concentration of -85‰, much more depleted than the last rainfall. However, the depletion of deuterium in the storm runoff is not as much different as the event 1 with a -54.4‰ as the lowest concentration in catchment D (against -56.7‰ in the event 1). Unfortunately no sample was collected during the peak of the storm flow due to its short duration. This can cause a mismatch between the peaks of discharge and the lowest isotopic concentration, cations and silica.

The concentration of the cations Ca^{2+} and Mg^{2+} in catchment D decreased during the secondary peak but the lowest concentration seems to be related with the second peak in the bedrock groundwater instead of the second peak in catchment D. In the other hand, the values of SiO_2 do not present significant changes (average concentration: 4.7 mg/l).

5.2.2. Three-component analysis

The previous chemical characterization of the responses of the groundwater and catchment runoff during the events can provide valuable information about the contribution of groundwater to the runoff in catchments using end-member mixing analysis (Gabrielli et al., 2012; Iwagami et al., 2010; Mulholland, 1993). The rainfall water and groundwater (subsurface water) are commonly considered as end member due to their major contribution to the runoff. The strong response to rainfall observed in bedrock groundwater and its significant chemical variation leads us to consider a variable contribution of the bedrock groundwater to the runoff. Moreover, the reduced response observed in the deposit cover Bh10 in comparison with the below bedrock response allows us to underestimate its contribution to the storm runoff. As a result, in this case additionally to the rainfall (Rf) two groundwater sources will be considered as end members; deep groundwater (DGw) and the shallow groundwater (SGw). The deep groundwater (*DGw*) corresponds to the pre event groundwater part of the base level. The shallow groundwater (*SGw*) represents the groundwater during the response. The chemical similarities (cation concentration and EC values) between the Bh10 water samples and the top samples during the response in Bh40 allow us to use both in the definition of the SGw sample.

The tracers selected for this three-component analysis are Silica and the Mg^{+2}. Silica is a very common and well known conservative tracer of groundwater (Iwagami et al., 2010; Katsuyama et al., 2005; McGlynn and McDonnell, 2003; Mulholland, 1993; Munyaneza et al., 2012). In the study area the concentration of silica marks a clear separation between water from superficial processes highly influenced by rainfall and water from deep processes. The particular characteristics of Mg^{+2} concentrations in this area allow us to clearly separate SGw and DGw contributions.

From the plots Mg^{+2} vs Silica concentration it is graphically analyze the contribution of the three end members to the storm runoff of catchment during the selected events (Figure 36).

In the event 1 the catchment D present clear cyclical variation starting and ending its cycle with concentration dominated by deep groundwater contribution. In the event 2 the smaller precipitations cause low levels of mixing between the end members. In this event catchment D has concentrations dominated by the DGw with a small mix during the storm response.

5.2.3. Hydrograph separation

Based on the three-component analysis a hydrograph separation is calculated for the two events analyzed (Figure 39). Table 5 shows the maximum contributions of the end member on each event. The contribution proportion of each end member to the catchment discharge during base flow and storm response is presented in Figure 40.

Table 5. Details in the contribution of the end members in the storm discharge in the three events analyzed.

	DGw (Deep Gw)		**SGw (Shallow Gw)**		**Rf (Rainfall)**	
	Peak of Contribution [l/s]	% of discharge	Peak of Contribution [l/s]	% of discharge	Peak of Contribution [l/s]	% of discharge
Event 1	14.7	33.9	28.1	35.7	22.2	30.4
Event 2	5.6	59	2.78	22	2.1	19

The analysis confirms the strong contribution of DGw during the base flow of catchment D, representing the 60% to 70% of the base flow (Figure 40). The contribution of DGw in the total storm flow decreases for higher rainfall events. For the SGw the relation is opposite; the contribution increase with an increase in the total rainfall amount of the event. The contribution of the most superficial water (Rf) seems to be similar for different event with a 20 to 30% of the total storm runoff.

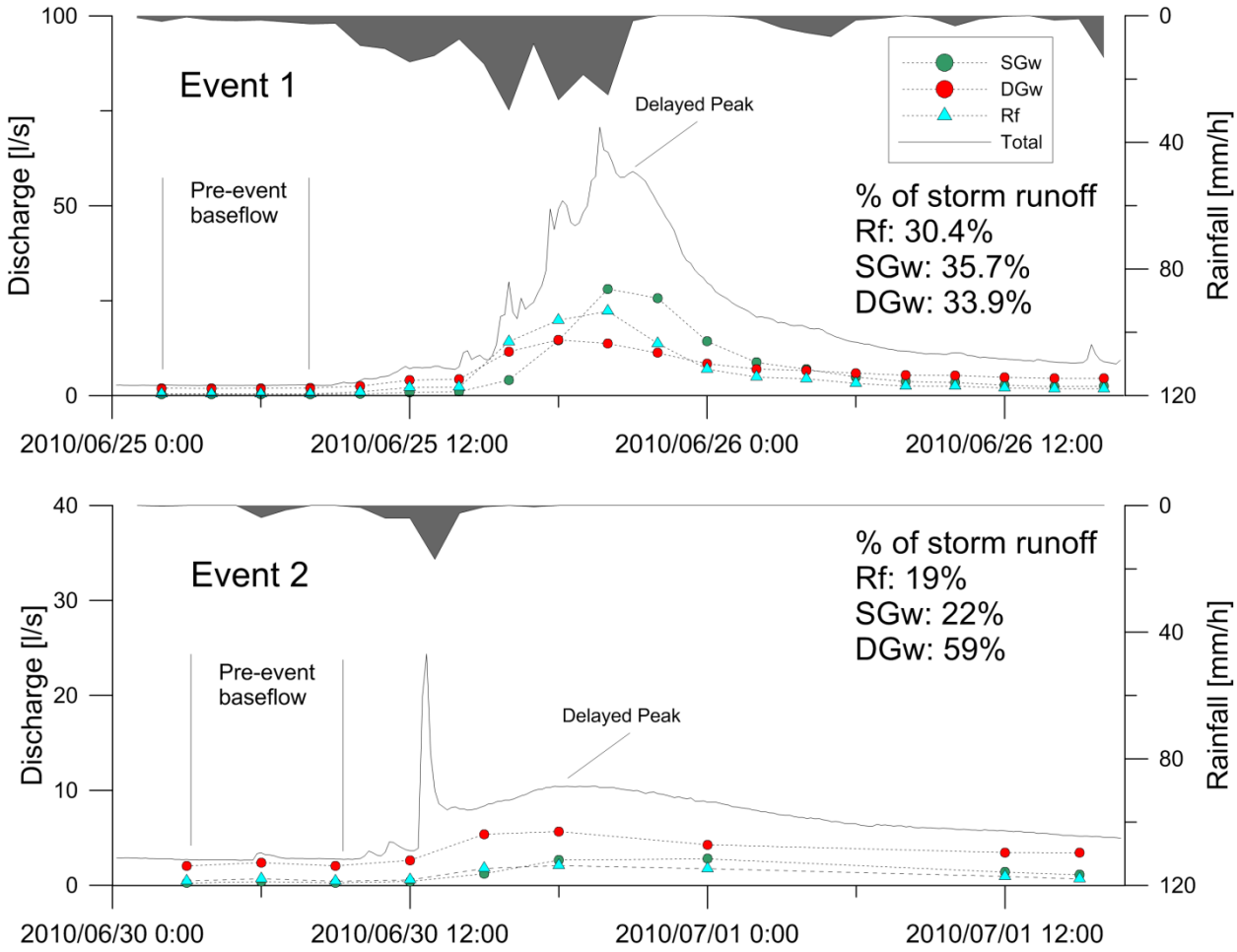

Figure 39. hydrograph separation for the two storm events analyzed in catchment D.

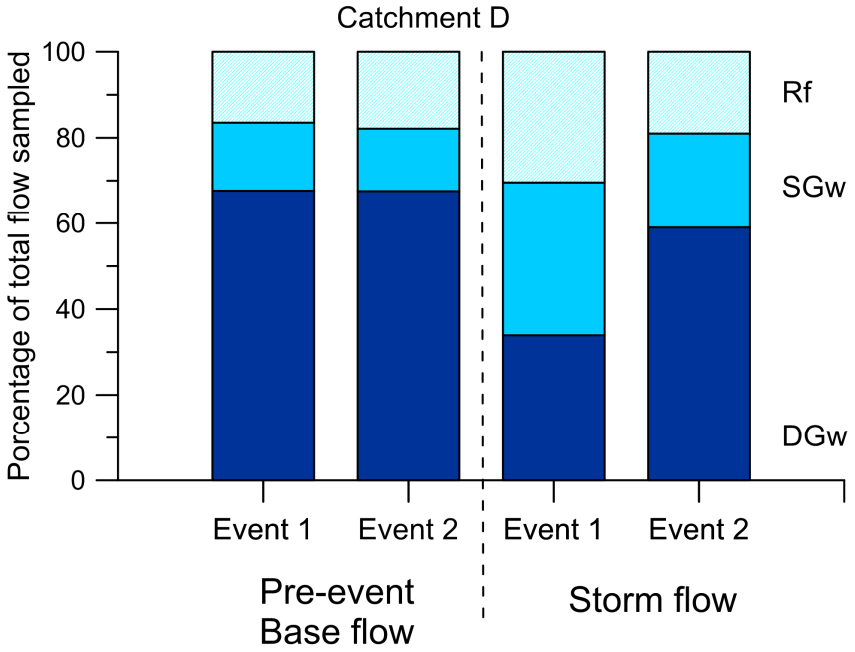

Figure 40. Proportion of contribution of the end members to the discharge of catchment D during the base level and during the storm.

5.3. Discussion: Interaction groundwater – catchment runoff

The observation in the hydrographs reveals three different characteristics of flow for three near catchments. These three different characteristics seem to be dependant in the underlain conditions.

Catchment M does not represent a natural discharge. Its stream is artificially canalized over the landslide deposit. This could affect the definition of the drainage area and therefore the calculation of the specific discharge. This catchment only shows discharge for precipitations over 20 mm/h approximately and does not present long recession curve. The 20 mm/h can represent a threshold limit for rainfall intensity required to exceed the infiltration rate and generate the superficial discharge. Another possibility is that this discharge represents the direct contribution of the soil and regolith cover observed in the borehole core over the bedrock. However the works for the landslide deposit stabilization and the artificial channel for catchment M (Photo 8) can affect the contribution of the shallow cover to the surface. It seems that the discharge in M represent the superficial processes in the small area uphill to the landslide scarp. The lack of long recession leads to infer a small interaction of the discharge with another deep storage or even shallow deposits over the bedrock. In the other hand, catchment U presents a longer and very linear recession. This recession seems to represents a linear discharge from a homogeneous reservoir which can correspond to the old landslide deposit that underlies a big portion of the stream.

The development of a delayed discharge in D indicates different flow path in the catchment whish are not observed in U or even in the very near catchment M. The delayed discharges and secondary peaks in hydrographs has been identified and studied since long time in different catchments. This delayed discharge are usually explained by delayed subsurface storm flows determined by pre-event settings of saturation (Agata, 1997; Anderson and Burt, 1978; Becker, 2005; Birkinshaw, 2008; Burt and Butcher, 1985; Graeff et al., 2009; Hihara,

1988; Iwagami et al., 2010; Masiyandima et al., 2003; Onda et al., 2001; Shiraki et al., 2007; Weyman, 1974; Zillgens et al., 2007). In catchments with relatively thick deposit cover, the generations of delayed responses has been mainly linked to the hydrogeological characteristics of the deposit, specifically its initial saturation level and the distribution of sediments in the catchment (Anderson and Burt, 1978; Birkinshaw, 2008; Burt and Butcher, 1985; Onda et al., 2001). Few studies were carried out in mountainous headwater catchments with relative thin deposits cover. These studies have suggested that the delayed discharges are influenced by the groundwater conditions under the deposit cover or directly subsurface flows through fractures in the underlying bedrock (Agata, 1997; Graeff et al., 2009; Kosugi et al., 2008; Onda et al., 2006). Moreover, Onda et al. (2006) proposed that double peak hydrograph could be a good indicator of the existence of subsurface flows through bedrock fractures in catchments with thin deposit cover. However, no direct measurements on bedrock groundwater were given in order to reinforce this statement.

In this study, the delayed discharge in catchment D is observed in most of the response throughout the year. Even though the Type I responses are associated to small rainfall events (Figure 32a and b), the conditions to distinguish from Type II responses are not clear. Contrary to the studies of Agata (1997) or Zillgens et al. (2007), in this study the pre-event discharge and the rainfall intensity do not explain correctly the generation of Type II responses (Figure 32b). The differences must be in the bedrock characteristics and the origin of the delayed response. In the mentioned studies, the formation of the delayed responses was clearly dominated by the saturation conditions of the soil (sediment) cover. These saturation conditions of soil were determined by the antecedent precipitations. In this study, the delayed responses seem to be determined by the rainfall distribution in short periods of time. Graeff et al. (2009) proposed that the generation of delayed responses are caused by the excess of a deep storages threshold in the catchments. This deep storage was related to the groundwater levels in the bedrock aquifer. Assuming similar process in this study, the generation of Type II discharges for small rainfall

events permit to assume a fast saturation of deep storage in the catchments allowing the generation of the delayed responses (Graeff et al., 2009; Zillgens et al., 2007). This agrees with the fast response of bedrock groundwater even for not normal rainfall events.

The saturation of deep storages in catchments also can be linked to the lag time between the peak of rainfalls and the secondary peak when it was observed. Even though the complexities behind the generation of secondary peaks, it is commonly observed that in catchment more influenced by the deposit cover, the secondary peak tends to have a long delays, in the order of days with minimum of one day delay (Anderson and Burt, 1978; Birkinshaw, 2008; Graeff et al., 2009; Weyman, 1974; Zillgens et al., 2007) and independent of the size of the catchment (Zillgens et al., 2007). Certainly this delay time can be reduced if the saturation conditions are sufficiently high. Examples of this were reported by Masiyandima et al. (2003) with delay times of the second peak from minutes to hours after the first peak. In this case, the catchment analyzed presented low relief, with shallow groundwater level in hydromorphic zone.

In headwater catchments with reduced deposit cover there is a tendency to present short lag time between the first and secondary peak. The longest delays commonly do not exceed the 24 hours approximately for the smaller rainfall events (Agata, 1997; Iwagami et al., 2010; Onda et al., 2001) (Table 6). One exception correspond to the case of Kosugi et al. (2011) and their study of delayed response in headwater catchment underlain by fractured granite. In the study the delay observed is in the order of days. The homogeneous distribution and the low frequency of the fracture system generate slow patterns of bedrock groundwater flow and longer delays in discharges. Under this combination of factors, the bedrock groundwater flow can behave as a flow in an unconsolidated media aquifer with low hydraulic conductivity at catchment scale.

Table 6. Review of studies of delayed discharge in catchment. Comparison with measurements of lag time between peak of rainfall and delayed peaks in discharge.

	Bedrock	Lag time Peak of Rainfall – Delayed peak in discharge
Agata and Tanaka, (1997)	Sedimentary	7-26 hrs
Iwagami et al. (2010)	Volcanic	9 hours
Kosugi et al. (2011)	Granite	2 days
This Study	Sedimentary	10 min – 16 hours

In catchment D also were observed relatively short lag times, with 16 hours to less than 1 hours delay between peaks. Faster delayed responses mean faster saturation conditions in the subsurface which can be related with the groundwater conditions that in this case correspond to bedrock groundwater (Graeff et al., 2009; Onda et al., 2006).

The direct correlation between the discharge in D and bedrock groundwater suggested an important correlation between them when the maximum in bedrock groundwater is reached. During the maximum of groundwater, the particular situation of stable levels suggested an important discharge of groundwater out of the bedrock. Under this situation, it was suggested that this discharge of groundwater contributes directly to surface processes. The peaks of the delayed discharge in D showed an important increase during the maximum level of bedrock groundwater. However, no clear evidences of any mechanism that suggested this direct contribution from groundwater bedrock to the discharge in D were found in the field.

The hypothesis of direct contribution of bedrock groundwater into the discharge of D during the maximum level was partially confirmed by the hydrograph separation. Generally, the contribution of bedrock groundwater (i.e. SGw and DGw) is similar to other studies that demonstrate an important contribution of bedrock groundwater in runoff (Table 7).

Table 7. Review of studies that measured the % of contribution of bedrock groundwater in the discharge of catchments.

	Bedrock	**% of contribution of Bedrock Groundwater to runoff**
Uchida et al. (2003)	Granite	50 - 95%
Kosugi et. al. (2006)	Granite	65-71%
Anderson and D. (2001)	Sedimentary (Sandstone)	93%
This Study	Sedimentary	69.6% - 81%

During the base level in the discharge of D, the high contribution of DGw, that represents the base level in bedrock groundwater, permit to infer a strong connection between groundwater and runoff during this time. This is also confirmed by the high concentrations of Ca^{+2}, Mg^{+2} in D during this period, compared with the values measured in catchment U. This high contribution also continues for small rainfall events as it is shown in the hydrograph separation for the event 2 (Figure 39).

The event 1 showed an increase in the contribution of SGw associated to the water that infiltrates in bedrock and generates the fast response of groundwater. This increase is not considerably higher than the rest of the end members. However the association of the peak of SGw contribution with the delayed peak in D in event 1 and no clearly in event 2 shows the importance of this end member contribution in the delayed peak. This can be interpreted as a fraction of the water that participates in the response of bedrock groundwater can also generates an increment in the discharge in D. The direct contribution as a flow of bedrock groundwater to

the runoff cannot be confirmed but the importance of the groundwater levels in the discharge is evidenced by the analysis. Graeff et al. (2009) had similar conclusions in the study of a headwater catchment with soil cover that does not exceed the 2 m depth. The study did not find evidence of direct discharge into the runoff such as bedrock spring as the reported by Onda et al. (2001) and Onda et al. (2006). In addition, the unclear chemical bound between bedrock groundwater and discharge during the maximum level leads to reject an eventual direct contribution of bedrock groundwater. Instead of that, it is proposed an interaction between sediment cover – bedrock groundwater as a responsible of the delayed responses in D.

Chapter 6: General Discussion

From the analysis presented in the previous chapter it is interpreted a hydrogeological model to explain the response of the studied hillslope to rainfall events.

6.1. Hydrogeological model of hillslope

The first step is to identify in the model the different hydrogeological features observed in borehole and field observations (Figure 41). The model in the figures respects the vertical and horizontal scale of the hillslope. The sediment and regolith cover has a depth of approximately 10 m in the area around the borehole; however in the rest of the hillslope its depth does not exceed 1.5 m. Below the weathered bedrock is separated in two zones that represent the fast response zone (PR) and slow recession zone (SR) defined by the groundwater fluctuations observed in Bh40 (Figure 12). These zones have been extended to the whole hillslope, up and down to the borehole point. These zones are arbitrarily projected parallel to the surface of the hillslope as a response of the deformation assumed in the hillslope. With this it is also inferred that the whole hillslope presents certain permeability and represents a potential aquifer. The only discontinuities considered are the sets of high degree fractures that cross the fractured bedrock. These structures have been inferred in the hillslope as a result of the step-like morphology observed in the hillslope.

In the model (from Figure 41 to Figure 44), the contribution of the bedrock groundwater to catchment D is represented by arrows in the foothill of the hillslope.

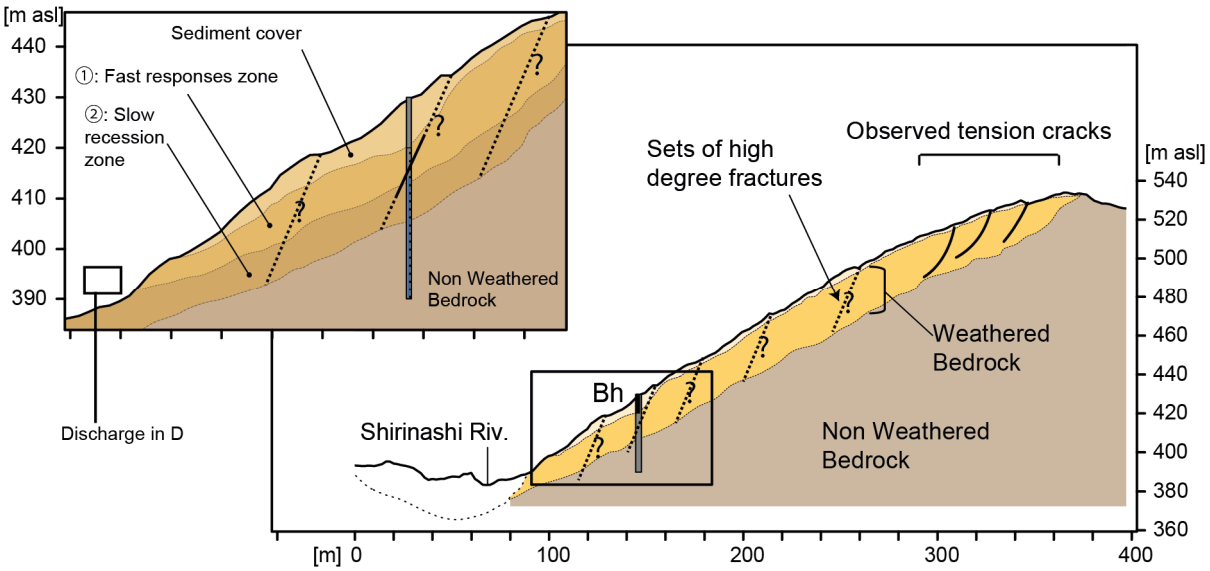

Figure 41. Geological and geomorphological elements included in the hillslope model.

During the base level, the water table in bedrock groundwater is located in the zone of slow recession (SR) (Figure 42). This slow recession represents the slow contribution of bedrock aquifer to maintain the base level in catchment D even during winter season (dry period). This explains the similar chemical characteristics during the base level of bedrock groundwater and the discharge of catchment D.

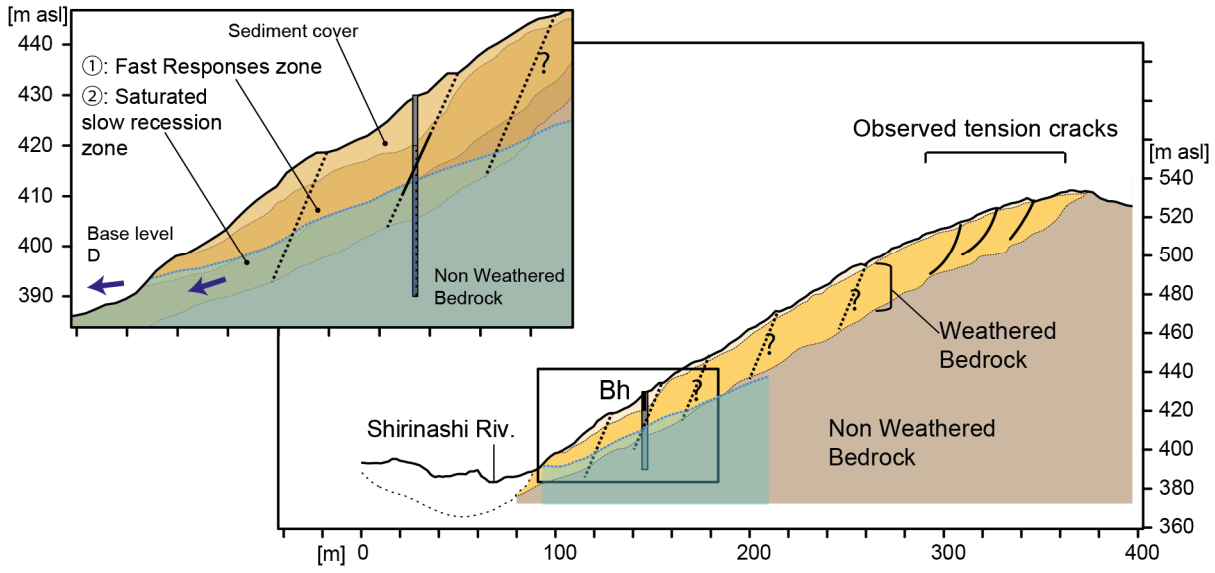

Figure 42. hillslope model representing the groundwater conditions during the base level (no rainfall).

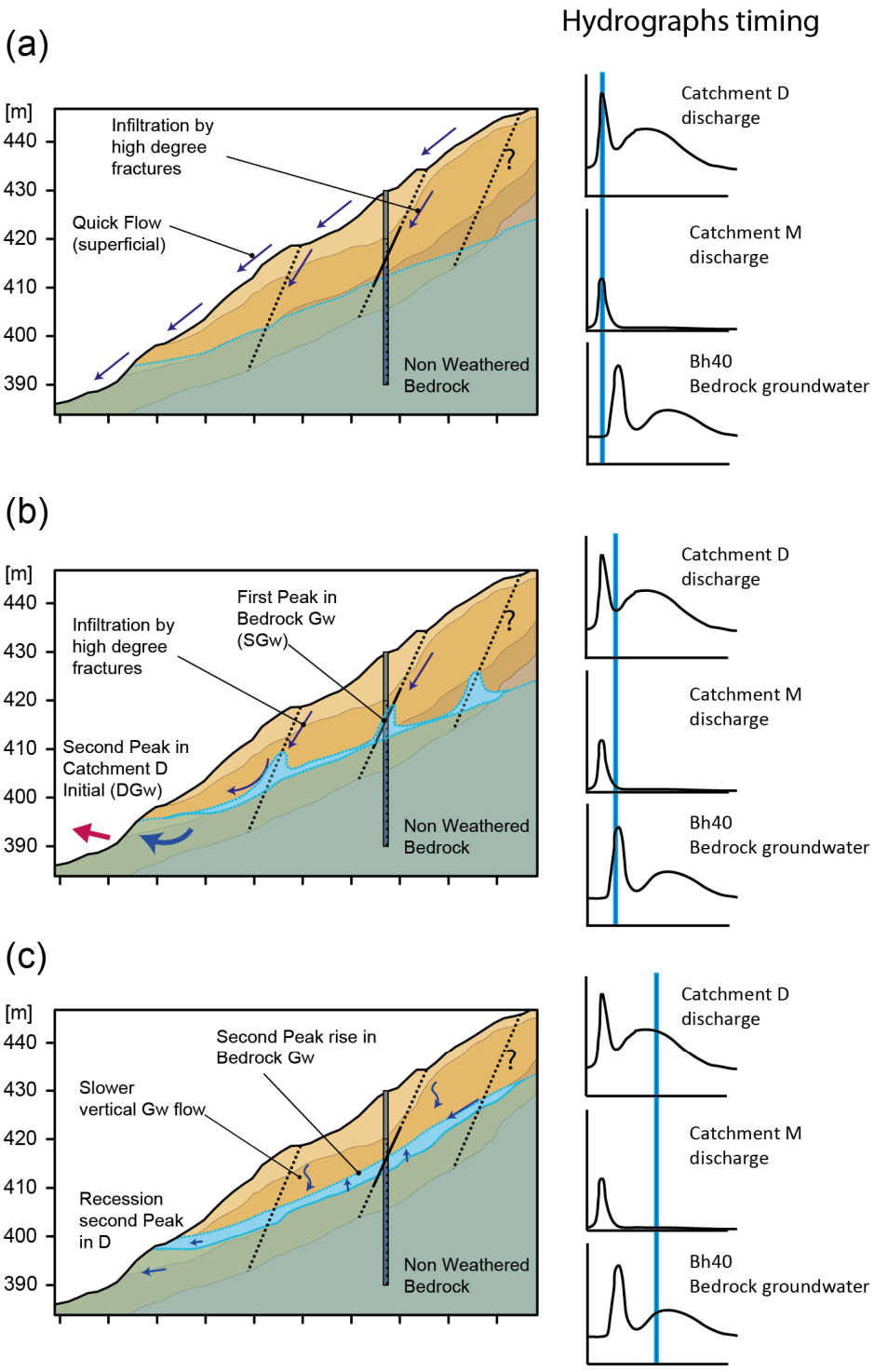

Figure 43. Hillslope model representing the groundwater flows during the double peak response in bedrock groundwater. (a) At the beginning of the storm the quick flow from the first peak in the catchment discharge (M and D) prior to the response of the bedrock groundwater. (b) Groundwater flows during the first peak in Bh40 (Lp). (c) Groundwater flows during the second peak in Bh40 (Lp).

The double peak responses in bedrock groundwater are observed under moderate rainfall conditions (below 80 mm of API_6) (Figure 43). Before the groundwater response, first response corresponds to the discharge in catchment D and M. This quick flow in D might correspond to superficial runoff in the areas near to the discharge point. In M the quick flow is only observed for rainfall over 20 mm/h has the same timing as the quick flow in D. After quick flow peak in discharge the first peak in bedrock groundwater is observed. This first peak in bedrock groundwater must represent the fast saturation of the high degree fractures system. This saturation must be produced by a mix of water between new water that infiltrate into the bedrock and water that remains in the unsaturated zone in bedrock or in the soil cover. This mechanism of fast infiltration by high degree fractures has been described by some authors, but its interaction with boreholes was not directly observed (Salve et al., 2012; Tsutsumi and Fujita, 2008). The infiltration of water of the first peak can generate in the bedrock groundwater a piston effect and produce the displacement of base level water (Mulholland, 1993). This displacement of water, given by possible a wave of pressure, can explain the peak of DGw observed in the hydrograph separation (Figure 39). The peak of base level water (DGw) comes before the secondary peak in discharge and represents the first contribution of bedrock groundwater in the discharge of catchment D. This "injection" of water eventually generates a rise of the water table of bedrock groundwater that generates after the secondary peak. Contrary to the first peak, this secondary peak represents a saturation level of the whole bedrock aquifer. The vertical infiltration of water by the fracture system of the bedrock (matrix) can also contribute to the secondary peak. This contribution is delayed because of the lower hydraulic conductivity of the fracture system of the bedrock matrix. The recession of the secondary peak in discharge of catchment D is observed during the rise of the secondary peak in bedrock groundwater. The decoupling between the delayed peaks in discharge and groundwater was reported by Becker (2005) and it was attributed to possible differences in the subsurface conditions across the catchment. The mechanism of contribution of bedrock groundwater into the discharge must have

higher hydraulic conductivity than the bedrock aquifer. This difference can generate the decoupling. The reduction of lag time for delayed peaks in bedrock groundwater and discharge in higher precipitations support the hypothesis of an important connection between bedrock groundwater and discharge under high saturated conditions of bedrock aquifer.

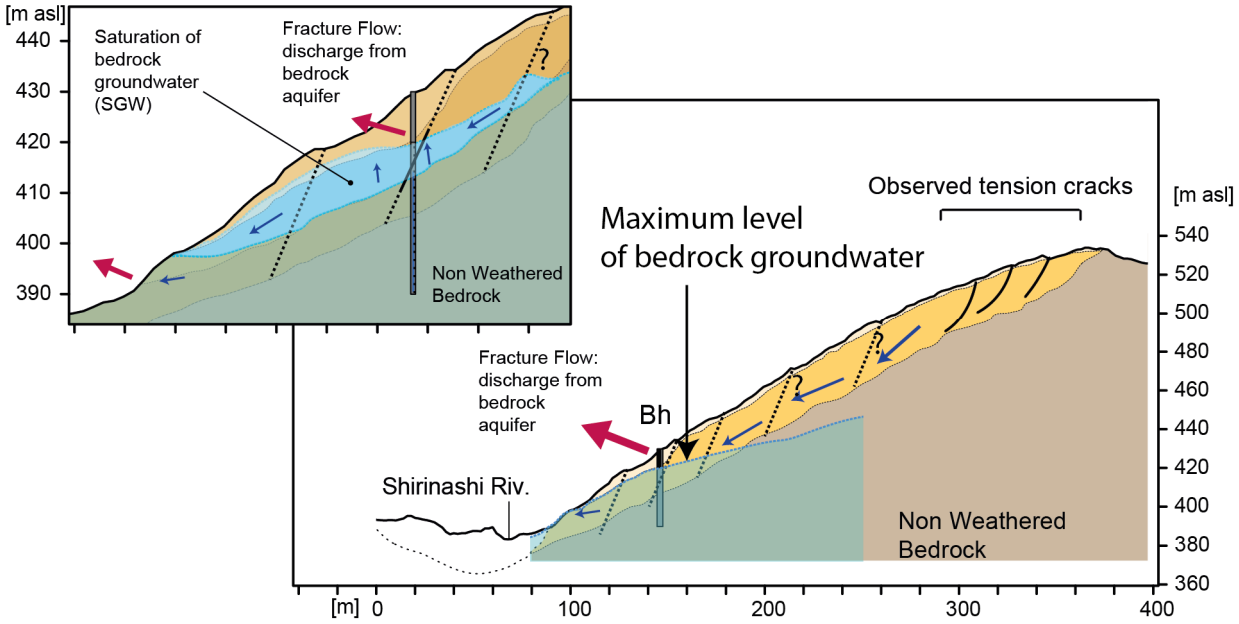

Figure 44. Hillslope model representing the situation during the maximum level of bedrock groundwater and the stabilizations of the water table.

For higher rainfall events, the maximum in bedrock groundwater is reached at 11.5 m bgs (Figure 44). The saturation of the bedrock aquifer is assumed in this situation. The maximum level in bedrock groundwater has important implications in the groundwater conditions of the hillslope. The maximum can represent a maximum for the groundwater level in the whole hillslope under the assumption of the whole hillslope bedrock is hydraulically connected. The stable maximum in groundwater level shows that the water table of bedrock aquifer is controlled by the mechanism that generates that stable maximum. The similar recession curve for all the single peaks can prove that the water table in the hillslope never exceeds the level of 11.5 m bgs (as measured in the borehole area).

The mechanism that generates the maximum level in bedrock groundwater was not clearly observed. The existence of a domain of horizontal or low angled fractures in the core sample allows inferring the participation of a specific set of fractures at the maximum level. The significant increase in the delayed peak in the discharge of D during the maximum demonstrate that this maximum situation affect the hydrological response of the hillslope. However, a direct connection between bedrock groundwater and storm runoff during the maximum level cannot be completely confirmed.

6.2. Implications in the generation of DSL in the area.

Several studies in DSL showed that a relevant factor, among others, to identify a hillslope prone to generates this catastrophic events correspond to the presence of gravitational deformation in the hillslope. Takahashi (2010) showed that in the area of Mt. Wanitsuka a particular interaction between groundwater and runoff is observed in zones of DSL occurrence. Now this study confirms that the fractural system, related to the gravitational deformation, can define sets of fractures that facilitate the interaction bedrock groundwater – runoff. Uchida et al. (2011) in its definition of a new method for assessing DSL susceptibility define three parameters to analyze in catchment susceptible to generate DSL. These parameters are: the presence of ancient DSL scars, evidence of gravitational deformation and the steepness and size of catchment. The study area can satisfy partially the first and second parameter therefore according this method the susceptibility to generate DSL is not critical.

The studied hillslope did not fail under the rainfall conditions of 2005. One of the reasons proposed in this study correspond to the mechanism that stabilize the bedrock groundwater at 11.5 m bgs approximately. This mechanism can partially facilitate the exfiltration of bedrock groundwater in the discharge of catchment D, but not in the same way in catchment M. The proximity of the hillslope to the catchment D could be one of the factors in the prevention of failure. Under this assumption, for farther zones in the hillslope to catchment D the interaction

bedrock groundwater - runoff cannot regulate the groundwater levels. This eventually generates the DSL by the excesses of groundwater pressure in the bedrock fracture below the safety factor. However, the gravitational deformation is a dynamic system where the hillslope slowly move downhill by gravitational forces. This implies that it is highly probable that the fracture system can change with time. Under this scenario, the mechanism that prevents the rise of groundwater levels in the hillslope can be blocked by a change in the fracture conditions. This could generate a rise in the groundwater levels and trigger the DSL in the hillslope (Figure 45).

It is necessary to mention that the rainfall event that generates the DSL in 2005 (DSL rainfall) was characterized by a long duration but moderate intensity (peak of 46 mm/h). The I-D correlation (average intensity versus duration) shows the characteristics of the DSL rainfall in Mt. Wanitsuka, compared with the maximum rainfall (Hp rainfall: rainfall that generates single peaks in bedrock groundwater) measured by this study during the study period (Figure 46). The difference is in the average intensity that is higher in the DSL rainfall. This average intensity is higher than the rainfall event that generates the DSL in Nara prefecture in 2011. The rainfalls measured in this study are characterized by average intensities below 10 mm/h. For all these rainfall events, the mechanism that controls the groundwater seems to prevent rise of the water table in the hillslope. However, the limits for this mechanism in terms of flow of water discharged from bedrock aquifer are still unknown. The progressive increase of the average intensity implies an increase of infiltrated water that hypothetically can exceed the discharge flow. Also, the rapid response during the maximum level of the bedrock groundwater (Figure 18) shows the high sensitivity of the water table to changes in the intensity of rainfall. A rapid increase of intensity can implies a rapid but effective rise of groundwater table that eventually can triggers the DSL by the rapid increase of groundwater pressure in fracture.

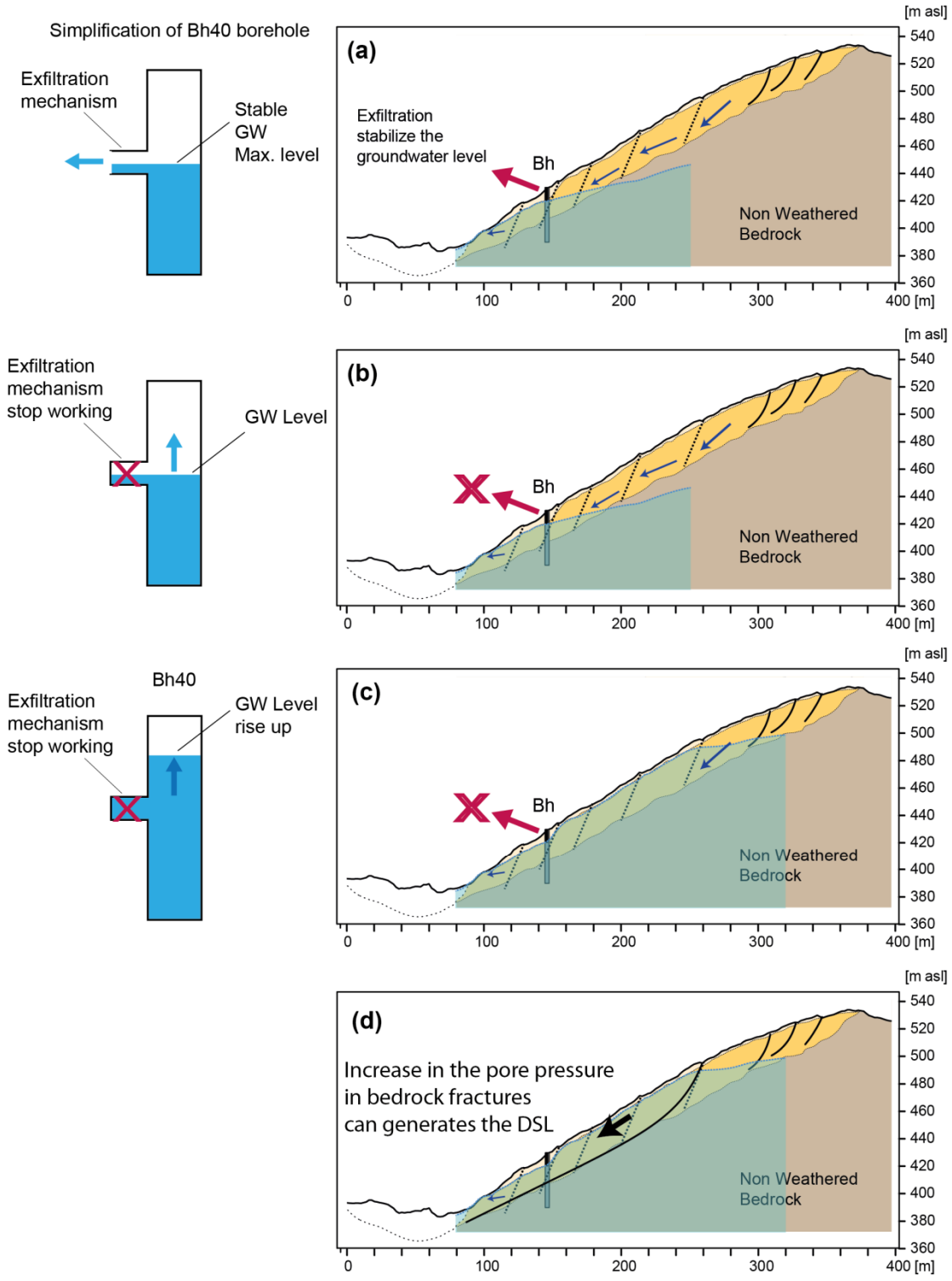

Figure 45. (a) Stable groundwater levels inferred for heavy rainfall events. The stop of the mechanism that allows the discharge from bedrock groundwater (b) can implies a rise of groundwater levels in the hillslope (c). The rise of groundwater implies an increase of the pore pressure in bedrock fractures that can generate the instability of the hillslope and trigger the DSL events.

The occurrence of DSL at the same time as the peak of intensity is not common; however there are few cases when that situation happens. An example of this corresponds the case of a relative deep landslide (10 – 15 m deep) in Minamata, Kumamoto prefecture (Kyushu Island) in 2003 (Sidle and Chigira, 2004; Tsutsumi and Fujita, 2008). This landslide occurred during the highest intensity of rainfalls (90 mm/h) but only with 250 mm of accumulated rainfall in 5 hours. The timing and rapid landslide occurrence was attributed to vertical fractures in bedrock (Weathered andesite) observed in the scarp of the landslide. These vertical fractures helped the rapid infiltration of water into the bedrock, similar mechanism to the presented in this study. Tsutsumi and Fujita (2008) made a model of the groundwater levels in the hillslope by numerical simulations. According to the study the model that considered the vertical infiltration of water by the vertical fractures could explain in a better way the timing of the landslides occurrence. The model also assumed hydraulic disconnection between fractures.

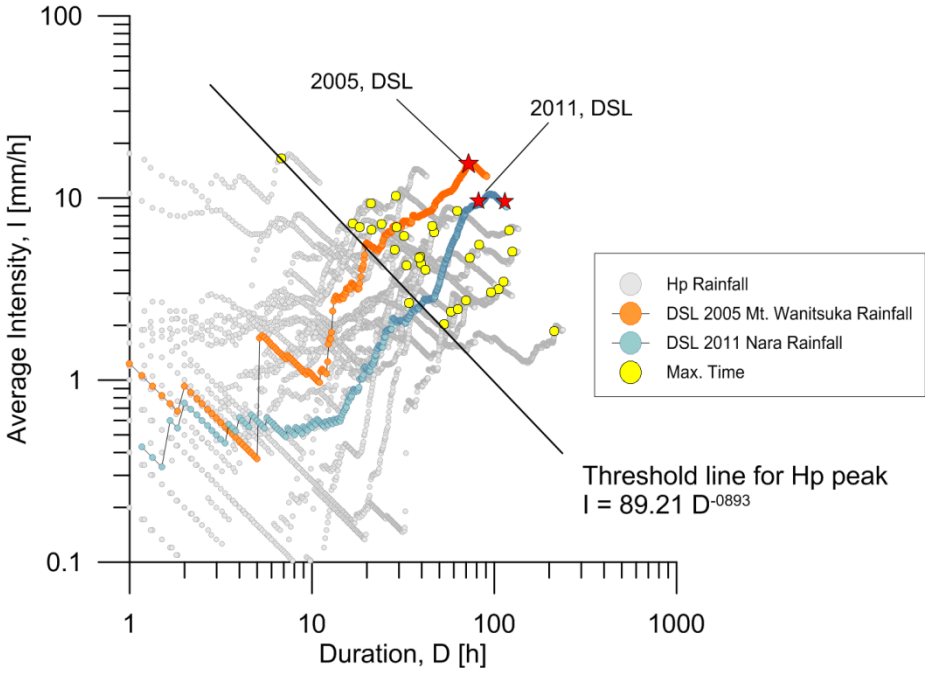

Figure 46. Graph I-D for the rainfall events that generates maximum peaks in Bh40 (Hp) and the rainfall that generates DSL event in Mt. Wanitsuka in 2005 (Orange dots) and in Nara prefecture in 2011 (Blue dots). Red stars: Estimated occurrence time of DSL event. Black solid line: threshold line of I-D conditions for the generation of maximum peaks (Hp).

In this study, the high fractured areas and the fracture system in bedrock permit the connection between eventual sets of vertical or high degree fractures that acts as conduits. This implies the greater storability of the bedrock aquifer compared to the case in Minamata. Also the existence of the discharge mechanism of bedrock groundwater increases the volume of water required to the increase of fracture pore pressure that triggered the DSL. Although, the high degree fracture system can still work during the saturated conditions of bedrock groundwater. In this terms, it is possible to assume that the high degree fracture system can be responsible of the timing of DSL occurred in Mt. Wanitsuka in 2005.

Chapter 7: Conclusions.

The role of the bedrock groundwater in the hydrological and hydrogeological response to rainfalls of mountainous hillslopes is still not well understood. This role has special importance in hillslopes with relatively deep fractured bedrock due to its implications in the generation of deep seated landslides. In order to understand this role, a series of hydrometric and hydrochemical observations were carried out in this study in a hillslope of Mt. Wanitsuka. In this mountain several deep seated landslide were observed recently after heavy rainfalls caused by the pass of typhoon in the area. The observations consisted in measurements of groundwater levels of the sediment cover and bedrock in the hillslope also the runoff of near catchments and rainfall in a hillslope with evidences of gravitational deformation. These observations revealed the significant response of bedrock groundwater to rainfalls compared to the response of the sediment cover of the hillslope. This response is represented by a rapid rise and also relatively fast decrease of groundwater levels in the bedrock. The rapid response of bedrock groundwater showed to be dependent on short time antecedent rainfall, characterized by API index with 6 hours half-life period. Also, the rapid response in bedrock is associated with a significant change in the chemical characteristics (EC, isotopic and major elements composition) of groundwater.

The characteristics of the bedrock groundwater response showed evidences to be highly controlled by different sets of fracture in the bedrock. The fracture system in bedrock is dominated by a set of high degree open fractures which act as conduits of groundwater. These open fractures are mainly responsible of the rapid rise of groundwater levels in bedrock. This fractural system observed in bedrock can be related with the gravitational deformation inferred in the studied hillslope. Also, this fractural system seems to be responsible in the interaction of the bedrock groundwater with superficial runoff processes. This interaction is represented as a delayed discharge observed in a catchment next to the hillslope analyzed (catchment D).

Another important fracture flow mechanism observed in bedrock determines a maximum level of bedrock groundwater at 11.5 m bgs approximately. This mechanism seems to have an active participation in the interaction bedrock groundwater – runoff of catchment D increasing the discharge of the delayed peak. At the same time, this mechanism is signed to be responsible of the prevention of the generation of DSL during pass of typhoon No14 in 2005 in the studied hillslope. However, the gravitational deformation is a dynamic process therefore the fracture system that controls the bedrock groundwater level can be modified in the future. In this situation, the mechanism that prevents the DSL under the rainfall events in 2005 probably cannot continue performing that role and eventually DSLs can occur in the future.

Acknowledgements

I would like to express my gratitude to all the people who helped me, in one way to another, in the completion of this research. My sincerest gratitude goes to Professor Yuichi Onda for having received me as a member of his laboratory and being my advisor. I would like to thank the members of the dissertation defense committee, all members of the University of Tsukuba: Professor Ryo Anma, who also helped me in the process previous of the entrance to the doctoral course, especially Professor Takehiko Fukushima and Professor Tsuyoshi Hattanji. My gratitude also goes to Dr. Tomoyuki Iida, member of the laboratory of Professor Onda, for his valuable help, time and advices in the last part of my research and in field work. I would like to thank many other members of the laboratory of Professor Onda: Shigeaki Baba for his hard work in fieldwork and for his help in my first steps of this research. My thanks also go to Teramage Tesfaye for his help in the enrollment process to this doctoral course and posterior advice. I would like to say thank you to Yoshitaka Komatsu for his valuable help in the research and in the everyday university life. Finally I want to thank Takehiro Noguchi and Yuichiro Yonei for their help in fieldwork.

Certainly for a foreign student the life abroad is a big challenge but also an important part of this achievement. In this part I would like to thank Mamiko Irie for her companion, support and help in the daily life. Also I want to thank my family for their support, most of the time at the distance but still very important for me.

References

Agata, Y., Tanaka, Y., 1997. Double-peak storm runoff observed at a hilly watershed in the Soya hills, northern Japan and the conditions in which it occurs with special respect to basin water storage. *Geographical Review of Japan*, **70A**, 798-812.(In Japanese, abstract in English).

Agliardi, F., Crosta, G., Zanchi, A., 2001. Structural constraints on deep-seated slope deformation kinematics. *Eng Geol*, **59**(1-2), 83-102.(In English).

Akther, H., Shimokawa, E., Teramoto, Y., Jitousono, T., 2011. Geomorphological features and prediction of potential sites for deep-seated landslides on Wanitsuka Mountain, Miyazaki Prefecture, Japan. *Journal of the Japan Society of Erosion Control Engineering.*, **63**(5), 14-21.(In English).

Anderson, M.G., Burt, T.P., 1978. Role of Topography in Controlling Throughflow Generation. *Earth Surf Proc Land*, **3**(4), 331-344.(In English).

Anderson, S.P., Dietrich, W.E., Montgomery, D.R., Torres, R., Conrad, M.E., Loague, K., 1997. Subsurface flow paths in a steep, unchanneled catchment. *Water Resour Res*, **33**(12), 2637-2653.(In English).

Baedke, S.J., Krothe, N.C., 2001. Derivation of effective hydraulic parameters of a karst aquifer from discharge hydrograph analysis. *Water Resour Res*, **37**(1), 13-19.(In English).

Banks, E.W., Simmons, C.T., Love, A.J., Cranswick, R., Werner, A.D., Bestland, E.A., Wood, M., Wilson, T., 2009. Fractured bedrock and saprolite hydrogeologic controls on groundwater/surface-water interaction: a conceptual model (Australia). *Hydrogeol J*, **17**(8), 1969-1989.(In English).

Becker, A., 2005. Runoff processes in mountain headwater catchments: recent understanding and research challenges. In: U. Hubert, H. Burgmann, A. Reasonar (Eds.), *Global Change*

and Mountain Regions: An Overview of Current Knowledge. Springer, Dordrecht, pp. 283-295.(In English).

Birkinshaw, S.J., 2008. Physically-based modelling of double-peak discharge responses at Slapton Wood catchment. *Hydrol Process*, **22**(10), 1419-1430.(In English).

Burt, T.P., Butcher, D.P., 1985. On the Generation of Delayed Peaks in Stream Discharge. *J Hydrol*, **78**(3-4), 361-378.(In English).

Caine, N., 1980. The Rainfall Intensity - Duration Control of Shallow Landslides and Debris Flows. *Geogr Ann A*, **62**(1-2), 23-27.(In English).

Chigira, H., Tsou, C.Y., Matsugu, Y., Hiraishi, N., Matsuzawa, M., 2013. Topographic precursors and geological structures of deep-seated catastrophic landslides caused by Typhoon Talas. *Geomorphology*, **201**, 479-493.(In English).

Chigira, M., 2009. September 2005 rain-induced catastrophic rockslides on slopes affected by deep-seated gravitational deformations, Kyushu, southern Japan. *Eng Geol*, **108**(1-2), 1-15.(In English).

Chigira, M., Kiho, K., 1994. Deep-Seated Rockslide-Avalanches Preceded by Mass Rock Creep of Sedimentary-Rocks in the Akaishi Mountains, Central Japan. *Eng Geol*, **38**(3-4), 221-230.(In English).

Coplen, T.B., Neiman, P.J., White, A.B., Landwehr, J.M., Ralph, F.M., Dettinger, M.D., 2008. Extreme changes in stable hydrogen isotopes and precipitation characteristics in a landfalling Pacific storm. *Geophys Res Lett*, **35**(21).(In English).

Craig, H., 1961. Isotopic variation in meteoric water. *Science*, **133**(26), 1702 - 1703.(In English).

Crosta, G.B., 2004. Introduction to the special issue on rainfall-triggered landslides and debris flows. *Eng Geol*, **73**(3-4), 191-192.(In English).

Deere, D.U., 1964. Technical description of cores for engineering purposes. *Rock Mechanics Engineering Geology*, **1**, 16 - 22.(In English).

Dewalle, D.R., Swistock, B.R., Sharpe, W.E., 1988. 3-Component Tracer Model for Stormflow on a Small Appalachian Forested Catchment. *J Hydrol*, **104**(1-4), 301-310.(In English).

Gabrielli, C.P., McDonnell, J.J., Jarvis, W.T., 2012. The role of bedrock groundwater in rainfall-runoff response at hillslope and catchment scales. *J Hydrol*, **450**, 117-133.(In English).

Gleeson, T., Novakowski, K., Kyser, T.K., 2009. Extremely rapid and localized recharge to a fractured rock aquifer. *J Hydrol*, **376**(3-4), 496-509.(In English).

Graeff, T., Zehe, E., Reusser, D., Luck, E., Schroder, B., Wenk, G., John, H., Bronstert, A., 2009. Process identification through rejection of model structures in a mid-mountainous rural catchment: observations of rainfall-runoff response, geophysical conditions and model inter-comparison. *Hydrol Process*, **23**(5), 702-718.(In English).

Haria, A.H., Shand, P., 2004. Evidence for deep sub-surface flow routing in forested upland Wales: implications for contaminant transport and stream flow generation. *Hydrol Earth Syst Sc*, **8**(3), 334-344.(In English).

Hihara, T., Susuki, K., 1988. The double peak hydrograph during storm events in a small watershed of the Tama hills, west of Tokyo. *Geographical Review of Japan*, **61A**, 804-815.(In Japanese with English abstract).

Hong, Y., Hiura, H., Shino, K., Sassa, K., Suemine, A., Fukuoka, H., Wang, G.H., 2005. The influence of intense rainfall on the activity of large-scale crystalline schist landslides in Shikoku Island, Japan. *Landslides*, **2**(2), 97-105.(In English).

Hooper, R.P., Christophersen, N., Peters, N.E., 1990. Modeling Streamwater Chemistry as a Mixture of Soilwater End-Members - an Application to the Panola Mountain Catchment, Georgia, USA. *J Hydrol*, **116**(1-4), 321-343.(In English).

Iwagami, S., Tsujimura, M., Onda, Y., Shimada, J., Tanaka, T., 2010. Role of bedrock groundwater in the rainfall-runoff process in a small headwater catchment underlain by volcanic rock. *Hydrol Process*, **24**(19), 2771-2783.(In English).

Jain, S.K., 1993. Calibration of Conceptual Models for Rainfall-Runoff Simulation. *Hydrolog Sci J*, **38**(5), 431-441.(In English).

Kabeya, N., Katsuyama, M., Kawasaki, M., Ohte, N., Sugimoto, A., 2007. Estimation of mean residence times of subsurface waters using seasonal variation in deuterium excess in a small headwater catchment in Japan. *Hydrol Process*, **21**(3), 308-322.(In English).

Kampf, S.K., Burges, S.J., 2007. A framework for classifying and comparing distributed hillslope and catchment hydrologic models. *Water Resour Res*, **43**(5).(In English).

Katsuyama, M., Ohte, N., Kabeya, N., 2005. Effects of bedrock permeability on hillslope and riparian groundwater dynamics in a weathered granite catchment. *Water Resour Res*, **41**(1).(In English).

Kondoh, A., Shimada, J., 1997. The origin of precipitation in eastern Asia by deuterium excess. *Journal of the Japan Society of Hydrology and Water Resources Research*, **10**, 627-629.(In English).

Kosugi, K., Fujimoto, M., Katsura, S., Kato, H., Sando, Y., Mizuyama, T., 2011. Localized bedrock aquifer distribution explains discharge from a headwater catchment. *Water Resour Res*, **47**.(In English).

Kosugi, K., Katsura, S., Mizuyama, T., Okunaka, S., Mizutani, T., 2008. Anomalous behavior of soil mantle groundwater demonstrates the major effects of bedrock groundwater on surface hydrological processes. *Water Resour Res*, **44**(1).(In English).

Lollino, G., Arattano, M., Allasia, P., Giordan, D., 2006. Time response of a landslide to meteorological events. *Nat Hazard Earth Sys*, **6**(2), 179-184.(In English).

Masiyandima, M.C., van de Giesen, N., Diatta, S., Windmeijer, P.N., Steenhuis, T.S., 2003. The hydrology of inland valleys in the sub-humid zone of West Africa: rainfall-runoff processes in the M'be experimental watershed. *Hydrol Process*, **17**(6), 1213-1225.(In English).

Matsuura, S., Asano, S., Okamoto, T., Takeuchi, Y., 2003. Characteristics of the displacement of a landslide with shallow sliding surface in a heavy snow district of Japan. *Eng Geol*, **69**(1-2), 15-35.(In English).

Mcdonnell, J.J., Bonell, M., Stewart, M.K., Pearce, A.J., 1990. Deuterium Variations in Storm Rainfall - Implications for Stream Hydrograph Separation. *Water Resour Res*, **26**(3), 455-458.(In English).

McGlynn, B.L., McDonnell, J.J., 2003. Quantifying the relative contributions of riparian and hillslope zones to catchment runoff. *Water Resour Res*, **39**(11).(In English).

Montgomery, D.R., Dietrich, W.E., 1994. A Physically-Based Model for the Topographic Control on Shallow Landsliding. *Water Resour Res*, **30**(4), 1153-1171.(In English).

Montgomery, D.R., Dietrich, W.E., Heffner, J.T., 2002. Piezometric response in shallow bedrock at CB1: Implications for runoff generation and landsliding. *Water Resour Res*, **38**(12).(In English).

Montgomery, D.R., Dietrich, W.E., Torres, R., Anderson, S.P., Heffner, J.T., Loague, K., 1997. Hydrologic response of a steep, unchanneled valley to natural and applied rainfall. *Water Resour Res*, **33**(1), 91-109.(In English).

Moriike, H., Onda, Y., Tsujimura, M., Horiuchi, S., Akanuma, J., Karaki, M., 2009. Determining the Long-term precipitation index by runoff monitoring of multi-scale nested catchments. *Journal of the Japan Society of Erosion Control Engineering.*, **62**(1), 32-39.(In japanese, abstract in English).

Mulholland, P.J., 1993. Hydrometric and Stream Chemistry Evidence of 3 Storm Flowpaths in Walker-Branch Watershed. *J Hydrol*, **151**(2-4), 291-316.(In English).

Munyaneza, O., Wenninger, J., Uhlenbrook, S., 2012. Identification of runoff generation processes using hydrometric and tracer methods in a meso-scale catchment in Rwanda. *Hydrol Earth Syst Sc*, **16**(7), 1991-2004.(In English).

Okunishi, K., Nakagawa, A., 1977. A large-scale landslide at Shigeto, Kochi Prefecture – Part 2. Effect of groundwater on the landslide, *Annuals, Disast. Prev. Res. Int.* Kyoto University, Kyoto, pp. 223-236.(In japanese, abstract in English).

Onda, Y., Komatsu, Y., Tsujimura, M., Fujihara, J., 2001. The role of subsurface runoff through bedrock on storm flow generation. *Hydrol Process*, **15**(10), 1693-1706.(In English).

Onda, Y., Mizuyama, T., Kato, Y., 2003. Judging the timing of peak rainfall and the initiation of debris flow by monitoring runoff. *Debris-Flow Hazards Mitigation: Mechanics, Prediction, and Assessment, Vols 1 and 2*, 147-153.(In English).

Onda, Y., Tsujimura, M., Fujihara, J.I., Ito, J., 2006. Runoff generation mechanisms in high-relief mountainous watersheds with different underlying geology. *J Hydrol*, **331**(3-4), 659-673.(In English).

Onda, Y., Uchida, T., Takahashi, S., Tanaka, K., Suzuki, R., Toda, H., 2010. Observation for deep groundwater level and runoff characteristics at Wanitsuka mountain, Miyazaki, Japan. *Journal of the Japan Society of Erosion Control Engineering.*, **63**(1), 53-56.(In Japanese).

Padilla, C., Onda, Y., Iida, T., Takahashi, S., Uchida, T., 2014. Characterization of the groundwater response to rainfall on a hillslope with fractured bedrock by creep deformation and its implication for the generation of deep-seated landslides on Mt. Wanitsuka, Kyushu Island. *Geomorphology*, **204**, 444-458.(In English).

Petley, D.N., Allison, R.J., 1997. The mechanics of deep-seated landslides. *Earth Surf Proc Land*, **22**(8), 747-758.(In English).

Rodhe, A., Bockgard, N., 2006. Groundwater recharge in a hard rock aquifer: A conceptual model including surface-loading effects. *J Hydrol*, **330**(3-4), 389-401.(In English).

Saito, H., Nakayama, D., Matsuyama, H., 2010a. Relationship between the initiation of a shallow landslide and rainfall intensity-duration thresholds in Japan. *Geomorphology*, **118**(1-2), 167-175.(In English).

Saito, H., Nakayama, D., Matsuyama, H., 2010b. Two Types of Rainfall Conditions Associated with Shallow Landslide Initiation in Japan as Revealed by Normalized Soil Water Index. *Sola*, **6**, 57-60.(In English).

Salve, R., Rempe, D.M., Dietrich, W.E., 2012. Rain, rock moisture dynamics, and the rapid response of perched groundwater in weathered, fractured argillite underlying a steep hillslope. *Water Resour Res*, **48**.(In English).

Sepulveda, S.A., Padilla, C., 2008. Rain-induced debris and mudflow triggering factors assessment in the Santiago cordilleran foothills, Central Chile. *Nat Hazards*, **47**(2), 201-215.(In English).

Shevenell, L., 1996. Analysis of well hydrographs in a karst aquifer: Estimates of specific yields and continuum transmissivities. *J Hydrol*, **174**(3-4), 331-355.(In English).

Shimada, J., Momota, H., Ono, Y., 1980. Role of groundwater in the bedrock for underground oil storage: a hydrological case study of small granite island. , International Society for Rock Mechanics Symposium. ISRM, Stockholm, Sweden., pp. 393 - 400.(In English).

Shiraki, K., Shinomiya, Y., Urakawa, R., Toda, H., Haibara, K., 2007. Numerical calculation of secondary discharge peak from a small watershed using a physically based watershed scale infiltration simulation. *J Forest Res-Jpn*, **12**(3), 201-208.(In English).

Sidle, R.C., Chigira, H., 2004. Landslides and debris flows strikes Kyushu, Japan. *EOS, Transaction,. American Geopgysical Union*, **85**(18), 145 - 156.(In English).

Sugawara, M., Watanabe, T., Osaki, E., Katsuyame, Y., 1984. Tank model with snow component, *Research notes of the National Research Center for Disaster Prevention*, Tsukuba, Japan.(In English).

Takahashi, S., 2010. Relationship between runoff characteristics and groundwater levels at different depth in Mt. Wanitsuka. Miyazaki Prefecture. Master Degree, *University of Tsukuba*, Tsukuba, Japan., 233 pp.(In Japanese).

Taniguchi, Y., 2008. Sediment disasters caused by typhoon no. 14, 2005, in Miyazaki Prefecture. *International Journal of Erosion Control Engineering*, **1**(1), 11-19.(In English).

Terlien, M.T.J., 1998. The determination of statistical and deterministic hydrological landslide-triggering thresholds. *Environ Geol*, **35**(2-3), 124-130.(In English).

Tsou, C.Y., Feng, Z.Y., Chigira, M., 2011. Catastrophic landslide induced by Typhoon Morakot, Shiaolin, Taiwan. *Geomorphology*, **127**(3-4), 166-178.(In English).

Tsutsumi, D., Fujita, M., 2008. Relative importance of slope material properties and timing of rainfall for the occurrence of landslides. *International Journal of Erosion Control Engineering*, **1**(2), 79 - 89.(In English).

Uchida, T., Asano, Y., Mizuyama, T., McDonnell, J.J., 2004. Role of upslope soil pore pressure on lateral subsurface storm flow dynamics. *Water Resour Res*, **40**(12).(In English).

Uchida, T., Asano, Y., Ohte, N., Mizuyama, T., 2003. Seepage area and rate of bedrock groundwater discharge at a granitic unchanneled hillslope. *Water Resour Res*, **39**(1).(In English).

Uchida, T., Yokoyama, O., Suzuki, R., Tamura, K., Ishizuka, T., 2011. A New Method for Assessing Deep Catastrophic Landslide Susceptibility. *International Journal of Erosion Control Engineering*, **4**(2), 32-42.(In English).

Uchida, Y., Yokoyama, O., Takezawa, N., Ishiduka, T., 2012. Assessment for deep catastrophic landslides susceptibility. In: G. Koboltschnig, J. Hübl, J. Braun (Eds.), 12th Congress INTERPRAEVENT 2012. http://www.interpraevent.at/, Grenoble / France, pp. 609-618.(In English).

Uemura, R., Yonezawa, N., Yoshimura, K., Asami, R., Kadena, H., Yamada, K., Yoshida, N., 2012. Factors controlling isotopic composition of precipitation on Okinawa Island, Japan: Implications for paleoclimate reconstruction in the East Asian Monsoon region. *J Hydrol*, **475**, 314-322.(In English).

Varnes, D.J., 1978. Slope movement types and processes. In: R.L. Schuster, R.J. Krizek (Eds.), *Landslides—Analysis and control: National Research Council*. Transportation Research Board, Washington, D.C., pp. 11–33.(In English).

von Ruette, J., Papritz, A., Lehmann, P., Rickli, C., Or, D., 2011. Spatial statistical modeling of shallow landslides-Validating predictions for different landslide inventories and rainfall events. *Geomorphology*, **133**(1-2), 11-22.(In English).

Weyman, D., 1974. Runoff processes, contributing area and streamflow in a small upland catchment. In: G. KJ, W. DE (Eds.), *Fluvial Processes in Instrumented watersheds*. Institute of British Geographers, UK, pp. 33-43.(In English).

Wilson, C.J., Dietrich, W.E., 1987a. The contribution of bedrock groundwater flow to storm runoff and high pore pressure development in hollows., Erosion and sedimentation in the Pacific rim. International symposium. International Association of Hydrological Sciences, Corvallis, USA., pp. 49-59.(In English).

Wilson, J.C., Dietrich, W.E., 1987b. The Contribution of Bedrock Groundwater Flow to Storm Runoff and High Pore Pressure Development in Hollows, Erosion and Sedimentation in the Pacific Rim. IAHS, Corvallis, OR.(In

Yano, K., 1990. Studies on deciding rainfall threshold from warning and evacuating from debris flow disaster by improving the decision method of preceding rainfall. *Journal of the Japan Society of Erosion Control Engineering.*, **43**(4), 3-13.(In Japanese).

Yokoyama, O., Uchida, T., Tamura, K., Suzuki, R., Inoue, T., 2011. Relationship between catastrophic landslides and geomorphological and geological features in Mt. Wanitsuka, Miyazaki Prefecture. . *Journal of the Japan Society of Erosion Control Engineering.*, **63**(5), 3-13.(In Japanese, abstract in English).

Zerathe, S., Lebourg, T., 2012. Evolution stages of large deep-seated landslides at the front of a subalpine meridional chain (Maritime-Alps, France). *Geomorphology*, **138**(1), 390-403.(In English).

Zhang, W.J., Chen, Y.M., Zhan, L.T., 2006. Loading/unloading response ratio theory applied in predicting deep-seated landslides triggering. *Eng Geol*, **82**(4), 234-240.(In English).

Zillgens, B., Merz, B., Kirnbauer, R., Tilch, N., 2007. Analysis of the runoff response of an alpine catchment at different scales. *Hydrol Earth Syst Sc*, **11**(4), 1441-1454.(In English).

Appendix

I. Yearly Data:

Rainfall

Groundwater level Bh10

Groundwater Level Bh40

EC values Bh10 and Bh40

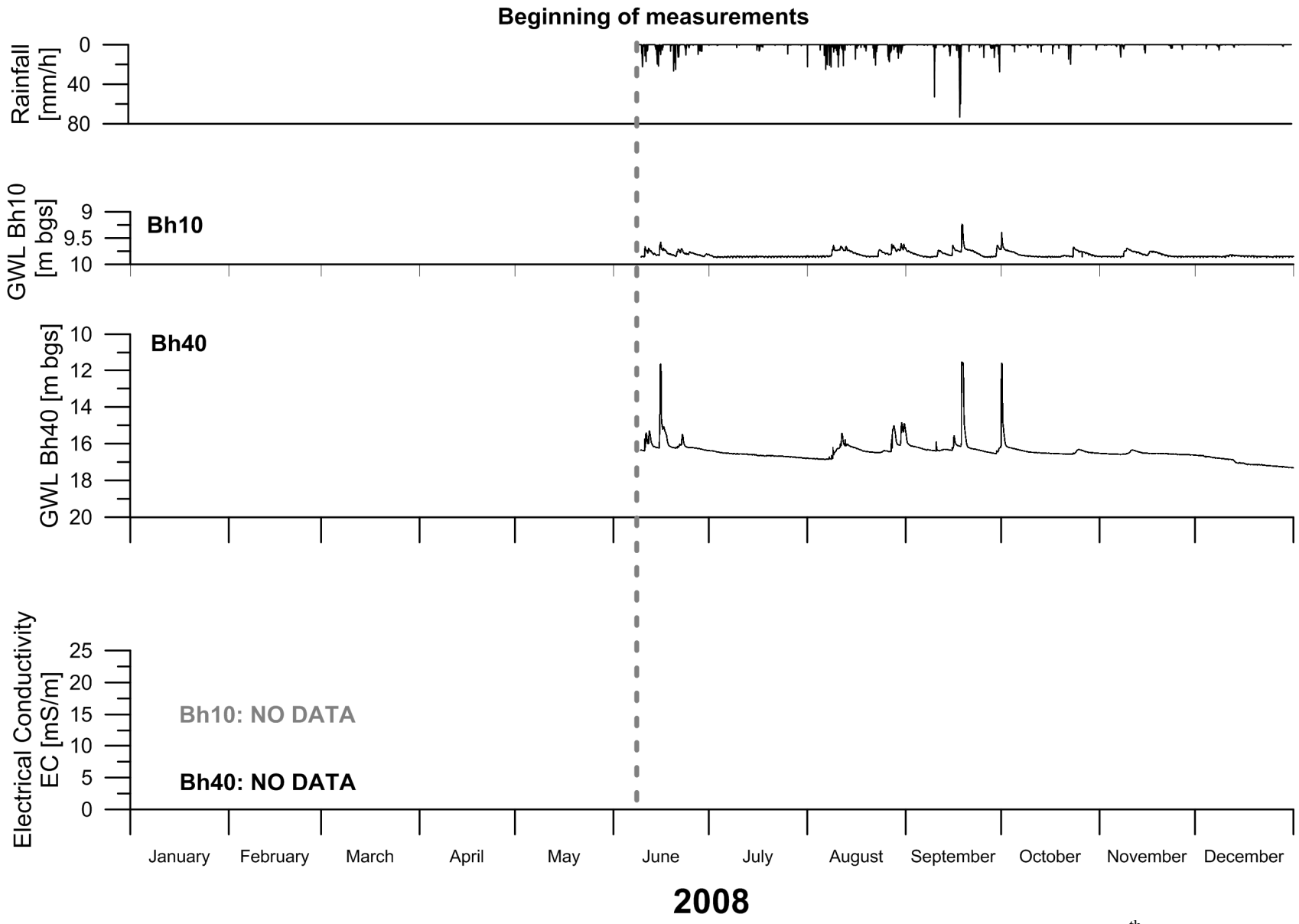

I-1. Yearly data 2008: Rainfall and groundwater level in Bh10 and Bh40. The measurements begin in June 6th of 2008.

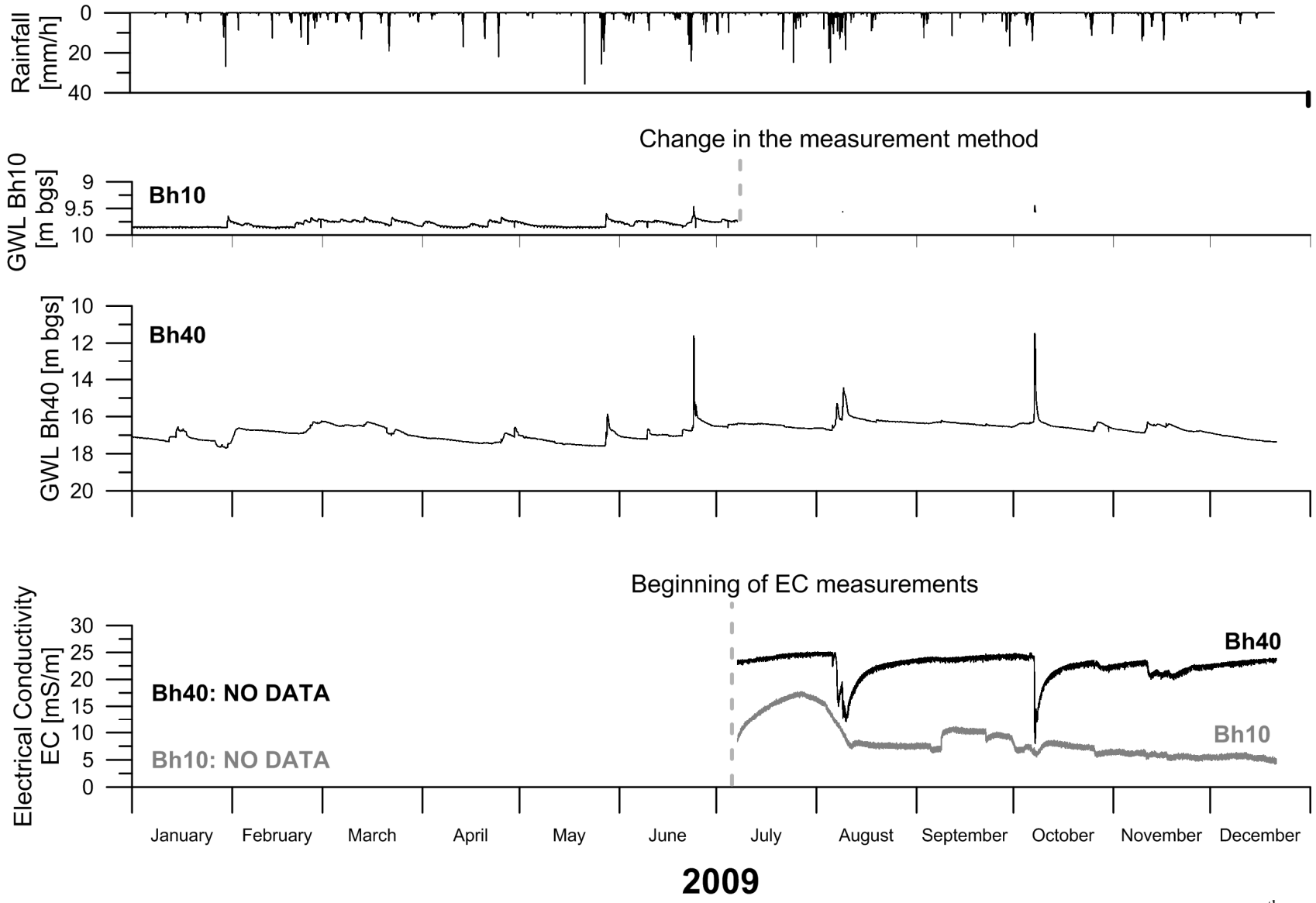

I-2. Yearly data 2009: Rainfall and groundwater level and EC values in Bh10 and Bh40. EC measurements begin in July 7th of 2008.

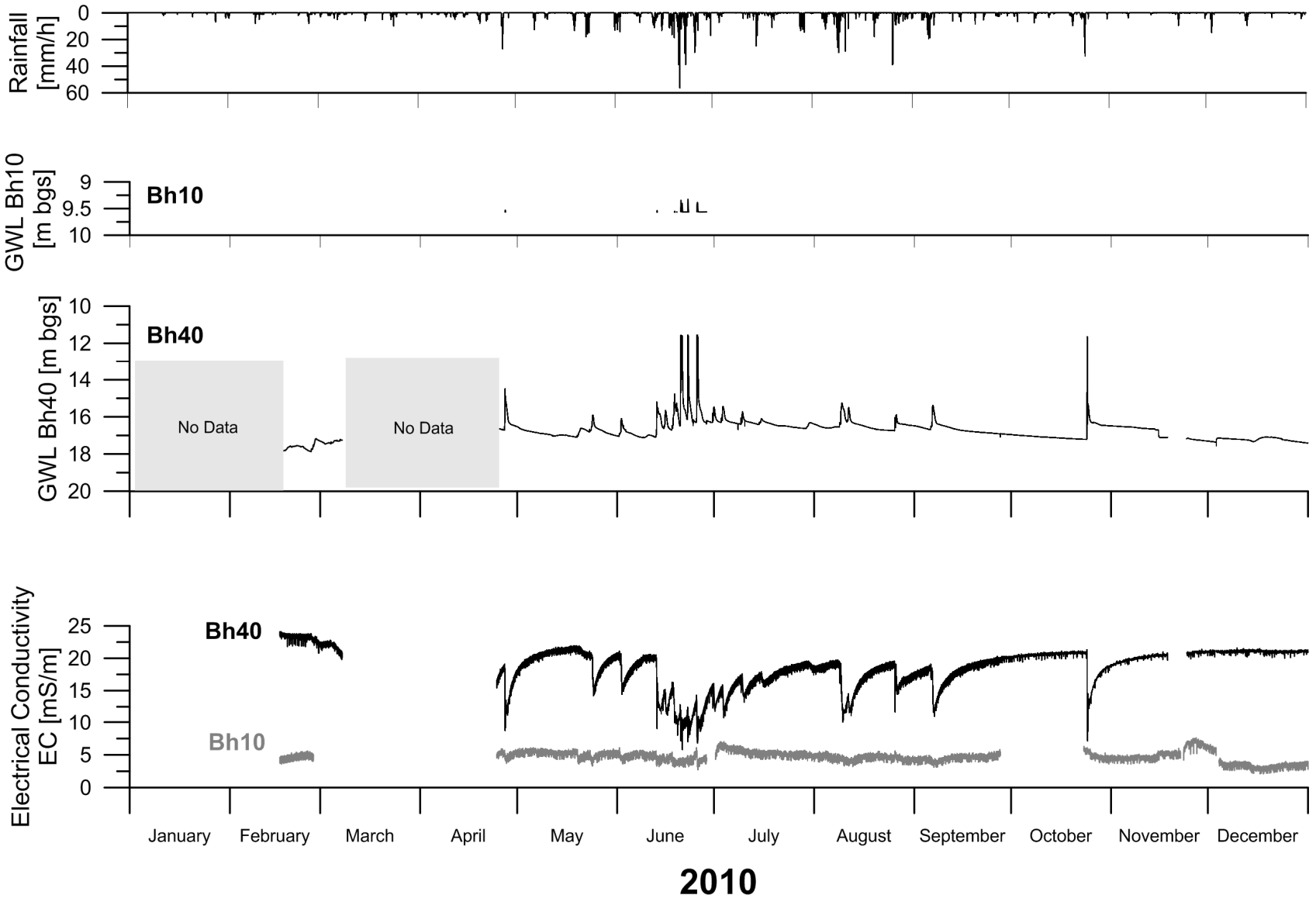

I-3. Yearly data 2010: Rainfall and groundwater level and EC values in Bh10 and Bh40.

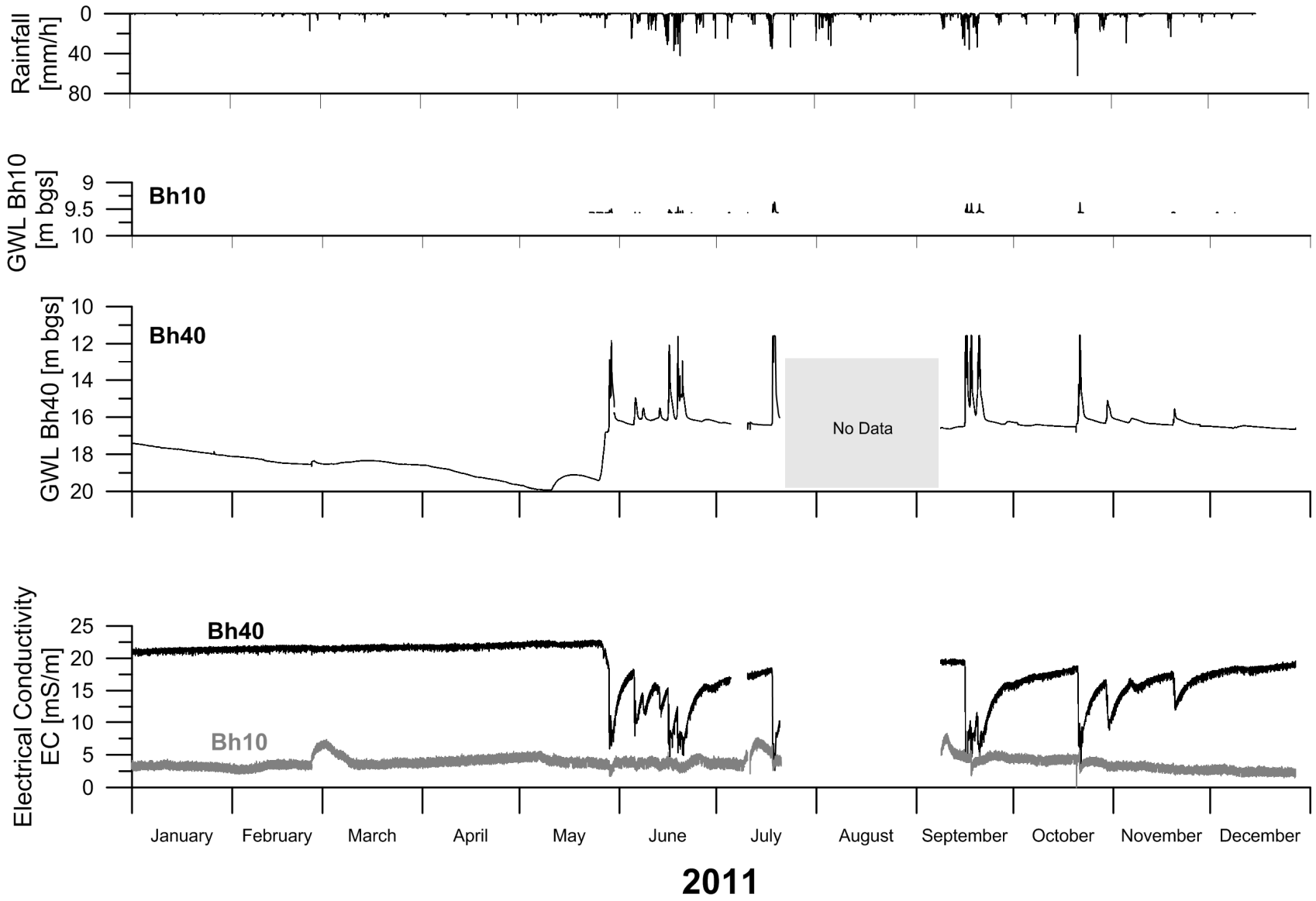

I-4. Yearly data 2009: Rainfall and groundwater level and EC values in Bh10 and Bh40.

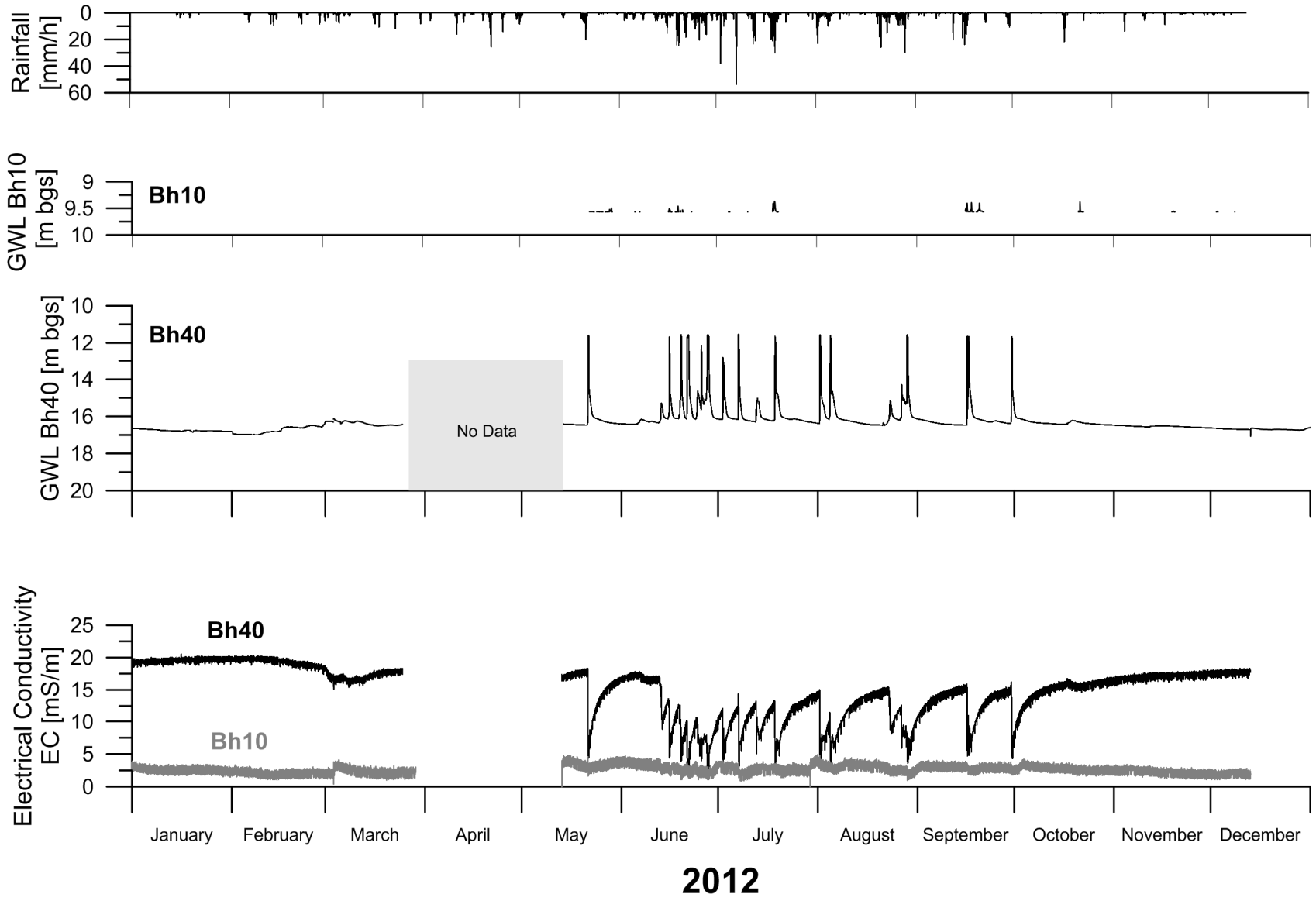

I-5. Yearly data 2009: Rainfall and groundwater level and EC values in Bh10 and Bh40.

II. Yearly Data:

Rainfall

Discharge Catchment D

Discharge Catchment M

Discharge Catchment U

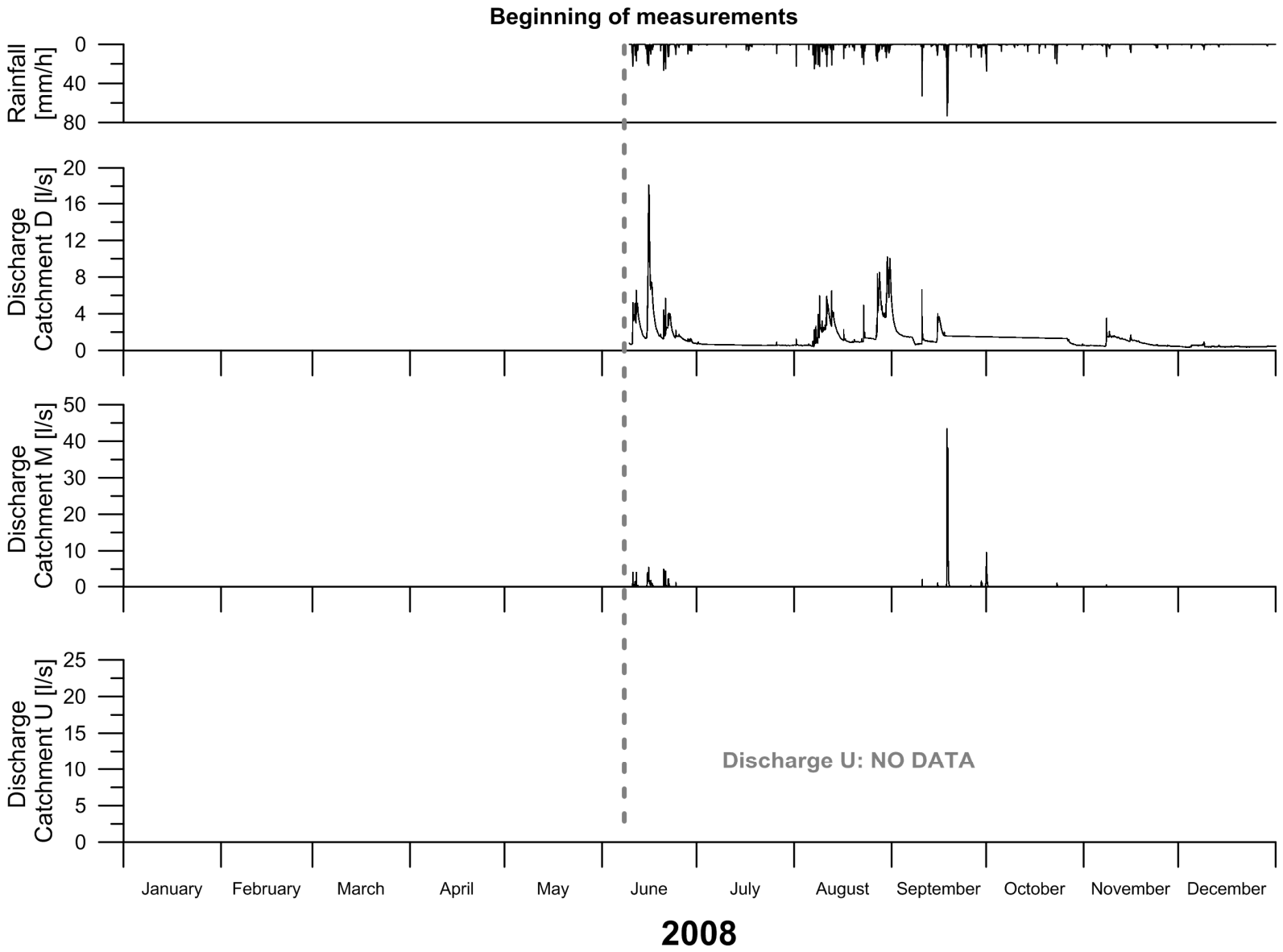

II-1. Yearly data 2008: Rainfall and Catchments discharges.

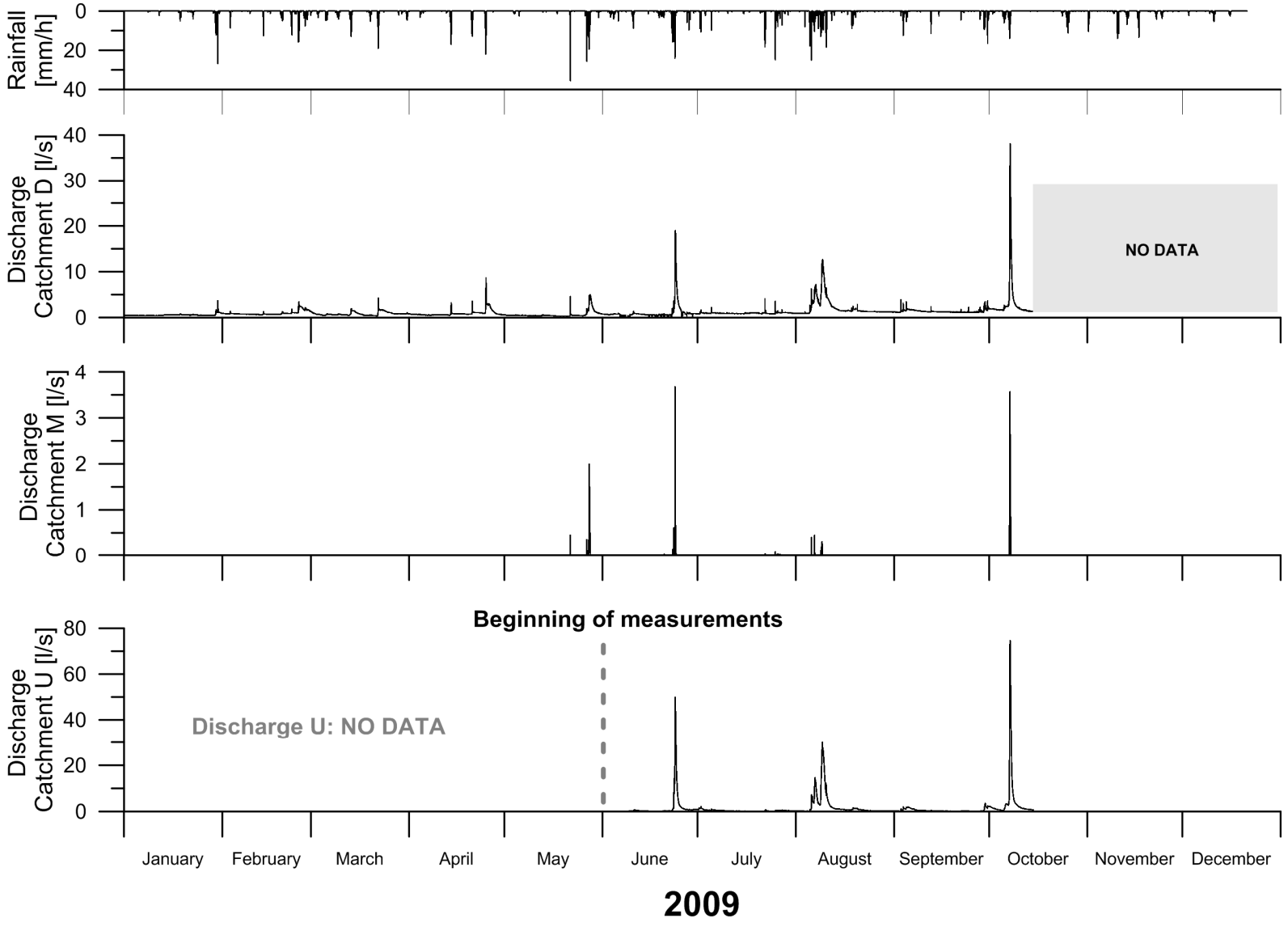

II-2. Yearly data 2002: Rainfall and Catchments discharges.

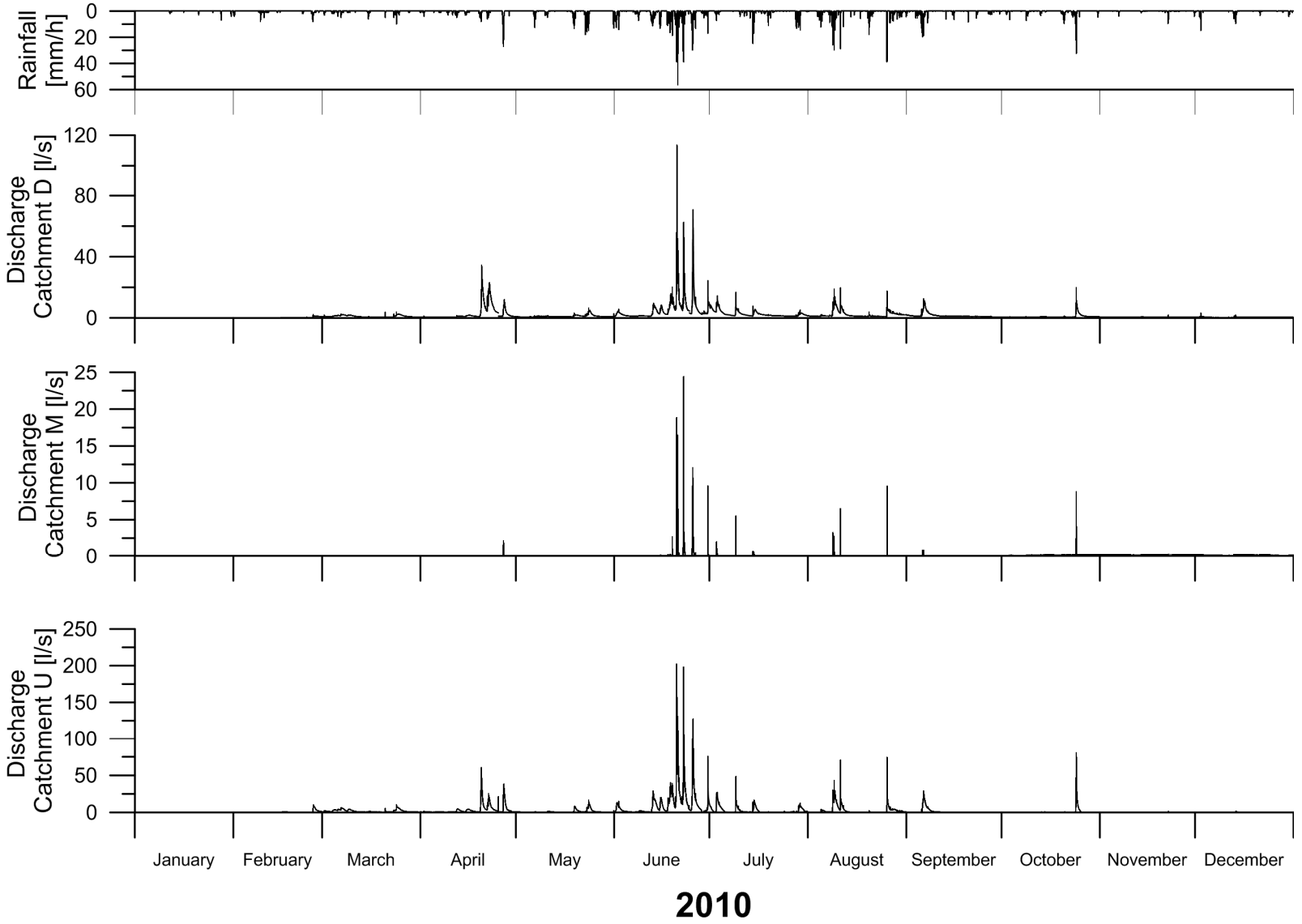

II-3. Yearly data 2010: Rainfall and Catchments discharges.

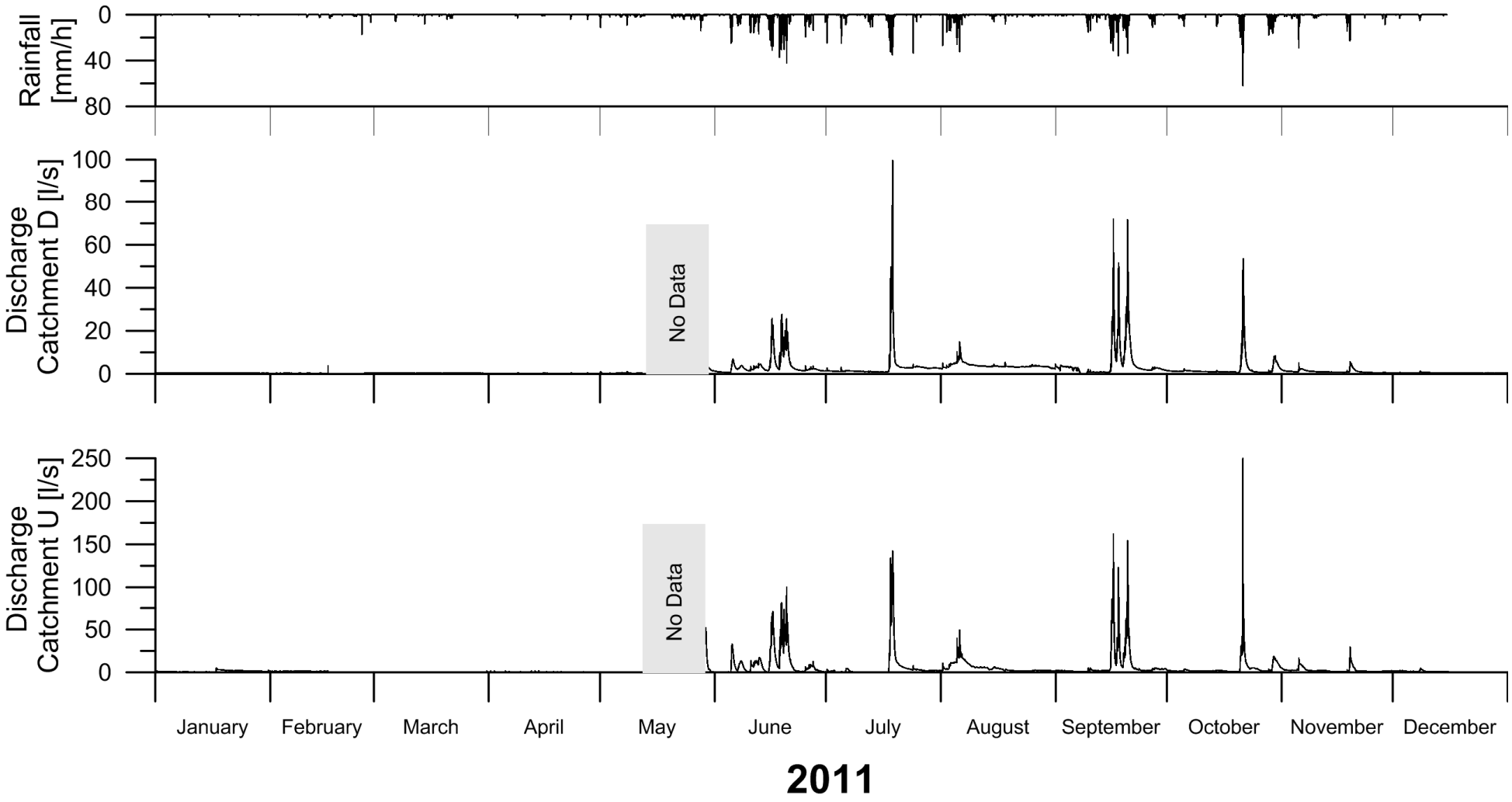

II-4. Yearly data 2011: Rainfall and Catchments discharges.

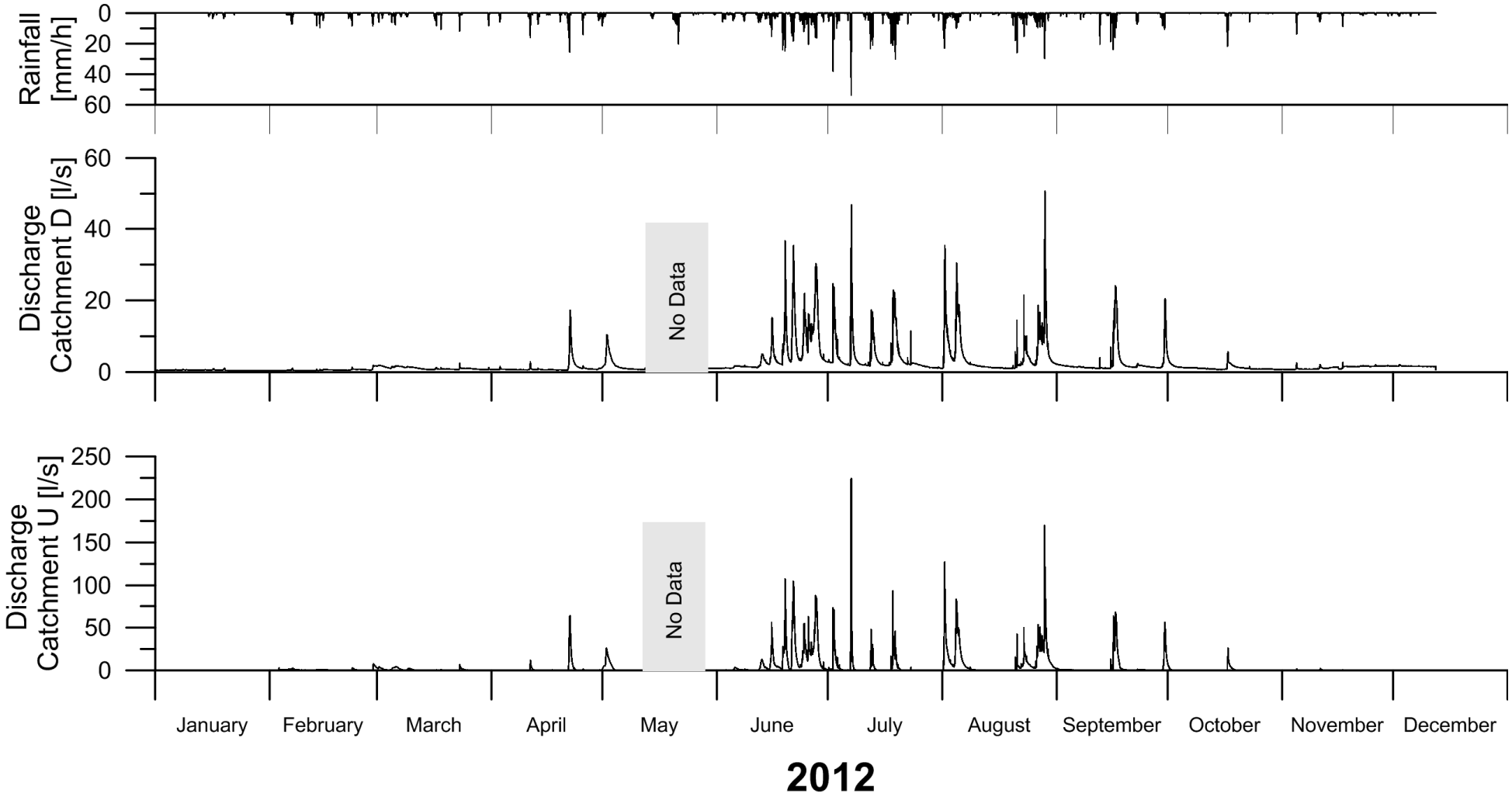

II-5. Yearly data 2012: Rainfall and Catchments discharges.